SOCIETY OF ECOLOGICAL CHEMISTRY AND ENGINEERING

ECOLOGICAL CHEMISTRY AND ENGINEERING A

CHEMIA I INŻYNIERIA EKOLOGICZNA A

Vol. 16 No. 11

OPOLE 2009

EDITORIAL OFFICE
Opole University, Chair of Chemical Physics
POB 313, ul. Oleska 48, 45–951 OPOLE
tel./fax +48 77 455 91 49
email: waclawek@uni.opole.pl
http://tchie.uni.opole.pl

SECRETARIES
Agnieszka Dołhańczuk-Śródka, tel. +48 77 401 60 45, email: agna@.uni.opole.pl
Małgorzata Rajfur, tel. +48 77 401 60 42, email: mrajfur@o2.pl

SECRETARIES' OFFICE
tel. +48 77 401 60 42
email: mrajfur@o2.pl

Ecological Chemistry and Engineering
is partly financed by Ministry of Science and Higher Education, Warszawa

ISSN 1898–6188

CONTENTS

SPIS TREŚCI

ECOLOGICAL CHEMISTRY AND ENGINEERING A

Vol. 16, No. 11 2009

Magdalena BOROWIEC, Marta HUCULAK,
Krystyna HOFFMANN and Józef HOFFMANN[1*]

ASSESSMENT OF SELECTED PESTICIDES CONTENT IN FOOD PRODUCTS IN ACCORDANCE WITH POLISH LAW IN FORCE

OCENA ZAWARTOŚCI WYBRANYCH PESTYCYDÓW W PRODUKTACH SPOŻYWCZYCH ZGODNIE Z OBOWIĄZUJĄCYM W POLSCE PRAWODAWSTWEM

Abstract: The tests covered the determination of the residue content of pesticides belonging to the groups of pyrethroids and dithiocarbamates in tomatoes and strawberries. Vegetables and fruits coming from the area of the Lower Silesian Province were tested. On the basis of the test results it has been established that: in none of the samples subjected to the chemical analysis for the dithiocarbamate residue content any exceedance of MAR defined in the Health Ministry Order of 16th May 2007 concerning the maximum allowable pesticide residue levels in foodstuffs or on their surface was found; in none of the samples subjected to the chemical analysis for the pyrethroid content any residues of: bifenthrine, cypermethrin, deltamethrin were found.

Keywords: insecticides, fungicides, toxicity, maximum allowable levels

Plant protectants contribute to better and higher-quality crops. However, their use in agriculture entails the risk of soil and surface water contamination. They also disturb the ages-old natural balance and can be toxic if used in larger quantities [1–3].

The increasing pollution of the natural environment with harmful compounds calls for periodic investigations and continuous monitoring. This is so because of the unintended (industry, transport, urbanization) and intended (agriculture) effects of human activity on the natural environment whose integral part are plant and animal food resources [4].

Besides the food nutritional value, food safety is a principal factor having a bearing on human health. Therefore food monitoring is essential in order to evaluate food quality with regard to the health of a population. Food quality monitoring is critical for assessing the exposure of the population to pesticide residues in foodstuffs. Pesticide

[1] Institute of Inorganic Technology and Mineral Fertilizers, Wroclaw University of Technology, ul. M. Smoluchowskiego 25, 50–372 Wrocław, Poland, phone 71 320 30 39, email: jozef.hoffmann@pwr.wroc.pl

tests indicate the pesticides which occur in the largest amounts in food, and the food products which most often contain their residues. It is necessary to monitor the residues of chemical plant protectants in food also because of their toxic action and common use in agriculture [5, 6]. According to the current concepts behind the various ecological programmes (HACCP, Sustainable Development, Good Agricultural and Veterinary Practice), it is crucial to determine the life cycle of products (pesticides in this case). By monitoring the content of pesticides in plant products one can assess the health safety of prospective consumers [7–9].

Pesticides

Pesticides are a widely used and so far the most effective way of protecting crops and plant products against pests. Besides having a beneficial effect on plant production such compounds may have adverse side effects due to the fact that generally they have toxic properties. The aim of determining the permissible levels of pesticide residues in the total mass or on the surface of foodstuffs is to protect the health of consumers [10–15].

Chemical substances which are to be used as pesticides should be characterized by:

– selective toxicity (high toxicity towards pests and low toxicity towards the other organisms),

– persistence in the environment (a time of residence in the environment sufficiently long for pest destruction),

– high degradability (once the function of a pesticide is fulfilled, it should quickly decay),

– no tendency to bioaccumulation in animal or plant organisms.

Pesticides are classified according to different criteria, the most important of which are: the application direction and mode of action, the chemical composition and toxicity.

According to toxicity, pesticides are divided into 5 classes. Class affiliation depends on LD_{50}, ie a lethal dose expressed in milligrams of a toxic substance per kilogram of body mass, which after a single administration causes death of 50 % of the tested population of animals. This applies to tests on animals and to acute toxicity determination. The classes of pesticide toxicity to mammals, being in force in Poland, are shown in Table 1 [16].

Table 1

Classes of pesticide toxicity to mammals, being in force in Poland [16]

Toxicity class	LD_{50} [mg/kg body mass]	Degree of hazard
I	up to 50	poisons
II	51–150	poisons
III	151–500	harmful substances
IV	501–5000	harmful substances
V	above 5000	practically harmless

With regard to their action, pesticides are divided into:

1) zoocides – animal control products:
   – insecticides – for the control of insects,
   – rodenticides – for the control rodents,
   – molluscicides – for the control molluscs (slugs and snails),
   – nematicides – for the control nematodes,
   – larvicides – for the control larvae,
   – aphidicides – for the control aphids,
   – ovicides – for the control insect and mite eggs;
2) fungicides – for the control fungi and oomycetes;
3) herbicides – for the control weeds;
4) growth regulators – stimulating or inhibiting plant life processes:
   – defoliants – removing leaves,
   – desiccants – removing moisture,
   – deflorants – removing excessive flowers;
5) acaricides (miticides)– for the control mites;
6) algicides – for the control algae;
7) bactericides – for the control bacteria.

Environmental persistence is the most decisive factor as regards the range of application of pesticides. As concerns their environmental persistence pesticides have been divided into four groups, as shown in Table 2.

Table 2

Division of pesticides with regard to their environmental persistence [16]

Group	Environmental persistence
Highly persistent	above 18 months
Persistent	up to 18 months
Non-persistent	up to 6 months
Fast decaying	up to 3 months

The pesticide residue level in crops depends on the pesticide decomposition time. The amount of the remaining pesticide must be reduced to zero or to a level harmless to people [17]. Pesticides are characterized by high biological activity and may have side effects, especially when introduced in higher doses into soil. Surface application pesticides do not penetrate deep into plants, remaining only on their surface. Some may penetrate deeper into plant tissues. The action of other pesticides is systematic – via the root system they penetrate the whole of the plant.

Chemical plant protectants when administered in the doses recommended by the manufacturer have only slight side effects which quickly disappear. Only when the dose is increased several times, the disturbances are stronger and longer lasting [14].

Insecticides

Insecticides are the most popular plant protectants used to kill insects. This group includes derivatives of chlorinated hydrocarbons. Since the latter do not undergo quick decomposition their accumulation in the environment is particularly dangerous. The half-life of chlorinated hydrocarbons in soil and the time of their activity against some pests are counted in years. The compounds are well soluble in the body where they are retained for a long period of time. The toxic residues of chemical plant protectants, taken up in small doses over a longer period, contribute to chronic poisonings. Since the substances accumulate slowly in the body, the poisonings progress latently without showing any pathological symptoms for years.

Synthetic pyrethroids belong to the group of insecticides which are derivatives of chrysanthemum acid, characterized by a wide spectrum of action against insects. Their toxicity to mammals is relatively low in comparison with, for example, phosphoorganic insecticides or carbamates. They have been passed as fit for use in the protection of vegetables, potatoes, fruits, plants grown for industrial purposes and forests. This wide range of their use creates a danger that they will be retained in plant and animal foodstuffs. Pyrethroids are generally characterized by considerable environmental persistence, high insecticidal activity and low toxicity towards warm-blooded organisms. Their drawback is low stability and quick decomposition under the influence of external factors, particularly light, whereby they are used only for pest control in closed spaced. In the 1970s light-resistant pyrethroids, such as cympermethrin and fenvalerate (Fig. 1), were produced [19].

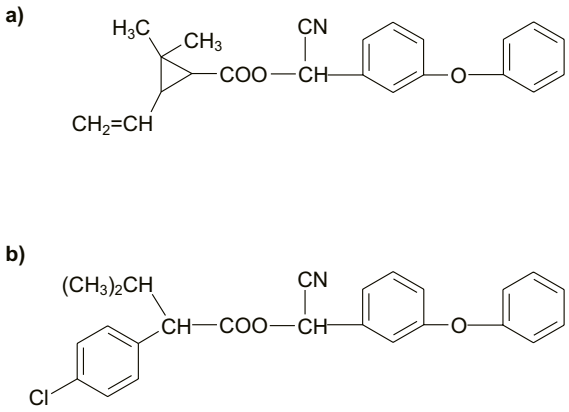

Fig. 1. Light-sensitive pyrethroids: a) cympermethrin (LD_{50} = 250–500 mg/kg – rat orally), b) fenvalerate (LD_{50} = 450 mg/kg – rat orally) [19]

Fungicides

Fungicides are substances which kill fungi. Fungicides include, among others, derivatives of dithiocarbamic acid whose chemical formula is as follows (Fig. 2) [19, 20]:

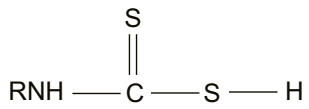

Fig. 2. Formula of derivative of dithiocarbamic acid [19, 20]

The principal fungicides are:

– inorganic substances – sulphur, barium and calcium polysulphides, copper(II) salts;

– organic substances – dithiocarbamates, benzimidazole (benomyl) derivatives and mercury- and tin-organic compounds.

Dithiocarbamates are one of the main groups among agricultural fungicides. Their toxicity is low. The probable lethal doses for humans range from 50 mg/kg (thiuram) to 5–15 g/kg (zineb). They get into the body via the alimentary canal and the respiratory system and accumulate either in the thyroid or the sexual glands. Most of them remain in the body for as long as a week (except for thiuram – retained up to a month), undergoing transformations to more toxic metabolites. They are solids characterized by different water solubility (lithium group salts – well soluble, heavy metals salts and disulphides – slightly soluble) [19].

Dithiocarbamates are analyzed in terms of CS_2.

Legal requirements

The maximum allowable residues (MAR) of pesticides in Poland are specified by the Health Ministry Order of 16th May 2007 concerning the maximum allowable pesticide residue levels in foodstuffs or on their surface.

The Order specifies [10]:

– the maximum allowable pesticide residue levels in plant foodstuffs or on their surface, except for grain, treated in Annex 1 to the Order;

– the maximum allowable pesticide residue levels in grain or on its surface, as wells as used for grain fumigation, treated in Annex 2 to the Order;

– the maximum allowable pesticide residue levels in animal foodstuffs or on their surface, treated in Annex 3 to the Order;

– the maximum allowable pesticide residue levels in baby (up to the 12th month of life inclusive) and small child (up to the age of 3 years) foodstuffs, specified in regulations issued on the basis of art. 26 of the act of 25 August 2006 concerning food and nutrition safety, treated in Annex 4 to the Order.

Materials and methods

Sample taking principles

The principles of taking pesticide residue samples are specified in the National Hygiene Institution procedure: ‘Methods of Taking Samples of Plant and Animal Products for Testing Compliance with MAR’ [21].

The sample size depends on the size of fruits or vegetables and the kind of plant product. Table 3 shows the minimum laboratory sample size to be used in tests for the presence of pesticides [21].

Table 3

Minimum laboratory sample size in pesticide content tests [21]

Product classification	Product	Minimum size of each laboratory sample
Small size fresh products, units < 25 g	Berries, peas, olives	1 kg
Medium size fresh products, units generally 25 g to 250 g	Apples, oranges	1 kg (at least 10 units)
Large size fresh products, units generally > 250 g	Cabbage, cucumbers, grapes (in bunches)	2 kg (at least 5 units)

Pesticide residue determination

Dithiocarbamate residue determination

The spectrophotometric determination of dithiocarbamates and thiuram disulphide consists in heating up a sample with hydrochloric acid and tin(II) chloride in order to release carbon disulphide from the residues of dithiocarbamates present in it. Carbon disulphide is removed from the system and purified through distillation and subsequently collected in an ethanol solution of copper(II) acetate and diethanolamine. The absorbance of the reaction products was measured at a wavelength of $\lambda = 435$ nm. The determination was made in accordance with Polish Standard PN-EN 12396-1:2002 [22].

The analytical sample was comminuted only to a degree allowing it to pass through the reaction flask neck since the rate of decomposition of dithiocarbamate residues increases with the degree of sample size reduction.

10 cm^3 of sodium hydroxide solution was added to the first washer connected to a Liebig condenser while 15 cm^3 of a colour reagent was added to each of the next two washers equipped with Widmer spirals. The weighed out 200 g analytical sample was placed in a three-necked flask. After the apparatus was properly closed, 240 cm^3 of tin(II) chloride solution in hydrochloric acid was added by means of a dropping funnel and the flask was heated until boiling. The system was kept boiling for 1 hour. The content of the first washer was transferred to a measuring flask with a capacity of 25 cm^3 and made up to the mark with ethanol. The absorbance of the reaction products was measured at a wavelength of $\lambda = 435$ nm against a reference prepared from 15 cm^3 of the colour reagent and 10 cm^3 of ethanol.

Pyrethroid residue determination

The pyrethroid residue testing consists in extracting pyrethroids from plant material into a methanol-water solution, back-extracting to *n*-hexane and determining the compounds in the hexane extract by gas chromatography [18].

The comminuted plant material sample was weighed out in the amount: strawberries – 50 g and tomatoes – 50 g. Then 100 cm^3 of methanol were added. The mixture was shaken in a mechanical shaker for 1 h. The obtained suspension was filtered under diminished pressure through a Büchner funnel, using hard filter paper previously wetted with methanol.

20 cm^3 of the filtrate, 20 cm^3 of *n*-hexane and 30 cm^3 of 5 % were taken into a separator of 250 cm^3 capacity and shaken for 5 minutes. The bottom methanol-water layer was drained into another separator and the hexane solution remaining in separator I was filtered through fluted filter paper (with 2 g of anhydrous sodium sulphate) into a round-bottomed flask with a capacity of 250 cm^3.

Solvent (*n*-hexane) in the amount of 10 cm^3 was added to the methanol-water solution in separator II and then extracted for 5 minutes. The methanol solution was transferred to separator III and the hexane solution was filtered into the round-bottomed flask. Extraction was repeated one more time using 10 cm^3 of *n*-hexane and the obtained filtrate was combined with the other ones collected in the flask. The sodium sulphate left on the funnel was rinsed out with 10 cm^3 of *n*-hexane.

The hexane solution was evaporated on a vacuum pan to a volume of about 1 cm^3 at a temperature of 40 ^oC and spread on a column (filled in the following way: a wad of glass wool in the column outlet, about 2 g of anhydrous sodium sulphate, 17 g of Florisil and then about 2 g of anhydrous sodium sulphate; the column was washed out with 50 cm^3 *n*-hexane in order to clean it from substances making chromatographic analysis difficult).

The sample was eluted with 150 cm^3 of a mixture of acetone and *n*-hexane at a ratio of 2:98. The eluate was thickened on the vacuum pan to a volume of about 5 cm^3 and quantitatively transferred to a measuring flask with a capacity of 10 cm^3 and made up to the mark with *n*-hexane.

Results and discussion

Results of chemical analyses of dithiocarbamate residues in fruits and vegetables

Eight samples of strawberries and eight samples of tomatoes, taken in the Lower Silesian province, were tested for the presence of dithiocarbamates.

The dithiocarbamate residue content was calculated as a mass fraction of residue w, in milligrams per kilogram of the product, expressed in terms of CS_2 [22]:

$$w = \frac{m_c}{m_t}$$

where: m_c – the mass of released carbon disulphide (read off the analytical curve) [μg];
m_t – the mass of the tested material (prior to the removal of any parts, eg stones) [g].

The arithmetic mean of two simultaneously performed determinations was adopted as the result. Table 4 shows the dithiocarbamate residue content in strawberry and tomatoes samples, in terms of carbon disulphide.

Table 4

Dithiocarbamate residue content in strawberry and tomatoes samples in terms of CS_2 in mg/kg of strawberries/tomatoes

Sample no.	Dithiocarbamate residue content in sample in terms of carbon disulphide [mg/kg]	
	strawberries	tomatoes
1	0.100	0.090
2	0.125	0.090
3	0.095	0.005
4	0.090	0.100
5	0.095	0.110
6	0.085	0.155
7	0.085	0.095
8	0.190	0.090

The above results showed no exceedance of the allowable dithiocarbamate content, which for strawberries is 2.0 mg/kg of the product (according to the Health Ministry Order of 16th May 2007). The tested samples contain slight amounts of dithiocarbamate residues and so they do not pose hazard to living organisms. No exceedance of the allowable dithiocarbamate residue content, which is 3.0 mg/kg of the product for tomatoes, was determined in any of the samples. The slight amounts of the pollutants in the tested plant material are within the limits of MAR, defined in Annex 1 to the Health Ministry Order of 16th May 2007.

Results of chemical analyses of pyrethroid residue content

The pyrethroid content in the plant material [mg/kg] of the product was calculated from this formula [18]:

$$C_x = \frac{C \cdot V_1 \cdot V_3}{m \cdot V_2}$$

where: C_x – the concentration of the tested substance, mg/kg of the product;
C – the concentration in the extract obtained from the analyzed sample [$\mu g/cm^3$];
m – the sample mass taken for analysis [g];
V_1 – the volume to which the thickened eluate was made up [cm^3];
V_2 – the amount of filtrate taken for analysis [cm^3];
V_3 – the amount of solvent taken for extraction [cm^3].

Sixteen samples (eight samples of tomatoes and eight samples of strawberries) were tested for pyrethroid residue content. The pyrethroid residue content in the strawberries and tomatoes samples is shown in Table 5.

Table 5

Pyrethroid residue content in strawberries and tomatoes samples [mg/kg] of strawberries/tomatoes

Sample No.	Pyrethroid residue content [mg/kg]					
	bifenthrine		cypermethrin		deltamethrin	
	strawberries	tomatoes	strawberries	tomatoes	strawberries	tomatoes
1	< 0.006*	< 0.01*	< 0.02*	< 0.04*	< 0.03*	< 0.05*
2	< 0.006*	< 0.01*	< 0.02*	< 0.04*	< 0.03*	< 0.05*
3	< 0.006*	< 0.01*	< 0.02*	< 0.04*	< 0.03*	< 0.05*
4	< 0.006*	< 0.01*	< 0.02*	< 0.04*	< 0.03*	< 0.05*
5	< 0.006*	< 0.01*	< 0.02*	< 0.04*	< 0.03*	< 0.05*
6	< 0.006*	< 0.01*	< 0.02*	< 0.04*	< 0.03*	< 0.05*
7	< 0.006*	< 0.01*	< 0.02*	< 0.04*	< 0.03*	< 0.05*
8	< 0.006*	< 0.01*	< 0.02*	< 0.04*	< 0.03*	< 0.05*

* Below the determinability limit.

No pyrethroids were found in the tested strawberries and tomatoes samples. According to the Health Ministry Order of 16 May 2007 concerning the maximum allowable pesticide residue levels in foodstuffs or on their surface, the Maximum Allowable Pyrethroid Residue Levels in the strawberries are [7]:

– bifenthrine – 0.5 mg/kg of the product,
– cypermethrin – 0.05 mg/kg of the product,
– deltamethrin – 0.2 mg/kg of the product;

and the Maximum Allowable Pyrethroid Residue Levels in the tomatoes are [10]:

– bifenthrine – 0.2 mg/kg of the product,
– cypermethrin – 0.5 mg/kg of the product,
– deltamethrin – 0.3 mg/kg of the product.

Conclusions

The tests covered the determination of the residue content of pesticides belonging to the groups of pyrethroids and dithiocarbamates in tomatoes and strawberries. Fruits and vegetables coming from the area of the Lower Silesian Province were tested. On the basis of the test results it has been established that:

– In none of the samples subjected to the chemical analysis for the dithiocarbamate residue content any exceedance of MAR defined in the Health Ministry Order of 16th May 2007 concerning the maximum allowable pesticide residue levels in foodstuffs or on their surface was found.

– In none of the samples subjected to the chemical analysis for the pyrethroid content any residues of: bifenthrine, cypermethrin, deltamethrin were found, which is in compliance with the Health Ministry Order of 16th May 2007 concerning MAR of plant protectants in foodstuffs or on their surface.

The use of chemical plant protectants in the manufacturer recommended doses guarantees that the side effects are slight and quickly recede. Only when the dose is increased many times, the disturbances are stronger and last longer.

References

[1] Häfner M.: Ochrona środowiska, Polski Klub Ekologiczny, Kraków 1993.
[2] Wybieralski J.: Chem. Inż. Ekol. 1998, **5**(1–2), 113–118.
[3] Przybulewska K. and Nowak A.: Ecol. Chem. Eng. 2003, **10**(S2)**,** 233–243.
[4] Meinhardt B.: Stan zanieczyszczenia roślin na terenie miasta Wrocławia i okolic, Bibl. Monit. Środow., Wrocław 1994.
[5] Góralczyk K., Ludwicki J. K., Czaja K. and Struciński P.: *Monitoring pozostałości pestycydów w żywności w Polsce*, Roczn. Państ. Zakł. Hig. 1998, **49**(3), 331–339.
[6] Karłowski K., Andrzejewska E., Urbanek-Karłowska B., Windyga B. and Wojciechowska-Mazurek M.: Propozycje zmian w Polskim ustawodawstwie żywnościowym w zakresie substancji dodatkowych, zanieczyszczeń chemicznych i mikrobiologicznych, PZH, Warszawa 1997.
[7] Luning P.A., Marcelis W.J. and Jongen W.M.F.: Zarządzanie jakością żywności. Ujęcie technologiczno-menadżerskie – GHP, HACCP, TQM, ISO, WNT, Warszawa 2005.
[8] Kowalski Z.: Czystsze produkcje jako strategia ochrony środowiska naturalnego, Mentor, Kraków 1998.
[9] Hoffmann J.N. and Radosiński E.: Polish J. Chem. Technol. 2007, **4**, 8–13.
[10] Rozporządzenie Ministra Zdrowia z dnia 16 maja 2007 r., DzU 2007, nr 19 z dnia 4 lipca 2007 r., poz. 817.
[11] *Educational and Informational Strategies to Reduce Pesticide Risks*, Prev. Med. 1997, **26**, 191–200.
[12] Richardson M.: Water Sci. Technol. 1998, **8**, 19–25.
[13] Nikonorov M.: Zanieczyszczenia chemiczne i biologiczne żywności, WNT, Warszawa 1980.
[14] Nowak A.: Chem. Inż. Ekol. 1997, **6**(4), 869–893.
[15] Smoczyński S. and Amarowicz R.: Chemiczne skażenia żywności, WNT, Warszawa 1988.
[16] www.pestycydy.republika.pl, last actualization: 4 April 2002.
[17] Żabicki W. and Kulik Z.: Podstawowe wymagania higieny w produkcji, przechowywaniu i obrocie środkami spożywczymi, Krajowy Związek Rewizyjny Spółdzielni: SCh, Warszawa 1994.
[18] Opracowanie zbiorowe, Metody badania pozostałości pestycydów, Wyd. Metod. PZH, Warszawa 1988.
[19] Tsuji R., Isobe N. and Kawasaki H.: Toxicology 1996, **106**, 131–137.
[20] Kędzierska I. and Kędzierski W.: Ekologiczna profilaktyka chorób uwarunkowanych przez czynniki środowiskowe, Wyd. Med., Warszawa 1997.
[21] Państwowy Zakład Higieny. Zakład Toksykologii Środowiskowej, Metody pobierania próbek produktów pochodzenia roślinnego i zwierzęcego dla celów badania zgodności z NDP pestycydów, Warszawa 2002.
[22] Polish Standard PN-EN 12396-1:2002, Żywność o niskiej zawartości tłuszczu Oznaczanie pozostałości ditiokarbaminianów i disiarczku tiuramu.

OCENA ZAWARTOŚCI WYBRANYCH PESTYCYDÓW W PRODUKTACH SPOŻYWCZYCH ZGODNIE Z OBOWIĄZUJĄCYM W POLSCE PRAWODAWSTWEM

Instytut Technologii Nieorganicznej i Nawozów Mineralnych
Politechnika Wrocławska

Abstrakt: Przeprowadzone badania obejmowały oznaczenia zawartości pozostałości pestycydów z grupy pyretroidów i ditiokarbaminianów w pomidorach i truskawkach. Badaniu zostały poddane owoce i warzywa

pochodzenia krajowego z terenu województwa dolnośląskiego. Na podstawie uzyskanych wyników można stwierdzić, że w żadnej z próbek poddanych analizie chemicznej, w kierunku zawartości ditiokarbaminianów nie stwierdzono przekroczeń NDP określonych w Rozporządzeniu Ministra Zdrowia z dnia 16 maja 2007 r. w sprawie najwyższych dopuszczalnych poziomów pozostałości pestycydów, które mogą znajdować się w środkach spożywczych lub na ich powierzchni; w żadnej z próbek poddanych analizie chemicznej, w kierunku zawartości pyretroidów nie stwierdzono pozostałości: bifentryny, cypermetryny, deltametryny.

Słowa kluczowe: insektycydy, fungicydy, toksyczność, najwyższy dopuszczalny poziom

ECOLOGICAL CHEMISTRY AND ENGINEERING A

Vol. 16, No. 11 2009

Ladislav LUX[1], Mikuláš MATHERNY[1*]
and Silvia RUŽIČKOVÁ[1]

DETERMINATION OF WATER SOLUBLE FLUORIDE IN GRAVITATION DUST SEDIMENT SAMPLES

OZNACZANIE ROZPUSZCZALNYCH W WODZIE FLUORKÓW W PRÓBKACH PYŁU ZAWIESZONEGO

Abstract: Total amount and chemical constitution of gravitation dust sediment in the residential agglomeration of Košice region, Eastern Slovakia was investigated. Samples were taken from two type of area – rural and urban type. Interval of the sampling was once in a month, the database for years 1996 to 2007 was completed in regular intervals. From collected data trends were evaluated. Water-soluble fluoride content, pH value and total amount of gravitation dust sediment parameters were investigated. For fluoride determination direct potentiometry method with ion selective electrodes (ISE) was used. For the calibration purpose the polynomial calibration of 2nd order was used. Method validation was done on the base of following statistical parameters: reliability, precision and repeatability. From collected data the short-term and long-term trends were evaluated.

Keywords: determination, gravitation dust sediment, validation analysis, air pollution

The data of atmospheric pollution in environment are for many reasons of great importance. Solid part of pollutants, small particles, can be according to its size divided into three groups. Particles with diameter more than 10 μm, particles with diameter from 10 μm to 1 μm, and particles less than 1 μm. Quantity, size, and constitution of small solid particles presented in atmosphere greatly influence the quality of environment [1–3]. Particles under the size of 1 μm (flying ash) do not sediment and/or their sedimentation rate is slow. Particles over size of 10 μm sediment fast as a part of gravitation dust sediment [4]. Particles with size from 1 μm to 10 μm can form, depending on conditions, part of airborne dust or gravitation dust sediment [5]. Part of gravitation dust sediment can be incorporated into soil. On the other hand, utilization of soil components by plants can influence the quality of food. The chemical composition of the total amount of dust can be of great interest [6–9]. The longer is the sampling

[1] Technical University of Košice, Faculty of Metallurgy, Department of Chemistry, Letná 9, SK-042 00 Košice, Slovak Republic; email: mikulas.matherny@tuke.sk

period, the higher is the reliability of trend evaluation, which can be achieved. Prescriptions and laws concerning air pollution regulation for region can be found *eg* in [10, 11].

The sediment part of dust influences also the soil quality. Estimated particle size of gravitation dust sediment can be between 10 and 50 μm [1]. In case of small particles, surface of particles and adsorption phenomena on particles surface can be a factor influencing the quality. Using simple model [12] the specific surface of gravitation dust sediment can be estimated roughly between 0.24 $m^2\ g^{-1}$ (for 10 μm ∅), and 0.024 $m^2\ g^{-1}$ (for 50 μm ∅). Different particles of the dust have different size (different relative specific surface adsorption) and this fact should be taken into account too. In the present study the water soluble fluoride content of gravitation dust sediments was evaluated. Direct potentiometry with fluoride ion selective electrode was used for its easy operation, low limit of detection and of reliable data supply [13]. Calibration process, validation and chemometrical characterization of method was used to enhance the reliability of the obtained data.

Experimental

Gravitation dust sediment samples were collected once a month into water containing vessels [14]. Fluoride content of samples was measured by direct potentiometry, using the fluoride ion selective electrode Crytur (Monokrystaly TURNOV, Czech Republic) based on LaF_3 monocrystal. Concentration range of used calibration solutions was from pF = 2.3 to pF = 7.3 (it means fluoride concentration $c_F = 5.10^{-3}$–5.10^{-8} mol/dm^3). For calibration polynomial function of 2nd order was used.

Results and discussion

The results and discussion of the obtained experimental and calculation data can be divided into three parts. The first part is evaluation of the univariant value. The second part is devoted to the calibration of the system of potentiometric determination of fluoride ions. The third part is focused on the long-term and short-term changes of fluoride content in environmental samples.

Evaluation of the univariant data

Set of potential → concentration values were submitted to the chemometric methods. Univalent field of data for direct potentiometric method in the concentration range pF ∈ ⟨2.3, 7.3⟩ was prepared for validation purposes. Validation of fluoride analysis requires determination of degree of repeatability for any given potential of indicating electrode. For statistical data evaluation QC.Expert™2.5 [15] was used. Statistical statements of univariant data should conventionally fulfil requirement of positive normal data distribution. It assures identity between arithmetic mean value ($\bar{I}(x)$), median value ($\tilde{I}(x)$), modus value ($\dot{I}(x)$) and half sum value ($\tilde{I}(x)_p$). Median is the mean value of all potential data; modus is the concentration value appearing with highest

Table 1

Results of the univariant value evaluation

Concentration	$mol \cdot dm^{-3}$	0	$5 \cdot 10^{-8}$	$1 \cdot 10^{-7}$	$5 \cdot 10^{-6}$	$1 \cdot 10^{-6}$	$5 \cdot 10^{-5}$	$1 \cdot 10^{-5}$	$5 \cdot 10^{-4}$	$1 \cdot 10^{-4}$	$5 \cdot 10^{-3}$	$1 \cdot 10^{-3}$	$5 \cdot 10^{-2}$
Concentration	pF	∞	7.3	7.0	6.3	6.0	5.3	5.0	4.3	4.0	3.3	3.0	2.3
No. measur.	N	12	17	15	17	17	17	17	17	17	17	17	12
Arithm. mean	$\bar{I}(x)$	282.7	261.5	258.7	245.9	238.5	207.4	189.4	148.9	128.6	87.4	67.2	21.8
Stand. dev.	$s(\bar{I})_x$	2.8	16.8	4.0	13.3	10.4	14.3	12.1	11.3	9.8	9.1	8.9	6.2
RSD	$s(\bar{I})_{x,r}$	1.02	6.42	25.6	5.48	4.40	6.90	6.40	7.59	7.62	10.4	13.2	28.4
Median	$\tilde{I}(x)$	282.4	232.1	255.4	245.3	238.6	205.6	190.2	148.8	128.8	88.8	65.8	21.9
Stand. dev.	$s(\tilde{I})_x$	4.6	10.2	6.4	4.9	3.6	6.4	5.6	5.1	4.4	5.1	4.6	3.9
RSD	$s(\tilde{I})_{x,r}$	0.57	3.89	2.51	2.00	1.51	3.11	2.94	3.43	3.42	5.75	6.99	17.80
Modus	$\dot{I}(x)$	281.7	263.1	249.6	244.3	238.8	202.4	191.6	148.7	129.4	91.2	63.3	23.8
Halfsum	$\tilde{I}(x)_p$	283.6	259.5	260.4	256.9	245.5	216.9	196.9	156.4	129.5	87.1	67.6	20.1
Asymmetry	$A(x)$	0.49	0.10	0.49	1.29	1.17	0.93	0.81	0.18	–0.02	–0.18	–0.02	–0.10
Test asym.	$t_{A(x)} \neq 0$	N	N	N	Y	N	N	N	N	N	N	N	N
Excess	$E(x)$	2.10	2.10	2.05	4.55	4.44	3.25	3.18	2.67	1.96	1.74	1.70	1.60
Test excess	$t_{E(x)} \neq 3$	N	N	N	N	N	N	N	N	N	N	N	N
Test norm.	t_{norm}	Y	Y	Y	Y	Y	Y	Y	Y	Y	Y	Y	Y
Test homog.	t_{horm}	Y	Y	Y	N	N	N	N	N	Y	Y	Y	Y
Justness Box-Cox tranformation		Y	N	N	Y	Y	N	N	N	N	N	N	N
Just mean	$\bar{I}(x)$	284.8	–	–	242.9	236.6	–	–	–	–	–	–	–

frequency in the given dataset. Data were tested for homogeneity and normality. Parallel statistical test of excess and asymmetry was realized. Theoretical ground of chemometric data evaluation can be found elsewhere [16]. Results of the validation procedure can be found in Table 1.

The agreement condition are within standard deviation value ($s(\bar{I})_x$) of arithmetic mean fulfilled for all concentration values except of concentration $c_F = 10^{-7}$ mol · dm^{-3}. For this concentration neither optimal diagonal nor optimal excess has been achieved. For that reason calibration points (1) and (17) for concentration $c_F = 10^{-7}$ mol · dm^{-3} were excluded from the dataset. Test of excess was tried for disagreement with 3 and it was confirmed for all concentration values and therefore it was no reason for data excluding. All other input data fulfilled positive statistical criteria, and, were used without need for corrections. Histograms (Fig. 1 and 2) confirm normal and/or rectangular data distribution. For concentration range $c_F \in \langle 5 \cdot 10^{-6}, 5 \cdot 10^{-4} \rangle$ mol · dm^{-3} slight differences from normal distribution were found, therefore for average potential

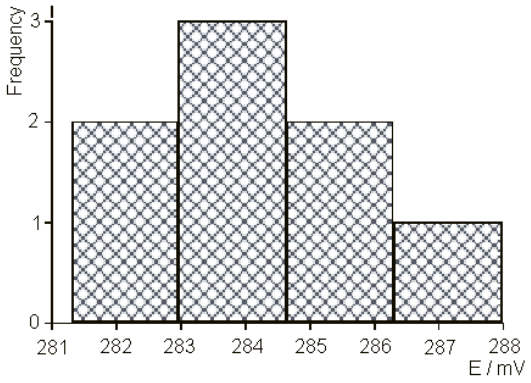

Fig. 1. Histogram of the normal distribution of potential values for the concentration of fluoride ions $c_F = 10^{-7}$ mol dm^{-3} (pF = 7)

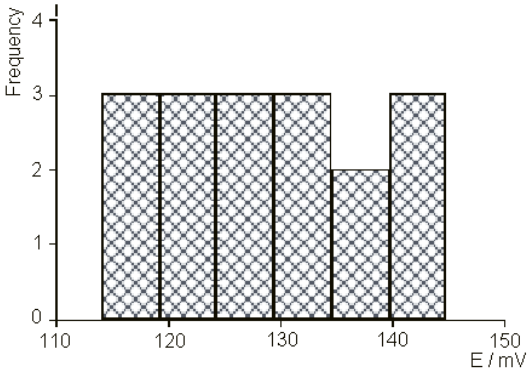

Fig. 2. Histogram of rectangular distribution of potential values for the concentration of fluoride ions $c_F = 10^{-4}$ mol dm^{-3} (pF = 4.0)

values Box–Cox correction was used. The necessary correction was minimal and it was necessary only for three data. All corrections were accepted for calibration line construction. In the concentration range $cF \in \langle 5 \cdot 10^{-6}, 5 \cdot 10^{-4} \rangle$ mol · dm^{-3} no optimal homogeneity of data was obtained. The reason of this phenomenon can be in uncertainties in potential measurements.

Potential values for blank sample (samples without fluoride content) were also measured. In this case a very good agreement between mean value, median value, modus and half sum was obtained. Parameters → diagonally and spoke were found as ideal, test confirmed homogeneity and normality of the set of measured data. Normal distribution of data was also confirmed. The relative precision (RSD) for arithmetic mean value was ± 1.01 % and ± 0.57 % for median value. These data confirm high precision and validity of measurements.

Evaluation of calibration procedure

Analytical calibration requires pair comparison of analytical concentration measured with concentration averages obtained from fluoride electrode potential data. After elimination of false data the construction of a new analytical calibration line followed. Using calibration module of QC.Expert (1) graphic and numeric parameters of calibration dependence were earned (Fig. 3.). Quadratic model of calibration was confirmed and confidence limits were evaluated. This dependence is in concentration interval $\Delta pF \in \langle 2.3, 5.3 \rangle$, respectively in $\Delta c \in \langle 5 \cdot 10^{-2}, 5 \cdot 10^{-5} \rangle$ mol · dm^{-3} linear, while for extreme low values $\Delta pF \in \langle 6.0, 7.3 \rangle$, respectively $\Delta c \in \langle 5 \cdot 10^{-8}, 1 \cdot 10^{-6} \rangle$ mol · dm^{-3} already bends. The value of correlation coefficient reaches r = 0.99 and coefficient of determination R = 98.01 %. It confirms that all calibration data are relevant and quadratic model is confirmed. Sensitivity of method in the interval studied is 80.6–78.4 what means, that linear trend in this interval is valid. Lower limit on calibration function expressed as dependence of E vs pF is $pF_L = 0.51$. This limit represents the highest concentration of F^-. Parameters of calibration function using median values were computed (Fig. 4). Even on the graphical projection relevancy of

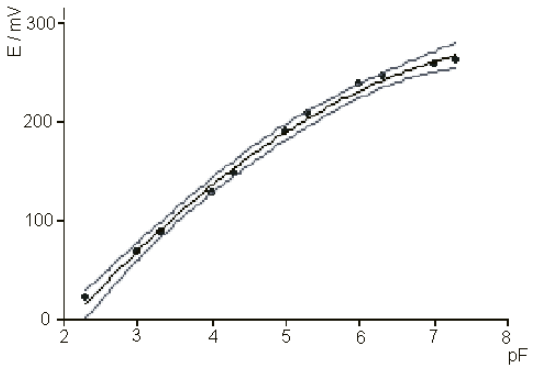

Fig. 3. Calibration line with confidence limits computed basing on calculated arithmetic mean values

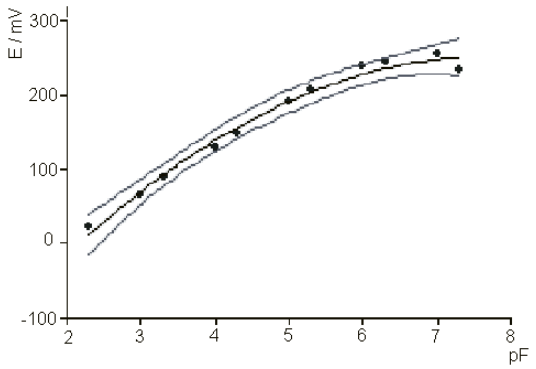

Fig. 4. Calibration line with confidence limits computed basing on calculated median values

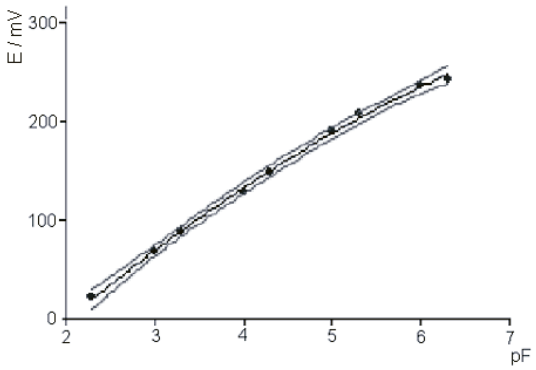

Fig. 5. Calibration line with confidence limits computed from the reduced arithmetic mean values

quadratic calibration model can be seen. The trend of confidence limit values, however, exhibits some decrease in precision level. The obtained limit of highest measurable F^- concentration is also worse as $pF_L = 0.90$. Calibration points fitted calibration line usually up to concentration pF = 6.3. In most cases, the last two points for pF = 7 and pF = 7.3 did not fit the calibration line, therefore were neglected for calibration line construction (Fig. 5). In the case, that measured potential value was in the range below concentration values pF = 6.3, these values were marked as “false detectable” “values under LOD”.

Analysis of environmental samples

Basis for assessment of environment load with gravitation dust sediment is the total amount of gravitation dust sediment. Chemical composition of dust sediment can supply additive information for environment quality evaluation. Results of analysis and correlation treatment of Cu, Cr, Fe, Mn, Ni, Pb, Sn, Ti and V have been already

presented [18, 19], but results concerning fluoride determination and comparison with total gravitation dust sediment were not yet published.

In all cases discussed here, total gravitation dust sediment and fluoride content for rural and municipal sampling place are presented. Two models of evaluation – "long-term" and "short-term" trends have been used. Long-term trend – *ie* change of year average values from 1996 to 2007 for rural sampling place (Fig. 6) and the same dependence for municipal sampling site (Fig. 7) measured in the same time period. Load of gravitation dust sediment expressed in $Mg \cdot kg \cdot km^{-2} \cdot year^{-1}$ unit changes from about 50 to 140 during period studied for rural sampling place and from 1100 to 2000 for municipal sampling sites. In both cases, slight decrease can be observed, at rural sampling sites rather monotonous, but at the municipal sampling sites higher scattering was observed. The reason of gravitation dust sediment decrease can be a result of improving environmental protection of industrial processes and heating technology in

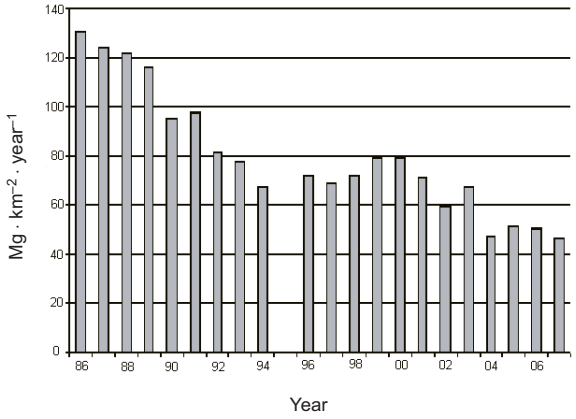

Fig. 6. Column diagram of annual content of gravitation dust sediment in the rural period from 1986 to 2007

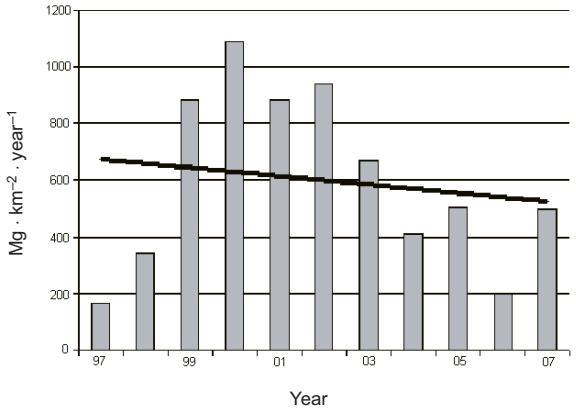

Fig. 7. The same dependence as the previous, but for municipal sampling place. The thick line is the extrapolated dependence of term trend

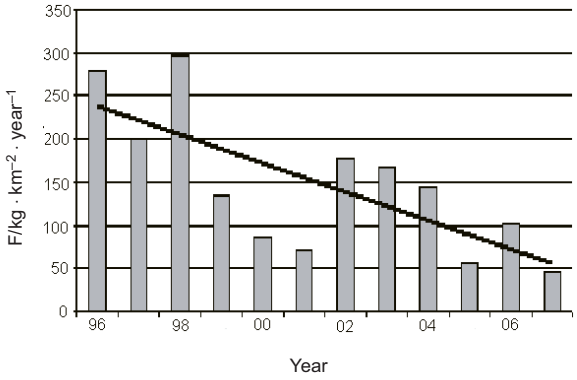

Fig. 8. Change of fluoride content in environmental samples in year period from 1996 to 2007. Rural sampling sites. Fluoride (F) content in [kg km^{-2} year^{-1}]. Time period from 1996 to 2007. The thick line is the extrapolated dependence of fluoride term trend

the region. Short term trend in total gravitation dust amount shows, that values measured in summer are usually higher than those in winter (Fig. 7, 8). This phenomenon is probably due to the heavy municipal traffic in summer time. Results of analyzed trends measured for environmental samples of rural and municipal origin are summarized in Table 2.

Table 2

Summary of the content of gravitation dust sediments and fluoride ions

Total amount of gravitation dust sediment [Mg km^{-2} year^{-1}]		
Rural sampling place		
	Long term trend	Short term trend
Period	1996–2007	1996–2007
Trend	Decrease 80 Mg → 50 Mg	Maximum in months: VI, VII, VIII
Municipal sampling place		
Period	1997–2007	1997–2007
Trend	Decrease 1100 Mg → 500 Mg	Maximum in months: V, VI, VII
Water soluble fluoride content [F/kg km^{-2} year^{-1}]		
Rural sampling place		
	Long term trend	Short term trend
Period	1997–2007	1997–2007
Trend	Decrease 300 kg → 100 kg	No plausible trend
Municipal sampling place		
Period	1997–2007	1997–2007
Trend	Decrease 200 kg → 50 kg	Minimum in months: V, VI, VII

During the years of research only a slight decrease in total amount of gravitation dust sediment at rural sampling sites has been seen. The minimal value is about

50 Mg km^{-2} year^{-1}, maximum measured value is about 130 Mg km^{-2} year^{-1}. Data for 1995 is missing. In the case of municipal sampling sites, the decrease is less significant, but the scattering of data is higher. The values for total gravitation dust sediment are much higher than those for rural sampling sites.

Using direct potentiometric method with ion-selective electrode and calibration procedure mentioned above, environmental samples were analyzed. Validation characteristics of analytical procedure allowed evaluate the "long-term" and "short-term" trends in fluoride content. Two projection models are studied, *ie* dependence of year averages during time from 1993 to 2007, (long-term trend) and change of monthly measured data within a year period (short-term trend). The changes in fluoride content in samples within a year period are presented in Fig. 9. Trends of fluoride content for given sampling sites are presented in Fig. 7. Change in fluoride content during ten-year-time period for municipal samples is presented in Fig. 8. The same dependence was observed for rural samples.

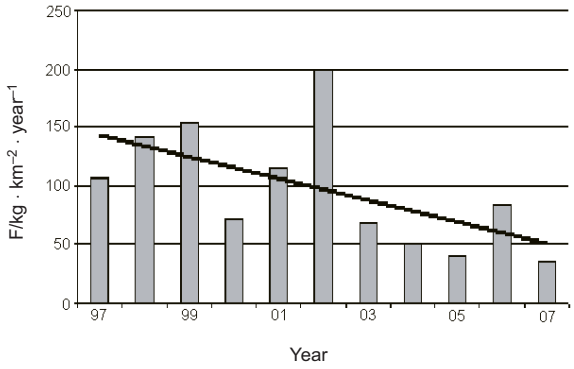

Fig. 9. Change of fluoride content in environmental samples in year period from 1997 to 2007. Municipal sampling sites. Fluoride (F) content in [F/kg km^{-2} year^{-1}]. Time period from 1997 to 2007. The thick line is the extrapolated dependence of term trend

Content of fluoride for two types of sampling sites differs only slightly. The range of maximum and minimum value is from 60 to 250, and from 70 to 160 kg km^{-1} year^{-1}, respectively. Values for rural sampling sites seems to be higher those value for urban sampling sites.

Conclusions

Water soluble part of fluoride content in gravitation dust samples can be determined by ion selective electrodes, using direct potentiometry. Fluoride content of environmental samples is in range from 140 to 50 F/kg km^{-2} year^{-1}, while slight decrease in fluoride content has been observed either in rural or in municipal sampling sites. Content of fluoride changes also within a year, but, there was no correlation between fluoride content and total dust sediment.

The estimated limit of detection for fluoride determination is 10^5g dm^3. Taking into account the sampling procedure, the sample volume, treatment of sample in analysis procedure, this limit can be expressed in units 20 kg km^{-2} year^{-1} That means, that lowest measurable fluoride content is as low as 20 kg km^{-2} year^{-1} the real fluoride content was almost in all cases higher than estimated LOD. Only in 12 cases from 336 measured data the fluoride content could not be measured because being lower than this value. Evaluation of long-term trend leads to the following conclusions. The amount of total gravitation dust sediment is much higher in the municipal samples (Table 2). Water soluble fluoride content in samples decreased in time period studied significantly both in rural samples, as well as in municipal samples. Changes in total dust and Fe content of dust have some similarities, in rural, as well as in municipal samples. In both cases "summer values" and "winter values" can be distinguished, the "summer" values are significantly higher, than "winter" ones. Both, Fe and total dust values are higher for municipal sampling sites than those for rural ones. For fluoride content the urban and rural data are fairly similar. No correlations were found for other elements.

Acknowledgement

The authors wish to thank to the Grant Agency of the Slovak Republic for the financial support of the research project 20-009404 (APVV), Prof. M. Meloun (Technical University Pardubice) for providing program QC-Expert for testing.

References

[1] Matherny M., Balgavá V. and Einax J.: Chem. Pap. (Bratislawa), 1994, **48**, 95–99.
[2] Uhrinova K., Flórián K., Matherny M. and Pliešovská N.: Sborník 21. ročníku Konference "Hutní Analytika" 2001. 2 THETA, Č. Tešín 2001.
[3] Matherny M.: Proc. 6th Conf. Environ. Mineral. Process, Ostrava. VŠB-Ostrava, 2002, 119–126.
[4] Malisa H. and Robinson J.W.: Analysis of Airborne Particles by Physical Methods. CRC Palm Beach, 1979.
[5] Balgavá V. and Matherny M.: J. Radioanal. Nucl. Chem., 1993, **170**, 171–180.
[6] Flórián K. and Pliešovská N.: Acta Chim. Hung., 1980, **103**, 301–310.
[7] Flórián K., Gálová M., Koller L., Krakovská E., Lux L., Matherny M., Nickel H. and Pliešovská N.: Acta Chim. Hung. – Models in Chemistry, 1992, **129**, 611–617.
[8] Lux L., Pliešovská N., Flórián K. and Uhrinová K.: Zborník 2. celoštátnej konferencie "Environmentálne problémy miest" , EXPO-EDUX, Košice 1999.
[9] Lux L., Pliešovská N., Flórián K. and Uhrinová K.: Zborník 4. celoštátnej konferencie "Environmentálne problémy miest" EXPO-EDUX, Košice 2001.
[10] Zákon o ovzduší č. 309/1991 Zb. z. Českej a Slovenskej federatívnej republiky, Praha 1991.
[11] Opatrenie Vlády SSR č. 8/1981, Vestník MZ SSR, Bratislava.
[12] Lux L., Stašková R. and Gálová M.: ACH – Models in chemistry, 1996, **133**(1–2), 115–127.
[13] De Marco R., Clarke G. and Pejcic B.: Electroanalysis, 2007, **19**, 1987–2001.
[14] VDI, Handbuch Reinhaltung der Luft. VDI Komission Reinhaltung der Luft, Blatt 2, Stutgart 1972.
[15] Kupka K.: QC.Expert™. Statistical softwarwe. TriloByte, Pardubice 2002.
[16] Meloun M., Militký J. and Forina M.: Chemometrics for analytical chemistry. Ellis Horwood, New York 1994.
[17] Uhrinová K., Flórián K. and Matherny M.: Chem Pap. (Bratislava), 2005, **59**, 230–234.
[18] Uhrínová K., Pliešovská N., Lux L., Flórián K. and Matherny M.: Proc. 4-th Int. Conference on Carpathian Euroregion Ecology, CERECO 2003, Miskolc-Tapolca, Hungary.
[19] Simeonova P., Simeonov V., Lux L., Dakova I. and Spanos T.: Ecol. Chem. Eng. 2005, **12**(7), 727–737.

OZNACZANIE ROZPUSZCZALNYCH W WODZIE FLUORKÓW W PRÓBKACH PYŁU ZAWIESZONEGO

Abstrakt: Określono całkowitą ilość i skład chemiczny grawitacyjnego opadu pyłu na osiedlu mieszkaniowym w aglomeracji regionu Koszyce, wschodnia Słowacja. Próbki pobierano z dwóch rodzajów powierzchni – typu wiejskiego i miejskiego. Próbki pobierano w regularnych odstępach czasu raz w miesiącu, w latach od 1996 do 2007 r. Na podstawie uzyskanych danych dokonano oceny trendów zmian rozpatrywanych parametrów. Badano stężenie rozpuszczalnych w wodzie fluorków, pH i parametry sumy grawitacyjnego opadu pyłu. Do oznaczenia fluoru zastosowano bezpośrednią metodę potencjometryczną z wykorzystaniem jonoselektywnej elektrody ISE. Do kalibracji wykorzystano wielomian 2 stopnia. Walidacji metody dokonano na podstawie następujących parametrów statystycznych: rzetelności, precyzji i powtarzalności. Na podstawie zebranych danych dokonano oceny trendów długo- i krótkoterminowych.

Słowa kluczowe: środowisko, grawitacyjny opad pyłu, walidacja analizy, zanieczyszczenie powietrza

ECOLOGICAL CHEMISTRY AND ENGINEERING A

Vol. 16, No. 11 2009

Henryk MATUSIEWICZ[1*] and Mariusz ŚLACHCIŃSKI[1]

INTERFACING MICROCHIP BASED CAPILLARY ELECTROPHORESIS SYSTEM WITH A MICROWAVE INDUCED PLASMA OPTICAL EMISSION SPECTROMETER (μCE-MIP-OES)

TECHNIKA SPRZĘŻONA W UKŁADZIE MIKROCHIP – ELEKTROFOREZA KAPILARNA W OPTYCZNEJ SPEKTROMETRII EMISYJNEJ PLAZMY MIKROFALOWEJ

Abstract: A microchip based capillary electrophoresis (μCE) system was interfaced with microwave induced plasma optical emission spectrometry (MIP-OES) to provide rapid elemental separation capabilities. This system uses an extremely low flow micro-cross-flow nebulizer sited directly at the liquid exit of the chip. A supplementary flow of buffer solution at the channel exit was used to improve nebulization efficiency. A small evaporation chamber has been incorporated into the interface in order to prevent the losses associated with traditional spray chambers, allowing the entire sample aerosol to enter the plasma. Syringe pumps were used to manipulate the flow rate and flow direction of the sample, buffer, and supplementary buffer solution. Sample volumes of 40 nanolitre can be analyzed. The feasibility of this hyphenated method for elemental separation was demonstrated by the on-line electrophoretic separation of Ba^{2+} and Mg^{2+} ions within 35 s using an 8 cm long separation channel etched in a glass base. Resolution of the Ba^{2+} and Mg^{2+} peaks was 0.9 using the chip-based μCE-MIP-OES system.

Keywords: microwave induced plasma, optical emission spectrometer, capillary electrophoresis, interface, chip technology

The microwave induced plasma (MIP) is a small low power plasma that has excellent high excitation efficiency for metal and non-metal elements [1]. The technique of MIP optical emission spectrometry (OES) would be excellent for the separation of elements, however due to the small size and low thermal temperature of the plasma (compared with its high excitation capability) it cannot be easily interfaced to liquid separation techniques such as high-performance liquid chromatography (HPLC) or capillary electrophoresis (CE). This problem could be overcome by using lab on a chip

[1] Department of Analytical Chemistry, Poznan University of Technology, ul. Piotrowo 3, 60–965 Poznań, Poland, phone 61 665 23 12, fax 61 665 25 71, email: Henryk.Matusiewicz@put.poznan.pl

technology for the separation as this provides rapid separation with nanolitre volumes of liquid. Laboratory on a chip devices provide an excellent opportunity for rapid on-chip pretreatment of samples, separation for speciation studies and the analysis of very small sample volumes..

The coupling of CE with analytical atomic spectrometry provides a very sensitive, element specific detection method in conjunction with high separation efficiency [2]. However, interfacing this technique remains challenging, primarily due to the flow incompability. Microfabricated analytical system using electrophoresis as a separation mechanism have been shown to reduce drastically separation times and to simplify instrumental design. Another advantage of microchip technology is that pre-etched channel networks can be used to provide several flow streams, omitting tube connectors and thus reducing dead volumes. In most microchip CE (μCE) systems, sample injection is achieved by the electrokinetic method [3]. Song et al [4,5] reported elemental speciation using μCE which was successfully interfaced with inductively coupled plasma mass spectrometry (ICP-MS) via a commercial low flow micro-nebulizer and miniaturized spray chamber. Hui et al [6] were the first to report on chip nebulizer. A chip based electrophoresis system was interfaced to ICP-OES by means of a cross-flow nebulizer.

This paper describes, for the first time, how a microchip based electrophoresis system was interfaced to an MIP-OES, incorporating a simplified small spray chamber in order to approach 100 % analyte transport efficiency. The sample and buffer solution were introduced into the separation channel of μCE chip by hydrodynamic injection with a microsyringe pumps. A voltage applied along the length of the channel separated the ions of interest, but a hydrodynamic flow was also used to shorten the overall analysis time. Barium and magnesium were used as test elements because of the strong emission of the elements in the MIP and similar ion mobilities of the ions. The analytical performance of the chip-based μCE-MIP set up was examined.

Materials and methods

An Echelle grating optical emission spectrometer (PLASMAQUANT 100, Carl Zeiss, Jena, Germany) using fibre-optical light-guides and photomultiplier tubes (PMT) and TE_{101} microwave plasma cavity assembly was used, and was essentially the same as previously described [7]. Instrument settings and operational parameters used for the experimental MIP-OES system are summarized in Table 1.

The MIP resonant cavity as an excitation source, specified previously [7], was used. The plasma is viewed axially with the axis of the plasma perpendicular to the plane of the entrance slit. Since the plasma torch, cavity, generator and gas flow have been described in detail in a previous paper [7], they will not be discussed again here, but briefly summarized only. The microwave generator is connected by means of a flexible cable to the rectangular resonant cavity of the TE_{101} design. The torch is a quartz capillary made of Suprasil (Heraeus, Hanau, Germany). Table 1 lists the MIP apparatus specifications and operating conditions for the generation of plasma.

Table 1

Instrumental parameters for the μCE-MIP-OES system

Mounting	Czerny-Turner in tetrahedral set-up
Focal length, mm	500
Spectral range, nm	193–852
Order lines	28^{th}–123^{rd}
Microwave frequency, MHz	2450
Microwave power, W	160
Microwave cavity	TE_{101} rectangular, water cooled
Microwave generator	700 W, MPC-01 (Plazmatronika Ltd., Wroclaw, Poland)
Plasma viewing mode	Axial
Plasma torch, axial position	Quartz tube, 3.0 mm i.d., air cooled
Argon flow rate, $cm^3\ min^{-1}$	700
Plasma supporting helium flow rate, $cm^3\ min^{-1}$	160
Plasma form	Annular
Supplementary buffer flow rate, $mm^3\ min^{-1}$	20
CE potential, kV	5
Read	On-peak
Integration time/s	0.1
Background correction	Fixed point
Determination	Simultaneous
Wavelength, nm (line type)	Ba 455.403 (II); Mg 285.213 (I)

Experiments were carried out on a laboratory-built μCE system (the detailed fabrication method has been reported previously [8]), which was composed of a 0–30 kV high voltage power supply (HVPS Spelman, Spisska Nova Ves, Slovakia) and two microsyringe pumps (Ascor, Warsaw, Poland) which were capable of providing 0.4–100 $mm^3\ min^{-1}$. These overcome the pulsation introduced through the use of peristaltic pumps at low flow rates. The microchip used in this μCE-MIP-OES system consisted of two (30 × 25 × 3 mm) glass plates. The design of the microchip, with the channel layout, is shown in Fig. 1 [4]. The gas flow rate was controlled by means of a mass flow controller (DHN, Warsaw, Poland). An external argon source was needed

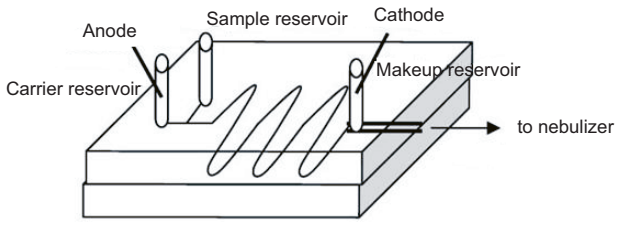

Fig. 1. Schematic diagram of the microfluidic chip

for the nebulization, as the MIP-OES is not able to provide the pressure required by this interface.

The microchip was interfaced to the MIP-OES via a commercially available, low flow rate concentric nebulizer (Micromist, Glass Expansion, Switzerland), as shown in Fig. 2 [4]. The uptake flow rate of the nebulizer was about 20 mm^3 min^{-1}. A miniature evaporation tube-shaped spray chamber (Model QuDIN, Epond, Vevey, Switzerland) fitted directly with the quartz plasma torch was used to obtain high sample introduction efficiency with the low flow rate nebulizer. The experimental conditions of the chip-based μCE system are summarized in Table 1. The instrument could be run in either a continuous flow mode to give a quick assessment of the instrument stability and the μCE separation or in time resolved acquisition mode for quantification of the peak areas.

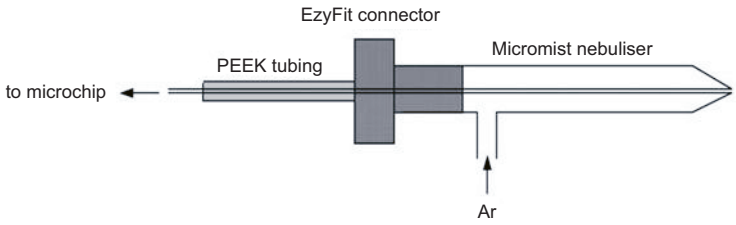

Fig. 2. Schematic diagram of the interface

A schematic diagram of the entire experimental sample introduction system set-up (μCE-MIP-OES) is shown in Fig. 3.

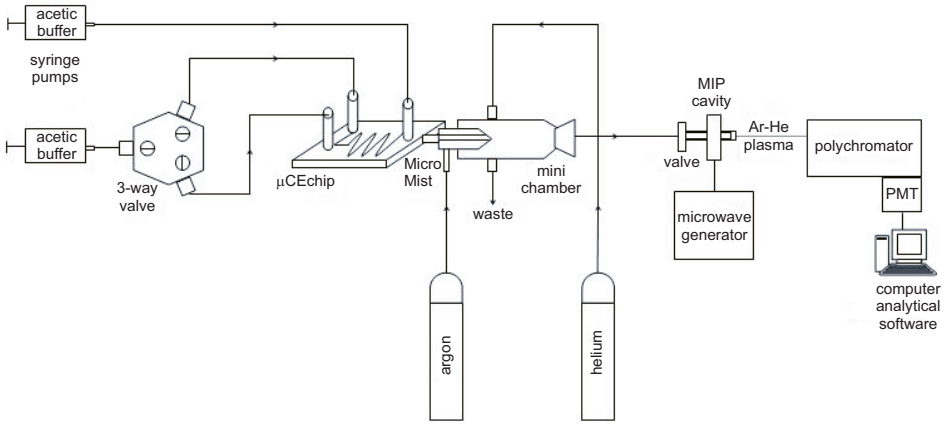

Fig. 3. Component diagram of the elaborated microchip based μCE-MIP-OES system (not to scale)

Sodium acetate buffer (60 mM) was prepared from sodium acetate for electrophoresis (≥ 99 % , Sigma-Aldrich Chemie, Steinheim, Germany) in doubly distilled water. The pH of the buffer was adjusted to 4.2 with acetic acid ((≥ 99 %,

Sigma-Aldrich Chemie, Steinheim, Germany). Stock solutions of 5000 mg dm^{-3} of Ba and Mg were prepared from barium di(acetate) and magnesium di(acetate) tetrahydrate ((≥ 99 %, Sigma-Aldrich Chemie, Steinheim, Germany) in doubly distilled water. The pH of the prepared stock solution was 6.0. The stock solution was mixed and diluted to the appropriate concentration with doubly distilled water immediately before use. The pH of the diluted solution was approximately 6.

Water was initially deionized (Model DEMIWA 5 ROSA, Watek, Czech Republic) and then doubly distilled in a quartz apparatus (Heraeus Bi18, Hanau, Germany).

Results and discussion

One of the problem with previous design of microchip sample introduction system for plasma spectrometry has been the low transport efficiency of the sample into the plasma [6]. In the experiments, a bulb-shaped spray chamber of relatively large volume was used. The large chamber may broaden the CE peak. Since the liquid flow rate in the chip is very low it should be possible to achieve 100 % transport of the sample out of the end of the chip to the microwave plasma. In order to achieve this a small cylindrical spray chamber of the volume of 10 cm^3 was used in the following study.

The optimization of wavelength was not carried out because the wavelengths used for the determination were pre-selected by the producer of the polychromator.

Preliminary analytical performance of the Ar/He-MIP was examined by measuring the S/B ratio of selected elements. However, substantial optimization of the gases parameters for the analytes was not undertaken, as this information was readily available from the literature on excitation and ionization conditions for MIP-OES with pneumatic nebulization [9] (and references cited therein). The comparison of these parameters obtained for mixed plasma with those presented for pure argon plasma and helium plasma with pneumatic nebulization shows that a mixed plasma allowed to achieve better detection limits than pure plasma gases. In addition, the mixed Ar + 20 % He MIP exhibits higher tolerance to water loading. As a result of the consideration on the above influences, an Ar/He-MIP was selected for all the subsequent experiments, for a plasma gas composition of ca 80 % Ar and 20 % He; this is in agreement with results presented earlier [9].

Two different types of experimental variables affect the method. These are as follows: first, variables controlling the emission response in the microwave plasma, that is, the microwave forward power of the microwave generator. Second, variables such as the argon carrier flow and sample uptake rate that regulate sample transport. Univariate optimization was used to establish the optimum experimental parameters. The parameters optimized are listed in Table 1.

The MIP is normally operated at low power levels in the range of 50–150 W. In this work, the stable Ar/He plasma could be maintained at a level of greater than 100 W forward power. Between 100 and 200 W, neither the intensities of spectral lines nor the S/B ratios showed such a dependence on the power that this would point to a pronounced optimum. In addition, the stability of the background and line signals did not significantly vary with power in the above-mentioned range. In general, for two

analytical lines of studied elements, S/B ratios usually tend to level off after the microwave power approaching 160 W (Fig. 4a). The intensities of spectral lines also level, but more slowly. As a result of this consideration on the above influences, an optimized power of 160 W was selected as an acceptable value and a practical working range.

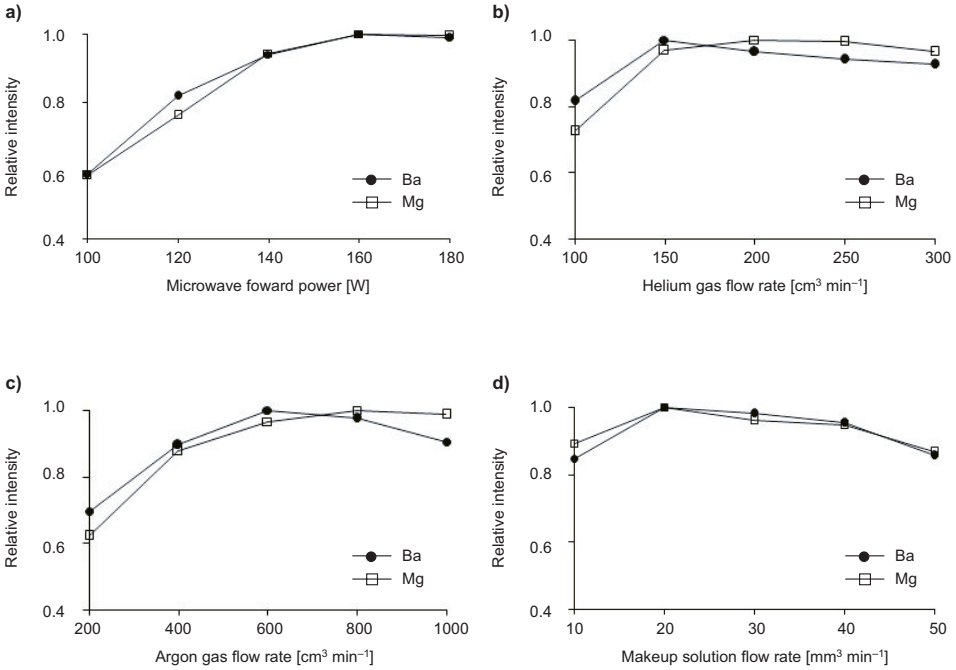

Fig. 4. Effect of the variables on the element's normalized emission intensity for microchip based μCE-MIP-OES system. Influence of (a) microwave forward power; (b) helium gas flow rate; (c) argon gas flow rate; (d) makeup solution flow rate on the emission intensity of the elements for continuous injection of 100 μg dm^{-3} Ba^{2+} and Mg^{2+} through makeup reservoir without application of voltage

The effect of plasma (support) helium gas flow rate was optimized in our experiments and was selected based upon previous experience and maintaining the plasma stability and plasma shape. Stable operation of the plasma was obtained at gas flow rates of 160 cm^3 min^{-1} (Fig. 4b).

It was also observed that the carrier Ar gas stream flow rate has a more significant influence on the emission intensities than the plasma support gas flow rate. The carrier Ar gas affects the formation of the plasma channel (an annular configuration) [10], the residence time of the analyte in the plasma, and the aerosol generation and transport efficiency [11]. To optimize the carrier (nebulizing) argon gas flow for multielement determination, the optimum flow for two elements was estimated in the total range of 200–1000 cm^3 min^{-1}. It was observed that the carrier argon stream flow rate has a significant influence on the emission intensities and thus proved to be a critical

parameter. In general, it was observed that when the flow rate was ranged between 200 and 1000 cm^3 min^{-1}, the emission intensities reached maximum at 700 cm^3 min^{-1}, and with further increase of the flow rate above these values, the emission intensities decreased for two elements (Fig. 4c). The maxima are the result of opposite effects of nebulizing gas flow on aerosol characteristics and transport and interaction of aerosol with the plasma. Increasing the nebulizing gas flow rate commonly causes a shift of both primary and tertiary drop size distributions to smaller droplet sizes. This in turn leads directly to higher analyte and solvent transport rates. However, these two transport rates exert opposite trends on net signal intensity. In addition, the higher the nebulizing-carrier gas flow, the smaller the residence time of droplets in the plasma. Therefore, the overall effect is shown as a maximum behaviour. Therefore, in this study, a 700 cm^3 min^{-1} carrier argon flow rate was chosen.

The makeup solution (buffer solution) also proved to be important for this work. When the sample pumping rate was greater than approximately 20 mm^3 min^{-1}, it was found that the signal intensities would not increase further and began to decrease (Fig. 4d). For pneumatic nebulization, the higher the liquid flow, the primary drop size distribution is shifted to bigger drop sizes. Nevertheless, the absolute amount of aerosol volume contained in smaller drop size is increased. Therefore, the higher the liquid flow, the higher the analyte and solvent transport rates, that finally show a behaviour of maximum on signal vs liquid flow. Therefore, a sample uptake rate of 20 mm^3 min^{-1} was chosen.

The analytical performance of the μCE-MIP-OES system is characterized by electrophoretic separation of a mixture of 1000 μg cm^{-3} each of Ba^{2+} and Mg^{2+}. The ion mobilities of Ba^{2+} and Mg^{2+} are similar and the ions carry the same charge. The degree of separation of the ions is an indicator of the resolving power of the μCE-ICP-OES system. Fig. 5 shows the electrophorogram of the Ba^{2+}/Mg^{2+} mixture. As can be seen in Fig. 5, the two ions are clearly beginning to separate on application of 5 000 V, and the separation was completed within 30 s. The migration times of Ba^{2+} and Mg^{2+} ions were

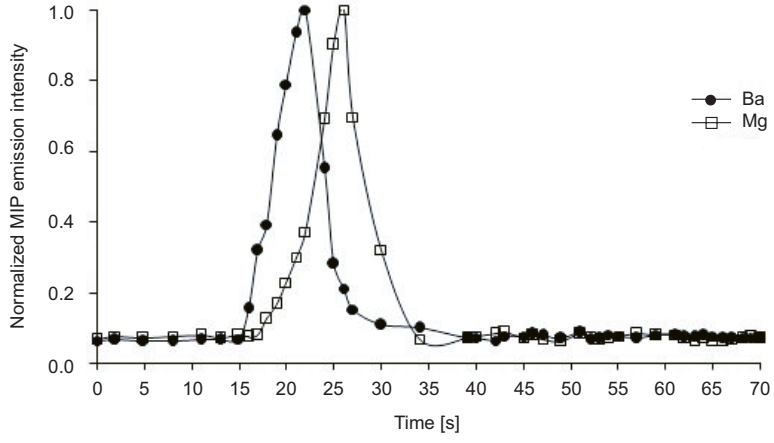

Fig. 5. Separation of Ba^{2+} and Mg^{2+} in a microchip based μCE-MIP-OES system. CE potential was 5 kV

22 s and 26 s, respectively. The half-intensity widths of the peaks were 3.7 s and 4.0 s, respectively. The resolution of the elution peaks was approximately 0.9.

Conclusions

A simple interface for chip-based μCE-MIP has been developed. The micro-concentric nebulizer converted the μCE effluent into fine aerosol for transport to the MIP. The small dimensions made it possible to place the entire device in the vicinity of the micronebulizer inlet and the makeup solution can therefore be introduced very near to the outlet of the separation channel. Sample and buffer solution flows in the μCE chip were manipulated using a pair of syringe pumps for flexible of solution flow rate and flow direction control. An evaporation tube-shaped spray chamber was used in order to facilitate the transport of the entire primary aerosol into the microwave plasma. At the moment the microchip system requires manual filling with background buffer and sample. Rapid CE separation of ions of the same charge and similar ionic mobility was demonstrated using Ba^{2+} and Mg^{2+} ions.

Acknowledgements

Financial support by the Committee of Scientific Research, Poland (Grant No. N N204 130935) is gratefully acknowledged.

References

[1] Skogerboe R.K. and Coleman G.N.: Anal. Chem. 1976, **48**, 611A.
[2] Maning C.A. and Kennedy R.T.: Anal. Chem. 1994, **66**, 280R.
[3] Zhang C. and Manz A.: Anal. Chem. 2001, **73**, 2656–2662.
[4] Song Q.J., Greenway G.M. and McCreedy T.: J. Anal. At. Spectrom. 2003, **18**, 1–3.
[5] Song Q.J., Greenway G.M. and McCreedy T.: J. Anal. At. Spectrom. 2004, **19**, 883–887.
[6] Hui A.Y.N., Wang G., Lin B. and Chan W.-T.: J. Anal. At. Spectrom. 2006, **21**, 134–140.
[7] Matusiewicz H.: Spectrochim. Acta, Part B 1992, **47**, 1221–1236.
[8] McCreedy T.: Anal. Chim. Acta 2001, **427**, 39–43.
[9] Jankowski K. and Jackowska A.: J. Anal. At. Spectrom. 2007, **22**, 1076–1082.
[10] Matusiewicz H. and Golik B.: Microchem. J. 2004, **76**, 23–29.
[11] Browner R.F., Canals A. and Hernandis V.: Spectrochim. Acta Part B 1992, **47**, 659–668.

TECHNIKA SPRZĘŻONA W UKŁADZIE MIKROCHIP – ELEKTROFOREZA KAPILARNA W OPTYCZNEJ SPEKTROMETRII EMISYJNEJ

Zakład Chemii Analitycznej
Politechnika Poznańska

Abstrakt: Opisano metodę rozdziału jonów Ba^{2+} od Mg^{2+} za pomocą mikrosystemu elektroforetycznego (μCE) w połączeniu z optyczną spektrometrią emisyjną (OES) plazmy indukowanej mikrofalowo (MIP). Roztwór próbki (ok. 40 nanolitrów) oraz roztwory buforowe wprowadzano do kanału separacyjnego o długości 8 cm za pomocą pomp strzykawkowych. Zaproponowany system umożliwia rozdział badanych jonów w ciągu 35 s oraz efektywne wprowadzenie próbki, w postaci aerozolu, do źródła wzbudzenia za pomocą układu mikrorozpylacz/minikomora mgielna.

Słowa kluczowe: plazma mikrofalowa, optyczna spektrometria emisyjna, elektroforeza kapilarna, aparatura, technologia chipowa

ECOLOGICAL CHEMISTRY AND ENGINEERING A

Vol. 16, No. 11 2009

Zenon SARBAK[1]

INFLUENCE OF MANGANESE AND MANGANESE-COPPER CATALYSTS SYNTHESIS ON DECOMPOSITION OF HYDROGEN PEROXIDE AND PHENOL OXIDATION

WPŁYW METOD SYNTEZY KATALIZATORÓW MANGANOWYCH I MANGANOWO-MIEDZIOWYCH NA ROZKŁAD NADTLENKU WODORU I UTLENIANIE FENOLU

Abstract: Characterisation of performance of manganese and manganese-copper oxide catalysts obtained by different methods of synthesis is presented. The specific surface area and catalytic activity were determined in decomposition of hydrogen peroxide and phenol oxidation. The catalytic performance of the catalysts studied was different in the two reactions.

Keywords: catalyst synthesis, hydrogen peroxide decomposition, phenol oxidation

Effective removal of organic compounds from industrial waste is still an important problem from the point of view of the environment protection. Catalytic oxidation of organic compounds in water solutions requires proper catalysts and oxidising agents. Usually the oxidising agents of organic compounds are molecular oxygen, ozone or hydrogen peroxide. The most often used catalysts are those that can be active at mild temperature and under atmospheric pressure. The catalysts used should decompose organic compounds to carbon dioxide and water or other environmentally friendly products. Moreover, the catalysts used in water solutions should have hydrophobic surface. Usually they are oxides of ignoble metals [1]. In the earlier published paper [2] the types of catalysts used in phenol oxidation were listed. The problems related to removal of phenol has been recently discussed in [3, 4]. Phenol is one of the organic compounds usually present in the industrial organic waste that are harmful to people and animals, in particular to microorganisms. This compound disturbs the processes of

[1] Laboratory of Adsorption and Catalysis, Faculty of Chemistry, Adam Mickiewicz University, ul. Grunwaldzka 6, 60–780 Poznań, Poland, email: sarbak@amu.edu.pl

self-purification of water and in concentrations high enough it totally inhibits photo-synthesis [1].

In our study phenol was removed from water environment by catalytic oxidation with hydrogen peroxide. The catalysts were synthetic oxides of manganese and manganese--copper obtained by four synthetic pathways: as a result of Mn^{2+} ions oxidation with $KMnO_4$ or by oxidation with $(NH_4)_2S_2O_8$, by reduction of Mn^{7+} ions with hydrochloric acid and by thermal decomposition of nitrates(V).

Experimental

Synthesis of the catalysts

Synthesis of the manganese and manganese-copper catalysts was performed along the four pathways described below.

Series I. Sample **1** was obtained by oxidation of Mn^{2+} ions by $KMnO_4$. Boiling solutions of $KMnO_4$ and $Mn(NO_3)_2$ were mixed and the mixture was maintained at boiling for 15 minutes. Sample **2** was obtained by oxidation of Mn^{2+} ions in the presence of Cu^{2+} by $KMnO_4$. Crystalline $KMnO_4$ was added to a mixture of $Mn(NO_3)_2$ and $Cu(NO_3)_2$ solutions at the molar ratio of 2:3; the mixture was kept at 95 ^oC for 15 minutes. Sample **3** was obtained by addition of a mixture of $Mn(NO_3)_2$ and $Cu(NO_3)_2$ solutions at the molar ratio 2:3 to a solution of $KMnO_4$, the mixture was kept at 95 ^oC for 15 minutes. Sample **4** was obtained by addition of a mixture of $Mn(NO_3)_2$ and $Cu(OH)_2$ solutions at the molar ratio 2:3 to a solution of $KMnO_4$; the mixture was kept at 95 ^oC for 15 minutes.

Series II. Sample **5** was obtained by reduction of Mn^{7+} ions by hydrochloric acid. To a solution of $KMnO_4$ heated to 80 ^oC, small portions of chloric acid were added (1:1). The addition was stopped when liberation of chlorine was no longer observed. Sample **6** was obtained as above, but later the mixture was washed with nitric(V) acid at 90 ^oC for two hours. Sample **7** was obtained as above, but in the presence of $KMnO_4$ solution, $Cu(OH)_2$ was precipitated and then the mixture was heated to 80 ^oC and small portions of hydrochloric acid (1:1). were added to it. After elimination of chlorine, washing and drying, the sample was washed with 3 M HNO_3 at 90 ^oC for 2 hours.

Series III. Sample **8** was obtained by oxidation of Mn^{2+} ions by $(NH_4)_2S_2O_8$. A solution of $MnSO_4$ was heated to 90 ^oC and a solution of $(NH_4)_2S_2O_8$ in 2M H_2SO_4 was dropwise added to the former one; the reaction lasted for 1 hour. Sample **9** was obtained by oxidation of Mn^{2+} ions by $(NH_4)_2S_2O_8$, after precipitation of $Cu(OH)_2$ in the presence of oxidised sample. A mixture of $MnSO_4$ and $Cu(OH)_2$ solutions was heated to 90 ^oC and to it small portions of $(NH_4)_2S_2O_8$ in 2M H_2SO_4 were added; the reaction lasted for 1 hour. Samples **1–9** were filtered off, washed with water to pH = 7 and full decolouration. The precipitates were dried at 120 ^oC for 8 hours. $Cu(OH)_2$ was precipitated with a solution of NH_4OH (1:3) from a water solution of $Cu(NO_3)_2$ at pH = 7.

Series IV. Sample **10** was obtained by thermal decomposition of fine powdered $Mn(NO_3)_2$ at 150 ^oC for 8 hours in the air atmosphere flown at the rate 30 cm^3/min. Sample **11** was obtained by thermal decomposition of powdered mixture of $Mn(NO_3)_2$ and $Cu(NO_3)_2$ (1:1) in the conditions described above.

Catalytic decomposition of H_2O_2

Catalytic decomposition of hydrogen peroxide was performed according to the procedure described in [2].

Catalytic decomposition of phenol

Catalytic oxidation of phenol of the initial concentration of 2500 ppm was performed with the use of H_2O_2, according to the procedure described in [2].

Results and discussion

The performance of oxide catalysts with manganese ions or manganese and copper ions, obtained in different procedures, was studied in the reactions of decomposition of hydrogen peroxide and phenol.

Table 1 presents the labelling of samples and their specific surface area values. The surface areas of samples **1**, **5**, **6**, **8** from among the samples containing only Mn ions, are 44, 54, 59 and 252 m^2/g, respectively. Sample **10** obtained as a result of thermal decomposition of $Mn(NO_3)_2$ has very small specific surface area of 2 m^2/g.

Table 1

Sample labelling and their textural characterisation

Samples	Labelling	Type of oxide preparation	Specific surface area BET [m^2/g]
Series I Oxidation of Mn^{2+} by $KMnO_4$	**1** **2** **3** **4**	Mn Cu-Mn Cu-Mn Cu-Mn	44 38 118 84
Series II Reduction of $Mn^{7+}$by HCl	**5** **6** **7**	Mn Mn Cu-Mn	54 252 70
Series III Oxidation of Mn^{2+} by $(NH_4)_2S_2O_8$	**8** **9**	Mn Cu-Mn	59 92
Series IV Thermal decomposition	**10** **11**	Mn Cu-Mn	2 30

According to decreasing values of the specific surface areas, the manganese oxide catalysts can be ordered as

$$\mathbf{6 >> 8 \approx 5 > 1 >> 10}.$$

The most effective procedure giving the manganese oxide samples of the largest surface area was the reduction of $KMnO_4$ by hydrochloric acid (1:1) at 80 ^oC followed by leaching with 3 M nitric(V) acid at 90 ^oC.

From among the samples obtained by oxidation of $Mn(NO_3)_2$, (series **I**) sample **3** has a large specific surface area of 118 m^2/g, while sample **2** has the specific surface area over three times smaller. Sample **3** was obtained by oxidation of a mixture of water solutions of manganese(II) and copper(II) nitrates(V) by $KMnO_4$, while sample **2** by oxidation of a mixture of manganese(II) and copper(II) nitrates(V) with crystalline $KMnO_4$ added upon boiling. Sample **4 (**obtained by oxidation of a mixture of $Mn(NO_3)_2$ and $Cu(OH)_2$ by $KMnO_4$ solution) has large specific surface area although by 30 % smaller than that of sample **3**.

From among the samples from series **II**, sample **7**, containing Mn and Cu ions, has the specific surface area over 3.5 times smaller than sample **6** containing only Mn ions.

From among the series **III** samples, sample **9** (obtained by oxidation of Mn ions in the presence of Cu ions by $(NH_4)_2S_2O_8$) has relatively large specific surface area but still over 20 % smaller than that of sample **3**.

From among series **IV** samples, sample **11**, obtained by thermal decomposition of a mixture of manganese(II) and copper(II) nitrates(V), has the smallest specific surface area of all samples considered. According to decreasing specific surface area, samples containing manganese and copper ions can be ordered as

$$\mathbf{3 > 9 > 4 > 7 >> 2 \approx 11}.$$

The above-discussed results prove that the reaction conditions and procedure influence the size of the specific surface area of the samples. The manganese-copper sample of the largest specific surface area was obtained by using a mixture of water solutions of manganese(II) and copper(II) nitrates(V) and $KMnO_4$ in solution. The manganese-copper sample of the smallest specific surface area was that obtained by thermal decomposition of a mixture of powdered manganese(II) and copper(II) nitrates(V).

Catalytic decomposition of hydrogen peroxide is characterised by the kinetic curves presented in Fig. 1. For the series of manganese catalysts their activity measured by the amount of liberated oxygen decreases as:

$$\mathbf{1 \approx 6 \approx 5 > 8 >> 10}.$$

The activities of samples **1, 5** and **6** were relatively high and similar, while that of sample **19** was the least active. The activity of sample **8** was relatively high, but lower than the activities of the manganese catalysts from series **I** and **II**. As follows from the results the catalytic activity of manganese catalysts in decomposition of H_2O_2 does not depend on the surface area because the activity of sample **6** of very large surface area was similar to those of samples **1** and **5,** whose surface areas were 5–6 times smaller.

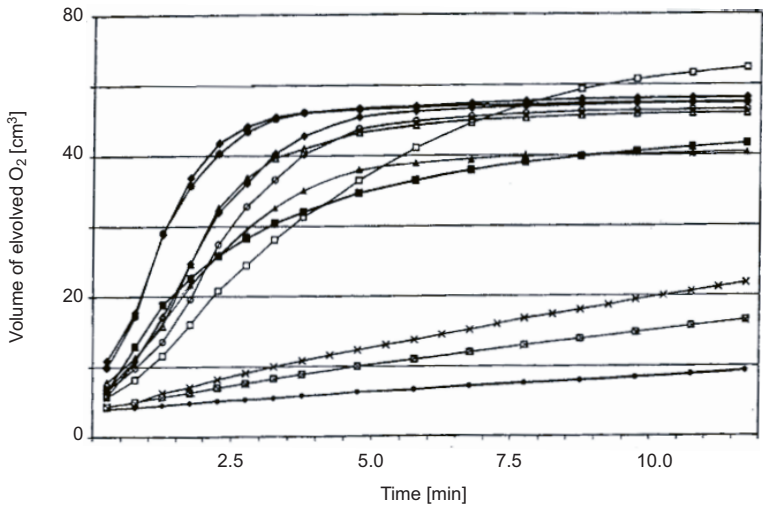

Fig. 1. Kinetic curves of catalytic decomposition of hydrogen peroxide: sample **1** – ◆, sample **2** – □, sample **3** – ▲, sample **4** – ×, sample **5** – Δ, sample **6** – ●, sample **7** – ◇, sample **8** – ■, sample **9** – ○, sample **10** – •, sample **11** – □

All manganese-copper catalysts, except for samples **4** and **11**, show high activity in H_2O_2 decomposition. The highest was the activity of sample **2**, according to decreasing activity in this reaction the manganese-copper catalysts can be ordered as:

$$\mathbf{2 > 7 \approx 9 > 3 >> 4 > 11}.$$

The catalytic activity of these catalysts in decomposition of H_2O_2 does not depend on their surface area. The catalyst of relatively small surface area (sample **2**) proved much more active than the catalyst of 3 times greater surface area (sample **3**). Moreover, the activity of the catalysts studied in this reaction was found practically independent of the method of the catalyst synthesis. It was shown that replacement of $Cu(NO_3)_2$ by $Cu(OH)_2$ (samples **4** and **9**) in the synthetic procedure gave catalysts of different activity. Sample **11** obtained by thermal decomposition of powdered mixture of $Mn(NO_3)_2$ and $Cu(NO_3)_2$ (1:1) is the least active in H_2O_2 decomposition, similarly as the manganese catalyst – sample **10** – obtained by thermal decomposition of fine powdered $Mn(NO_3)_2$.

The performance of the catalysts studied in phenol oxidation is completely different. Fig. 2 presents the kinetic curves obtained for the catalysts in phenol oxidation. According to decreasing activity after 4 hours of the reaction, the catalysts can be ordered as:

$$\mathbf{6 > 10 > 8 > 5 > 1}.$$

The most active is sample **6** obtained by reduction of Mn^{7+} ions and having the largest surface area. The next in the sequence is sample **10** of the smallest surface area,

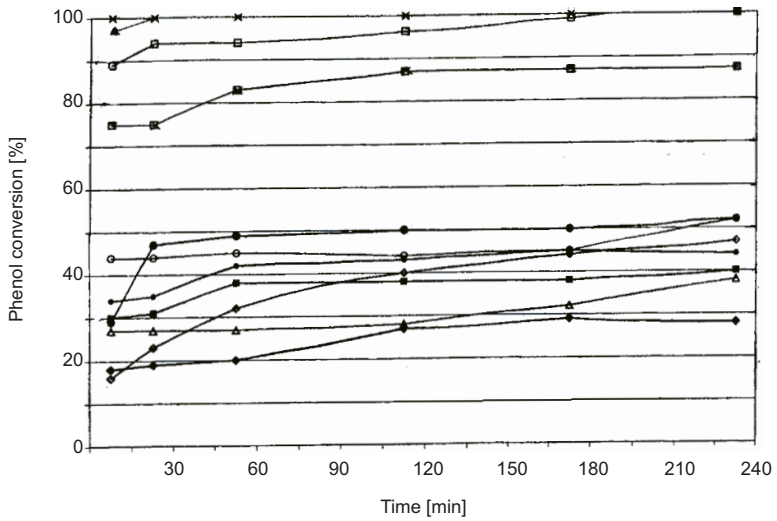

Fig. 2. Kinetic curves of catalytic oxidation of phenol: sample **1** – ◆, sample **2** – □, sample **3** – ▲, sample **4** – ×, sample **5** – Δ, sample **6** – ●, sample **7** – ◇, sample **8** – ■, sample **9** – O, sample **10** – •, sample **11** – □

obtained by thermal decomposition of fine powdered $Mn(NO_3)_2$. Samples **8**, **5**, **1** have the surface areas in the range 44–59 m^2/g, and their ability to phenol oxidation is lower than that of sample **10** of the specific surface area of 2 m^2/g. No correlation between the sample activity and specific surface area was found. The results obtained for samples **5** and **6** show that the reduction of Mn^{7+} ions by hydrochloric acid is insufficient to give an active catalyst, the activity considerably increases after washing with nitric acid.

According to decreasing activity in phenol oxidation the manganese-copper catalysts are ordered as:

$$\mathbf{3 = 4 \geq 11 > 2 >> 9 > 7}.$$

Series **I** samples obtained by oxidation of Mn^{2+} by $KMnO_4$ show high activity in this reaction. The low activity of sample **2** from series **I** can be explained by lower reactivity of $KMnO_4$ in the crystalline form than that in the form of solution (samples **3** and **4**). Surprisingly high was the activity of sample **11** obtained by thermal decomposition of powdered mixture of $Mn(NO_3)_2$ and $Cu(NO_3)_2$ (1:1).

As follows from the results, irrespectively of the synthetic procedure applied, the catalysts obtained have the surface catalytic active centres of different number and strength. The centres are of different type in manganese and manganese-copper samples, however, their exact identification needs further studies.

Conclusions

Manganese and manganese-copper catalysts were obtained by four different methods of synthesis. The specific surface area of the samples varied from 2 to 252 m^2/g. In

decomposition of H_2O_2 the activity of the catalysts obtained was different; the lowest was that of the sample obtained by thermal decomposition of powdered mixture of $Mn(NO_3)_2$ and $Cu(NO_3)_2$ (1:1). In phenol oxidation the catalytic activity was the highest for the samples obtained by oxidation of Mn^{2+} by $KMnO_4$ and it was surprisingly high for the sample obtained by the thermal decomposition of powdered mixture of $Mn(NO_3)_2$ and $Cu(NO_3)_2$ (1:1).

Acknowledgement

Assistance of Mr Robert Durski in part of experimental work is gratefully acknowledged.

References

[1] Jagiełło M.: *Zastosowanie ekstrakcji w stanie nadkrytycznym do analizy fenoli*. Ochr. Środow. 2004, **3**, 7–10.
[2] Sarbak Z.: Kataliza w ochronie środowiska, Wyd. Nauk. UAM, Poznań 2004.
[3] Bielicka-Daszkiewicz K.: *Usuwanie fenolu z wód ściekowych poprzez utlenianie*. Przem. Chem. 2008, **87**, 24–30.
[4] Nastaj J.K. and Kamińska A.: *Adsorpcja fenolu w wodnej fazie fluidalnej na adsorbentach polimerowych*. Przem. Chem. 2008, **87**, 300–308.

WPŁYW METOD SYNTEZY KATALIZATORÓW MANGANOWYCH I MANGANOWO-MIEDZIOWYCH NA ROZKŁAD NADTLENKU WODORU I UTLENIANIE FENOLU

Pracownia Adsorpcji i Katalizy w Ochronie Środowiska, Wydział Chemii
Uniwersytet im. Adama Mickiewicza w Poznaniu

Abstrakt: Przedstawiono wyniki badań nad wykorzystaniem tlenkowych preparatów manganowych i manganowo-miedziowych otrzymanych różnymi metodami syntezy. Dla otrzymanych preparatów wyznaczono wielkość powierzchni właściwej oraz określono aktywność katalityczną w rozkładzie nadtlenku wodoru i utlenianiu fenolu. Wykazano zróżnicowaną aktywność katalityczną preparatów w obu wymienionych reakcjach.

Słowa kluczowe: katalizatory Mn i Mn-Cu, rozkład nadtlenku wodoru, utlenianie fenolu

ECOLOGICAL CHEMISTRY AND ENGINEERING A

Vol. 16, No. 11 2009

Zenon SARBAK[1] and Krzysztof SURMA[1]

OXIDATION OF SOOT OVER TUNGSTEN AND PLATINUM-TUNGSTEN CATALYSTS SUPPORTED ON ALUMINA

UTLENIANIE SADZY NA KATALIZATORACH WOLFRAMOWYCH I PLATYNOWO-WOLFRAMOWYCH NANIESIONYCH NA TLENEK GLINU

Abstract: The paper reports results on soot oxidation in the presence of oxide catalysts that were alumina supported low (2 mass%) and high (20 mass%) loaded tungsten catalysts in one series and the catalysts as above with 0.3 mass% of platinum in another series. The model compound simulating Diesel soot was carbon carbonisate. The methods employed were differential thermal analysis (DTA) and thermogravimetry (TG). The tungsten catalysts were found to have similar activity in the process studied. The highest activity was established for the catalyst of 0.3 mass%Pt-2 mass%W/Al_2O_3.

Keywords: soot, oxidation, W/Al_2O_3, 0.3 Pt-W/Al_2O_3 catalysts, DTA/TG

Chemical composition of the exhaust gases emitted by Diesel engines differs considerably from that of spark-ignition engines [1]. During the work of compression--ignition engines at first soot nuclei are formed that are later developed in spherules and soot particles. This Diesel soot known also as particular matter [2] adsorbs on its porous surface some products of the fuel pyrolysis, including polycyclic aromatic hydrocarbons, heavy metals, sulphates, sulphuric acid and water. These products are known to have strong carcinogenic and mutagenic activities so it is of vital importance to remove them from the exhaust gases from Diesel engines. The concentration of Diesel soot can be reduced by changes in the construction of the engine leading to better combustion, by filtration of exhaust gases, by reducing the contents of sulphur, nitrogen and polycyclic aromatic hydrocarbons in the fuel, the use of proper lubricant oils or the use of alternative fuels.

One of the approaches is to capture the solid particles from the exhaust gases and oxidise them [3, 4]. At present this aim is realised on the two following ways. One of

[1] Laboratory of Adsorption and Catalysis in Environmental Protection, Faculty of Chemistry, Adam Mickiewicz University, ul. Grunwaldzka 6, 60–780 Poznań, Poland, email: sarbak@amu.edu.pl

them is based on the use of diesel particulate filter, capturing solid state particles from the exhaust gases.

The separated solid particles can be removed by combustion at high temperatures or in a catalytic reaction. The second way is based on the use of oxidising monolithic catalysts. The first solution has been applied in Diesel engines working in heavy vehicles, while the second one in motor-cars and delivery vans.

In the studies aimed at finding the most effective ways of Diesel soot removal a wide range of catalysts have been applied, including simple and complex metal oxides, platinum supported on oxides, spinels, perovskites and others [5–21]. In this study the activity of tungsten and platinum-tungsten catalysts supported on alumina was investigated in oxidation of carbonisate used as the model of Diesel soot.

Experimental

Origin and characterization of soot

The model of Diesel soot was the carbonisate produced by Gryfskand (former Hajnowskie Zaklady Suchej Destylacji Drewna), Hajnowka, Poland. The carbonisate was subjected to elemental analysis on Euro Vector model EA300 (Italy) and FT-IR study on Perkin Elmer apparatus.

Catalysts preparation

All samples were prepared by incipient wetness impregnation technique using water solution which contained desirable amounts of chloroplatinic acid or ammonium metatungstate. Two metallic catalysts were prepared in a two stage procedure. In the first stage tungsten was deposited on the alumina support (Alumina oxide – C, Degussa Corporation, USA) of the surface area equal to 93 m^2/g and was left to equilibrate for 3 hr at room temperature, then dried at 110 ^oC for 3 hr and finally calcined in air at 500 ^oC for 5 hr. Platinum was deposited in the second stage of preparation, then the sample was dried and calcined in the same conditions as in the first stage of impregnation.

A 0.3 mass% Pt/Al_2O_3 catalyst was prepared by impregnation of the alumina support with chloroplatinic acid by the incipient wetness followed by drying and calcinations in the same conditions as above.

Characterization of catalysts

Specific surface area, X-ray diffraction (XRD) FT-IR spectra and thermal analysis (DTA/TG) of so prepared samples were described earlier [22].

Catalytic measurements

The catalytic tests were conducted in derivatograph OD-102 of the system made by Paulik-Paulik-Erdey (Hungary). A portion of well-homogenised mixture of carbonisate

and catalyst at the mass ratio 1:29 was placed in ceramic crucible und heated to 1000 °C at the rate 13 °C min^{-1} in air flow at the rate of 30 cm^3/min [16]. The differential thermal analysis (DTA) and thermogravimetric (TG) curves were recorded. Analogous measurements in the same conditions were performed for the catalysts and the carbonisate (Fig. 1) separately.

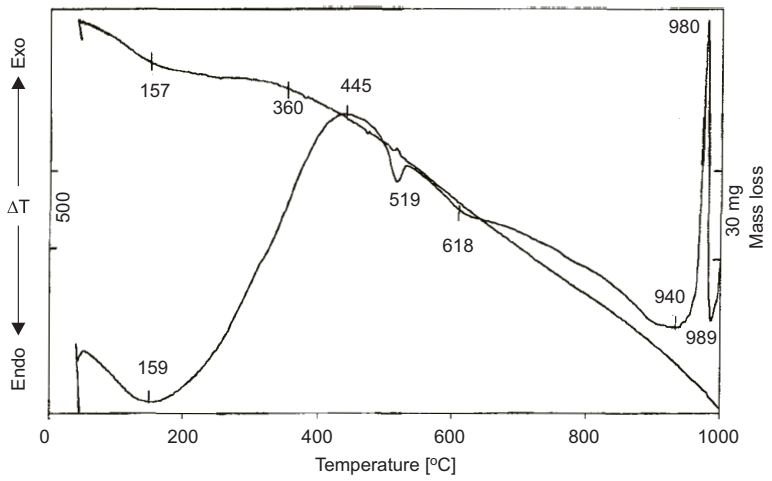

Fig. 1. DTA and TG curves of carbonisate oxidation

Results and discussion

According to the results of the elemental analysis the carbonisate contains 78.65 mass%C, 1.34 mass%H and 1.7 mass%N, the contents of the other components, such as minerals, were not determined. Its IR spectrum revealed bands characteristic of polycyclic aromatic hydrocarbons. In view of the above the carbonisate was assumed as relatively well simulating the particulate matters produced in Diesel engines. This conclusion was confirmed by the data reported in [23] on the thermogravimetric curve obtained for the soot collected from a one cylinder Diesel engine.

Table 1 presents the mass loss of the carbonisate during the reaction of catalytic oxidation. Assuming that the mass loss of the carbonisate during its heating (expressed as mg of carbonisate per g of catalyst) is a measure of the catalyst activity in the reaction of the carbonisate oxidation, the catalysts studied can be arranged in the following series according to decreasing activity:

$$0.3\ \text{Pt-2W/Al}_2\text{O}_3 > 20\text{W/Al}_2\text{O}_3 \approx 2\text{W/Al}_2\text{O}_3 \approx 0.3\ \text{Pt-20W/Al}_2\text{O}_3 > > 0.3\ \text{Pt/Al}_2\text{O}_3 \geq \text{Al}_2\text{O}_3$$

The highest activity was noted for the catalyst 0.3 Pt-2W/Al_2O_3, which is related to the fact that tungsten species were covered with “islands” of metallic platinum particles

[24]. The increase in the catalytic activity of this catalyst was a consequence of synergic interaction between these two components. The platinum catalysts containing 20 mass%W the tungsten species are covered with platinum species that are additionally impregnated with other tungsten species. This system was found less active in the reaction studied as the metallic platinum particles were not able to get engaged in the catalytic process [24].

Table 1

Carbonisate mass loss during catalytic oxidation

Catalyst	BET surface area [m^2/g]	Mass loss [mg/g catalyst]
Al_2O_3	93	2.45
0.3* Pt/Al_2O_3	93	36
$2W/Al_2O_3$	83	57
$20W/Al_2O_3$	70	60
$0.3Pt\text{-}2W/Al_2O_3$	95	78
$0.3Pt\text{-}20W/Al_2O_3$	74	55

* Numerical values proceeded element symbol = mass%.

The course of DTA curves recorded on the temperature programmed oxidation permits following the qualitative and quantitative changes in the components of the carbonisate.

The DTA curves of pure carbonisate (Fig. 1) show two exothermic effects with the maxima at 445 and 980 °C as well as three endothermic effects with the minima at 159, 519 and 618 °C.

In the presence of Al_2O_3 the course of DTA curve is different than that for pure carbonisate (Fig. 2). The exothermic maxima are moved towards higher temperatures of

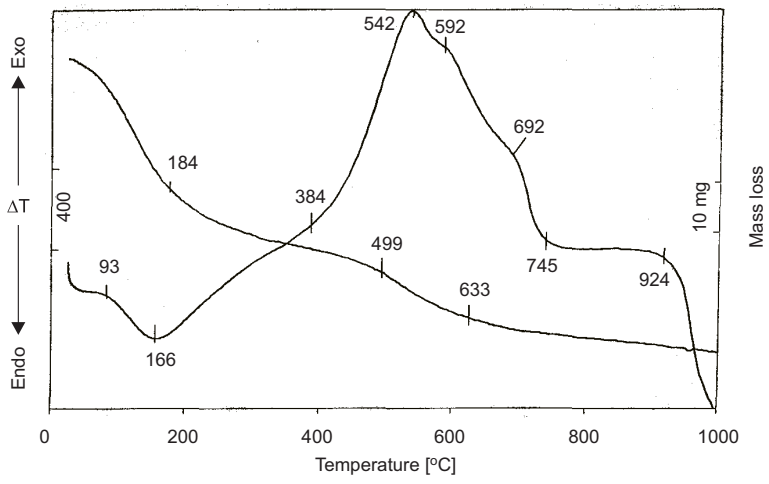

Fig. 2. DTA and TG curves of carbonisate oxidation over Al_2O_3

542, 592 and 692 °C. The exothermic effect with a maximum at 980°C disappears. However, the total mass loss of carbonisate is very low (Table 1) and it means that components of carbonisate undergo only transformation into another components.

Introduction of a small amount of platinum (0.3 mass%) onto Al_2O_3 results in a shift of the exothermic effect maximum from 445 °C noted for the carbonisate without catalyst (Fig. 1) to 531 °C (Fig. 3) and brings a great increase in the activity in the carbonisate oxidation reaction (Table 1).

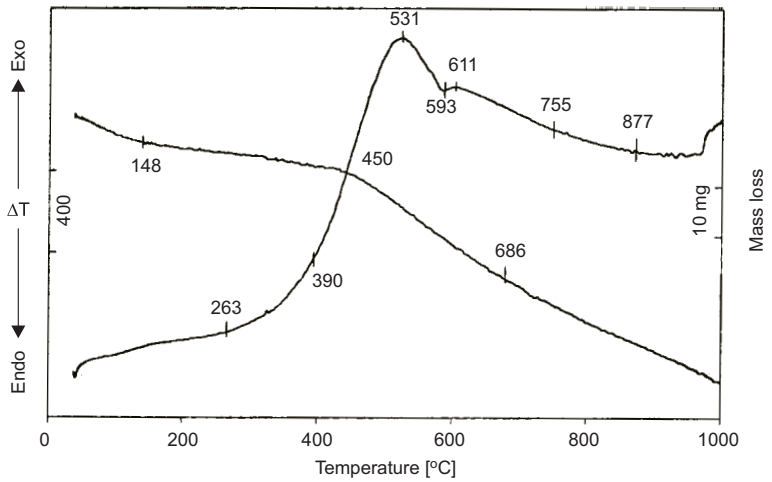

Fig. 3. DTA and TG curves of carbonisate oxidation over $0.3Pt/Al_2O_3$

After introduction of tungsten in the amount of 2 mass% or 20 mass% on Al_2O_3, the DTA curves (Fig. 4, 5) show the disappearance of the exothermic effect at 980 °C

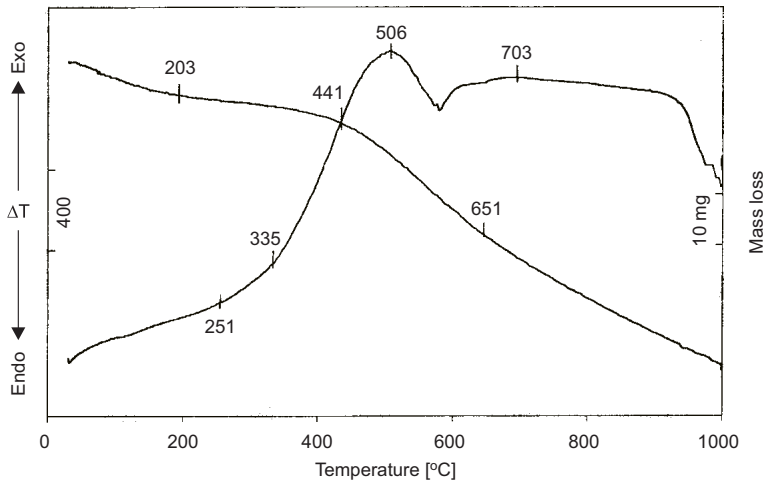

Fig. 4. DTA and TG curves of carbonisate oxidation over $2W/Al_2O_3$

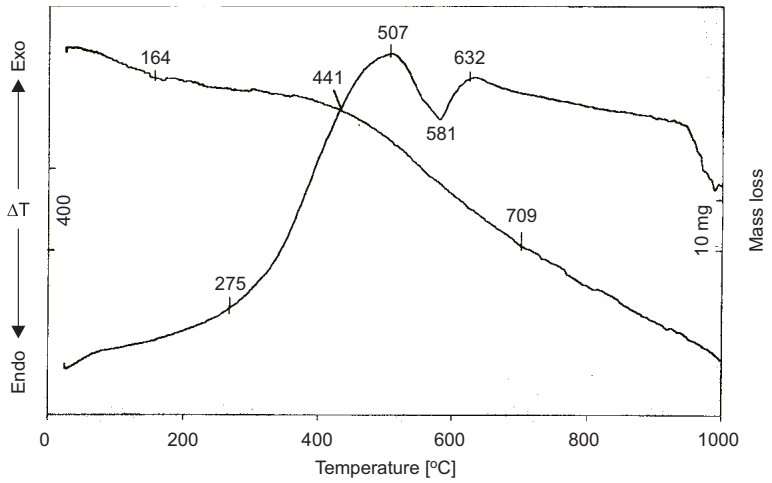

Fig. 5. DTA and TG curves of carbonisate oxidation over $20W/Al_2O_3$

observed on the DTA curve of the carbonisate (Fig. 1). The other thermal effects appear at similar temperatures: the exothermic effect at 506–507 °C and the endothermic effect at 579–581 °C.

The addition of platinum to the W/Al_2O_3 catalysts does not produce significant changes in the DTA curves (Fig. 6, 7) relative to the curve obtained for the carbonisate. The maxima and minima of the thermal effects are shifted towards higher temperatures. The most active catalyst proved 0.3 mass%Pt-2mass%W/Al_2O_3, while the activities of the other catalysts with tungsten and tungsten and platinum were at similar level and lower.

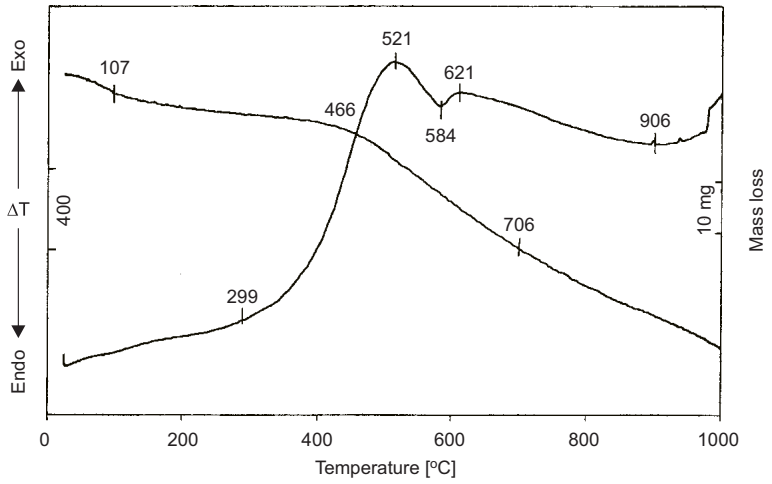

Fig. 6. DTA and TG curves of carbonisate oxidation over $0.3Pt\text{-}2W/Al_2O_3$

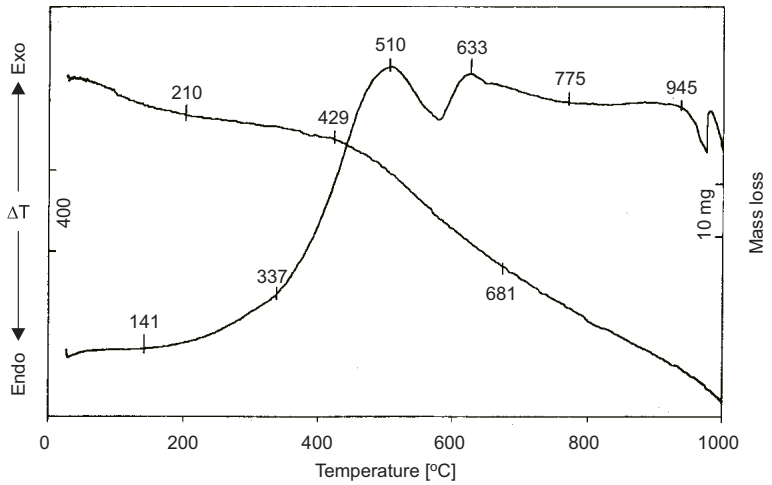

Fig. 7. DTA and TG curves of carbonisate oxidation over 0.3Pt-20W/Al_2O_3

Conclusions

1. Aluminium oxide is not effective as a catalyst of carbonisate oxidation.
2. Impregnation of Al_2O_3 with a small amount of platinum leads to a significant increase in the catalyst activity.
3. The low and high loaded tungsten catalysts are characterised by similar catalytic activity.
4. The highest activity in the carbonisate oxidation reaction was noted for the catalyst 0.3 mass%Pt-2mass%W/Al_2O_3.
5. DTA and TG have been found to be fast and effective methods permitting evaluation of the activity of the carbonisate oxidation catalysts.

References

[1] Sarbak Z.: Catalysis in Environmental Protection, Adam Mickiewicz University Press, Poznań 2004 (in Polish).
[2] Bockhorn H.: Pollutants from Combustion, Vove-Ul C. (ed.), Kluwer Academic Publishers, Dordrecht 2000, 205–215.
[3] Cimbelli P., Palma V., Russo P. and Vaccaro S.: Catal. Today 2002, **73**, 363–367.
[4] Roberts J.T.: Environmental Catalysis, Grassian V.H. (ed.), CRC Press, Boca Raton 2005, 177–185.
[5] Obuchi A., Oi-Uchisawa J., Enomoto R., Liu S., Nanba T. and Kushiyama S.: Stud. Surf. Sci. Catal. 2000, **130**, 1559–1564.
[6] Pruvost C., Lamounier J.F., Courcot D., Abi Aad E. and Aboukais A.: Stud. Surf. Sci. Catal. 2000, **130**, 2159–2163.
[7] Teraoka Y., Shangguan W.F. and Kagawa S.: Res. Chem. Intermed. 2000, **26**, 201–211.
[8] Mescia D., Canda E., Russa N., Fino D., Saracco G. and Specchia V.: Catal. Today 2006, **117**, 369–375.
[9] Tikhomirov K., Kröcher O. and Wokaun A.: Catal. Lett. 2006, **109**, 49–57.
[10] Darcy P., Da Costa P., Mellottée H., Trichard J.-M. and Djega-Maridasseou G.: Catal. Today 2007, **119**, 25–32.

[11] Fino D., Cauda E., Mescia D., Russo N., Saracco G. and Specchia V.: Catal. Today 2007, **119**, 257–263.
[12] Nejar N. and Illán-Gómez M.J.: Catal. Today 2007, **119**, 257–272.
[13] Aouad S., Saab E., Abi Aad E. and Aboukaď s A.: Catal. Today 2007, **119**, 273–278.
[14] Krishna K. and Makkee M.: Topics Catal. 2007, **42–43**, 229–234.
[15] Dhakad F., Rayalu S.S., Kumer R., Doggali P., Bakardjieva S., Subrt J., Mitsuhashi T., Haneda H. and Labhsetwar N.: Catal. Lett. 2008, **121**, 137–145.
[16] Sarbak Z. and Surma K.: Principles and Metods for Accelerated Catalyst Desing and Testing, Derouane E.G. et al (eds.), Kluwer Academic Publishers, Dordrecht 2002, 432–436.
[17] Sarbak Z.: Przem. Chem. 2003, **82**, 1–8.
[18] Sarbak Z. and Surma K.: J. Therm. Anal. Calorim. 2003, **72**, 159–163.
[19] Sarbak Z. and Surma K.: J. Therm. Anal. Calorim. 2006, **83**, 223–227.
[20] Sarbak Z. and Surma K.: Ecol. Chem. Eng. 2006, **13**, 291–295.
[21] Sarbak Z., Surma K. and Wieczorek K.: Polish J. Chem. Technol. 2008, **10**, 57–63.
[22] Sarbak Z.: Appl. Catal. A 1999, **177**, 85–90.
[23] Neeft J.P.A.: Catalytic oxidation of soot, Ph.D.Thesis, Technische Universiteit Delft, Delft 1995.
[24] Sarbak Z. and Jóźwiak W.K.: Przem. Chem. (sent for publication).

UTLENIANIE SADZY NA KATALIZATORACH WOLFRAMOWYCH I PLATYNOWO-WOLFRAMOWYCH NANIESIONYCH NA TLENEK GLINU

Pracownia Adsorpcji i Katalizy w Ochronie Środowiska, Wydział Chemii
Uniwersytet im. Adama Mickiewicza w Poznaniu

Abstrakt: Przedstawiono wyniki utleniania sadzy w obecności katalizatorów tlenkowych osadzonych na tlenku glinu i zawierających 2 i 20 % mas. WO_3 oraz 0,3 % mas.Pt. Jako model symulujący sadzę Diesla wybrano karbonizat. Efektywność utleniania karbonizatu badano metodami różnicowej analizy termicznej (DTA) oraz termograwimetryczną (TG). Wykazano, że w badanym procesie, katalizatory wolframowe miały podobną aktywność utleniającą. Największą aktywnością charakteryzował się katalizator 0,3 % mas.Pt-2 %mas. W/Al_2O_3.

Słowa kluczowe: sadza, utlenianie, W/Al_2O_3, 0,3 $Pt\text{-}W/Al_2O_3$, DTA/TG

ECOLOGICAL CHEMISTRY AND ENGINEERING A

Vol. 16, No. 11 2009

Tomasz GROBELSKI[1],
Jadwiga FARBISZEWSKA-KICZMA
and Teresa FARBISZEWSKA[2]

EFFECT OF HETEROTROPHIC BIOLEACHING ON EFFECIENCY OF AUTOTROPHIC BIOLEACHING OF METALS FROM TOXIC WASTE HEAPS IN ZLOTY STOK REGION

WPŁYW BIOŁUGOWANIA HETEROTROFICZNEGO NA EFEKTYWNOŚĆ BIOŁUGOWANIA AUTOTROFICZNEGO METALI Z TOKSYCZNYCH ZWAŁOWISK ZŁOTOSTOCKICH

Abstract: The results of two step bioleaching (autotrophic after heterotrophic) of mine wastes from heap "Jan" in Zloty Stok were presented. The results of the performed processes are very promising. 67 % of arsenic was extracted and exceedance of its permitted quantities in soil was reduced 3 times.

Keywords: biotechnology, bioleaching; bioreactor, heterotrophic bacteria, autotrophic bacteria, mineral wastes

Zloty Stok – a small town built at the feet of the Zlote Mountains is one of the most popular tourist centre in The Klodzko Land and is the place where the oldest gold mine in Poland is located. The first historical document mentioning the existence of the settlement and mining works in the surroundings of Zloty Stok goes back to 1273. Exploited deposits were mainly gold bearing arsenic ores: loellingite ($FeAs_2$) and arsenopyrite (FeAsS). The peak of gold mining in Zloty Stok fell for the 16th century when up to 150 kg of gold were recovered every year. The mine was closed in 1962 [1]. This seven centuries lasting exploitation of arsenopyrite deposits and smelting activities left surroundings of Zloty Stok mine with waste heaps containing high levels of metals, especially arsenic [2]. Considering this toxic waste heaps lying in the heart of the tourist

[1] Process Engineering Department, Faculty of Natural and Technical Sciences, Opole University, ul. R. Dmowskiego 7/9, 45–365 Opole, Poland, gaga@uni.opole.pl, kif@uni.opole.pl, grobeel@wp.pl

[2] Biotechnology and Molecular Biology Department, Faculty of Natural and Technical Sciences, Opole University, ul. kard. B. Kominka 4, 45–032 Opole, Poland.

region, remediation is inevitable and strongly recommended. By using bioleaching, the remediation method which allows metals recovery, there is possibility to turning waste heaps into unconventional ore deposits [2].

Study of bioleaching of sulphide minerals associated with metaloorganic and organic matter in case of copper shales showed that preliminary heterotrophic (neutral) bioleaching of the mineral material provides better efficiency of its further autotrophic (acid) bioleaching. Combination of this two processes allows for increasing the yield of metals in the leaching solution [3, 4]. The results were encouraging and suggested conducting similar two step bioleaching process in case of the mineral material from the waste heaps of Zloty Stok. To verify two step bioleaching efficiency in case of gold bearing arsenic ores two processes were performed and obtained results were compared: classical autotrophic bioleaching and two step autotrophic after heterotrophic bioleaching.

Experiment I

Test material was obtained from the waste heap "JAN", placed near road Zloty Stok – Ladek Zdroj. Samples from three characteristic places were taken. Material was crushed, sieved and averaged. Graining was 0.1–0.3 mm. Material contains: Ni – 151.0 ppm; Cu – 331.0 ppm; As – 4.54 %; Cd – 1.05 ppm; Cr – 71.7 ppm; Co – 22.8 ppm; Tl – 0.95 ppm and Pb – 62.0 ppm. Before bioleaching material was treated with 10N sulphuric acid in order to lower the pH level. After treatment chemical analyses were made. Material after pretreatment contains: Ni – 122.0 ppm; Cu – 310.0 ppm; As – 3.72 %; Cd – 0.36 ppm; Cr – 51.5 ppm; Co – 10.5 ppm; Tl – 0.59 ppm and Pb – 43.0 ppm.

The sample of pretreated mineral material (350 g) was placed in a tank bioreactor Biostat 5L with 3000 cm^3 2K solution and 500 cm^3 cultures of active strains of autochthonic autotrophic bacteria *Acidithiobacillus ferrooxidans* and *Acidithiobacillus thiooxidans* in ratio 1:1 [5]. Process was performed 30 days at temperature 35 ^oC, pH = = 2. The system was constantly stirred (200 rpm) and aerated. At the end of the process material was flushed, dried and chemical analysis was made. The results were: Ni – 82.0 ppm; Cu – 253.0 ppm; As – 3.4 %; Cd – 0.26 ppm; Cr – 42.6 ppm; Co – 10.1 ppm; Tl – 0.52 ppm and Pb – 31.0 ppm.

Experiment II

The second process of bioleaching of the material from heap "JAN" was performed in two steps. In the first step the sample of prepared mineral material (350 g) was placed in tank bioreactor Biostat with 3500 cm^3 leaching medium consisted of mineral solution inoculated with selected active strains of heterotrophic bacteria *Bacillus lentu*, *B. laterosporus*, *B. cereus* and *B. brevis* isolated from examined material [5]. These bacteria are known by their ability to oxidation of organic and metalorganic matter and their resistance to high arsenic concentrations. Process lasted 20 days, at temperature 25 ^oC, pH was in range (6.5–7.0). The system was constantly stirred (200 rpm) and aerated. At

the end of the process chemical analysis of material was made. The results were: Ni – 121.0 ppm; Cu – 298.0 ppm; As – 2.95 %; Cd – 1.03 ppm; Cr – 79.1 ppm; Co – 18.0 ppm; Tl – 0.73 ppm and Pb – 62.0 ppm.

After heterotrophic bioleaching material was filtered, dried and subjected to standard pretreatment before autotrophic leaching. The chemical analysis of the pretreatment material was made. The results were: Ni – 113.0 ppm; Cu – 279.0 ppm; As – 2.2 %; Cd – 0.38 ppm; Cr – 55.9 ppm; Co – 11.4 ppm; Tl – 0.59 ppm and Pb – 34.2 ppm.

The sample of material (180 g) was placed in tank bioreactor Biostat with 1300 cm^3 2K solution and 500 cm^3 cultures of active strains of autochthonic autotrophic bacteria *Acidithiobacillus ferrooxidans* and *Acidithiobacillus thiooxidans* in ratio 1:1 [4]. Process was performed 35 days at temperature 35 ^oC, pH = 2. The system was constantly stirred (200 rpm) and aerated.

At the end of the process chemical analysis of material was made. The results were: Ni – 82.0 ppm; Cu – 207,0 ppm; As – 1.5 %; Cd – 0.10 ppm; Cr – 39.8 ppm; Co – 10.1 ppm; Tl – 0.52 ppm and Pb – 32.5 ppm.

Results and discussion

The total amounts of extracted metals in the first experiment – autotrophic bioleaching of raw material – included chemical leaching during pretreatment and further autotrophic bioleaching are presented in Table 1.

Table 1

The total amounts of extracted metals

Element	Chemical leaching	Autotrophic bioleaching	Total leaching
	[%]		
Ni	19.20	32.8	45.70
Cu	6.40	18.4	23.60
As	18.00	8.6	25.10
Cd	68.57	21.2	75.24
Cr	28.20	17.3	41.60
Co	54.00	3.8	55.00
Tl	0.00	11.9	11.90
Pb	30.60	27.9	50.00

All of the monitored metals, except thallium, were found in the leachate after chemical pretreatment and all of them were found in the leachate after autotrophic bioleaching. The highest yield was obtained for nickel. The total extraction was: 75.24 % Cd; 55.0 % Co; 50.0 % Pb; 45.7 % Ni; 41.6 % Cr; 25.1 % As; 23.6 % Cu and 11.9 % Tl.

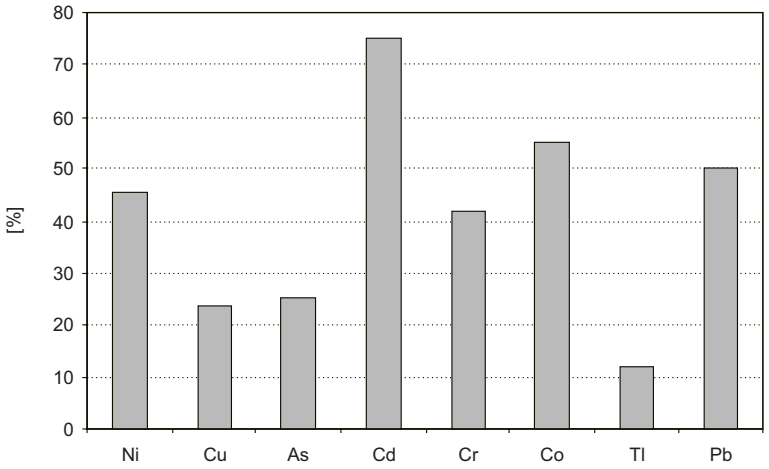

Fig. 1. The efficiency of autotrophic bioleaching of monitored metals from the raw material

The total amounts of extracted metals in the second experiment – autotrophic bioleaching of material after heterotrophic bioleaching – included chemical leaching in the middle stage are presented in Table 2.

Table 2

The total amounts of extracted metals

Element	Stage I Heterotrophic bioleaching	Stage II Chemical leaching	Stage III Autotrophic leaching	Total leaching
	[%]			
Ni	19.9	6.6	27.4	45.7
Cu	9.97	6.4	25.8	37.5
As	35.0	25.4	31.8	67.0
Cd	1.9	63.1	73.7	95.0
Cr	0.0	22.0	28.8	44.5
Co	21.0	36.7	11.4	55.0
Tl	0.0	0.0	11.9	11.9
Pb	0.0	45.0	5.0	47.6

The best yield was obtained for cadmium (95.0 %), arsenic (67.0 %) and cobalt (55.0 %). The yields of nickel (45.7 %), chromium (44.5 %) and copper (37.5 %) could also be considered as satisfying.

The heterotrophic bioleaching of chromium, thallium and lead was not observed while arsenic (35.0 %), cobalt (21.0 %) and nickel (19.9 %) has been leached very well. The chemical leaching of cadmium (63.1 %), lead (45.0 %) and cobalt (36.7 %) was significant, as well as autotrophic leaching of cadmium (73.7 %).

Comparison of the results of experiment I (autotrophic leaching) and experiment II (autotrophic leaching after heterotrophic) shows that heterotrophic leaching led prior to autotrophic had a positive impact on the results obtained in case of cadmium, copper and arsenic (Fig. 2.).

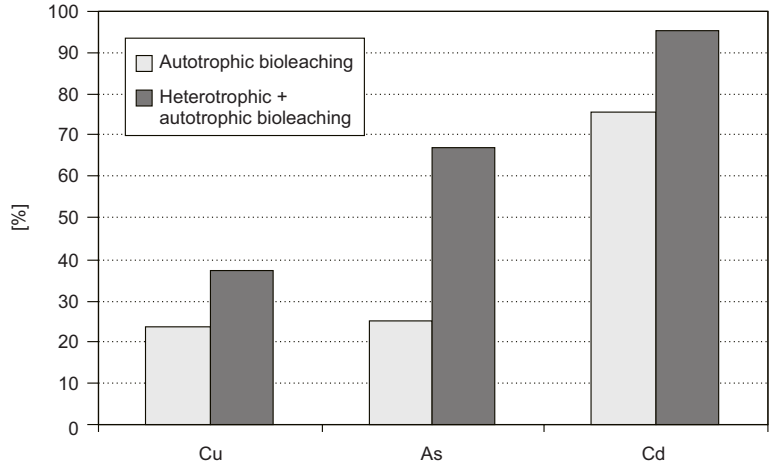

Fig. 2. Comparison of Cu, As and Cd extraction in autotrophic and heterotrophic + autotrophic bioleaching

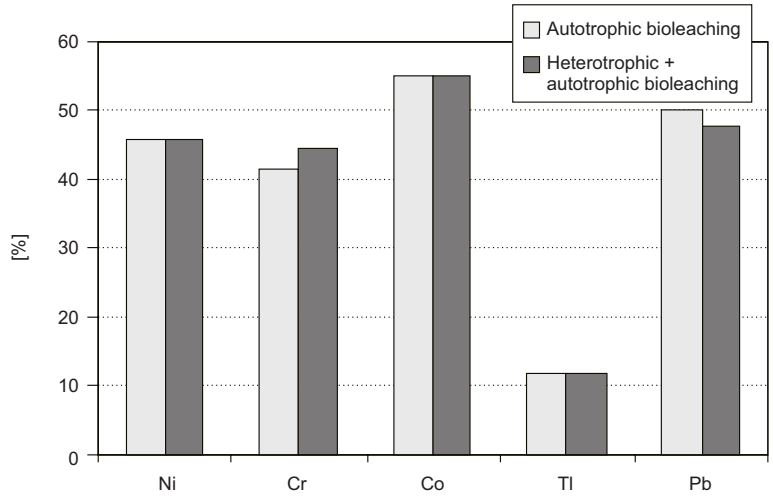

Fig. 3. Comparison of others metals extraction in autotrophic and heterotrophic + autotrophic bioleaching

Conclusions

The efficiency of recovery of the most toxic arsenic equals 67 % in experiment II and was almost three times better than in experiment I. Such a good extraction level is

sufficient reason to introduce two step bioleaching as a remediation process for Zloty Stok waste heaps.

However the concentration of arsenic in the material from heap "Jan" was reduced from 45.4 g/kg (4.54%) to 15 g/kg (1.5 %) i.e. three times and exceeds the permitted quantities 300 times for the class C soils and 700 times for the class D soils, reduction of its concentration by 67 % can be considered as a success [6]. There are strong evidences that two step bioleaching can be more effective using tube bioreactors [2, 7, 8].

Acknowledgements

The authors wish to acknowledge the support received from PBZ-KBN-111/T09/2004.

References

[1] Muszer A.: *Historia górnictwa w Złotym Stoku*. XXXV Seminarium. Fizykochemiczne Problemy Mineralurgii 1998, (7–9), 109–117.
[2] Grobelski T. and Farbiszewska-Kiczma J.: Detoksykacja zwałowisk odpadów byłej kopalni rud arsenopirytowych (in press).
[3] Grobelski T., Farbiszewska-Kiczma J. and Farbiszewska T.: *Bioleaching of Polish Black Shale*. Physicochemical Problems of Mineral Processing 2007, (41), 259–264.
[4] Farbiszewska T., Farbiszewska-Kiczma J. and Grobelski T.: *Bioleaching of Black Shale Talvivaara Ore*. Ecol. Chem. Eng. 2007, **14**(8), 793–798.
[5] Farbiszewska-Kiczma J., Farbiszewska T. and Grobelski T.: *Izolacja bakterii hetero- i autotroficznych z hałdy odpadów "JAN" w Złotym Stoku*, XXV Międzynarodowa Konferencja Naukowa "Inżynieria procesowa w Ochronie Środowiska", Opole–Zakopane, 31.05–2.06.2007, Opole 2008, 25, 23–29.
[6] http://www.mos.gov.pl/2prawo/rozporzadzenia_ms/02.165.1359_zalacznik.shtml
[7] Grobelski T., Farbiszewska-Kiczma J. and Farbiszewska T.: *Bioleaching of Polish Black Shale*, Physicochemical Problems of Mineral Processing 2007, (41), 259–264.
[8] Farbiszewska-Kiczma J. and Farbiszewska T.: *Bioługowanie odpadów po wzbogacaniu polskich rud miedzionośnych*, Conference proceedings "Perspectives for applying bioleaching technology to process shale-bearing copper ores", BIOPROCOP '06, Lubin 19.06.2006, Lublin 2006, 107–125.

WPŁYW BIOŁUGOWANIA HETEROTROFICZNEGO NA EFEKTYWNOŚĆ BIOŁUGOWANIA AUTOTROFICZNEGO METALI Z TOKSYCZNYCH ZWAŁOWISK ZŁOTOSTOCKICH

[1] Katedra Inżynierii Procesowej
Uniwersytet Opolski
[2] Samodzielna Katedra Biotechnologii i Biologii Molekularnej
Uniwersytet Opolski

Abstrakt: Przedstawiono wyniki badań dwuetapowego bioługowania (neutralnego i kwaśnego) odpadów pogórniczych zdeponowanych na hałdzie "Jan" w Złotym Stoku. Uzyskane wyniki dowiodły słuszności podjętych badań. Wyługowaniu uległo na przykład 67 % arsenu zawartego w materiale. Taki wynik spowodował, że przekroczenie dopuszczalnego poziomu zawartości arsenu w glebie zmalało trzykrotnie.

Słowa kluczowe: biotechnologia, bioługowanie, bakterie heterotroficzne, bakterie autotroficzne

ECOLOGICAL CHEMISTRY AND ENGINEERING A

Vol. 16, No. 11 2009

Stanisław KALEMBASA[1] and Agnieszka GODLEWSKA[1]

YIELDING AND MACRONUTRIENTS CONTENTS AT ITALIAN RYEGRASS ON A BACKGROUND OF ORGANIC FERTILIZATION AND LIMING

PLONOWANIE ORAZ ZAWARTOŚĆ MAKROELEMENTÓW W ŻYCICY WIELOKWIATOWEJ NA TLE NAWOŻENIA ORGANICZNEGO I WAPNOWANIA

Abstract: The pot experiment dealt with the evaluating the influence of sewage sludge with coal ash mixture as well as additional mineral fertilization and liming on yield and macronutrients contents at Italian ryegrass. Tested sludge originated from the purification plant in the city of Siedlce (industrial and municipal sewage) that were finally subjected to methane fermentation process. Italian rajgras was tested plant, in which dry matter yield and macronutrients concentrations were determined. Applied mixtures significantly increased the plant yield as well as magnesium and phosphorus contents, while decreased calcium and potassium levels. Liming considerably increased the amount of calcium and phosphorus in Italian ryegrass.

Keywords: Italian ryegrass, yield, macronutrients, sludge, hard coal ash, mixture, liming

A fast development of sewage purification methods and replacing the individual flat heating with municipal central heating has been recently observed, namely in small centers. Hard coal used in industry and for heating purposes is ground (fractions 1–20 mm in diameter), which allows for its better combusting and more efficient energy utilization. Achieved ashes of 1 mm particle diameter is transported to dumps and it has to be often wetted with water, because it is a source of dusting and threats the natural environment [1]. Mixing and further applying for crops fertilization can be one of the ways to utilize both waste products: hard coal ash and sewage sludge. It would make possible to use these wastes and to reduce their amounts stored.

Present study aimed at evaluating the fertilization value of sewage sludge with hard coal ash mixture as well as additional mineral nutrition and liming; the influence of that mixture on macronutrients contents at Italian ryegrass was also examined.

[1] Department of Soil Science and Plant Nutrition, Academy of Podlasie, ul. B. Prusa 14, 08–110 Siedlce, Poland, phone/fax: 25 643 12 87, email: kalembasa@ap.siedlce.pl

Material and methods

The three-factor pot experiment in completely randomized design with three replications was set in a greenhouse at Podlasie University in Siedlce. Following factors were examined:

I fertilization (sewage sludge with hard coal ash mixture at the ratio of 2:1 recalculated onto dry matter) taking into account two levels of experimental factor:

– 15 % of mixture amount in relation to the total soil weight;
– 30 % of mixture amount in relation to the total soil weight.

The amount of macronutritions introduced into the soil in materials used for fertilization applied in the 15 % to the soil mass was as follows: N – 0.28 g, P – 0.38 g, K – 0.14 g, Ca 0.84 and Mg – 0.22 g.

Sewage sludge applied in the experiment originated from the purification plant in Siedlce (industrial and municipal sewage) that were subjected to methane fermentation process and partially dehydrated on Bellmer press with flocculants addition at the final processing stage; hard coal ash originated from Energy Plant in Siedlce.

II liming (without or with liming according to 1 H_h of soil in a form of $CaCO_3$);

III mineral nutrition (without or with NPK nutrition). The mineral fertilization was applied once before sowing in forms of urea (285 mg/pot), triple superphosphate (320 mg/pot), and potassium sulfate (470 mg/pot).

The soil used for experiment consisted of light loamy sand collected from 0–20cm lessive soil layer. Before experiment, pH_{KCl} was 4.59 unit, while nitrogen and potassium contents 1.0 and 7.9 g · kg^{-1}, respectively. Pots were filled with 2 kg of soil and moisture content during vegetation period was maintained at 60 % level of the field water capacity. Italian ryegrass (*Lolium multiflorum* L.) was tested plant.

Four cuts of tested grass were harvested during the vegetation period, and then dry matter yield as well as total nitrogen (autoanalyzer CHNS/O 2400, Perkin-Elmer), phosphorus, potassium, calcium, and magnesium (ICP-AES technique after sample combustion) were determined in ground plant samples. Raw plant material was combusted at 450 ^oC in muffle furnace, then flooded with HCl/H_2O (1:1), and evaporated till dryness. Such prepared samples were dissolved in 10 cm^3 of diluted HCl (10 %) and transferred to measure flasks using 10 % HCl through hard filter paper.

Significant treatments effects and interactions ($P < 0.05$) were identified by analysis of variance (F Fisher-Snedecor's test) by applying FR Anal. Ver 4.1 software.

When significant treatment effects occurred means were separated using Tukey's for test $LSD_{(0.05)}$. Correlation coefficients for the relationship of the estimated factors were calculated.

Results and discussion

The waste activated sludge used in the experiment and consisting the mixture (Table 1) differed with their chemical composition. Sewage sludge originating from purification plant in Siedlce contained 5.57 g · kg^{-1} of nitrogen and phosphorus more than hard coal ash. The content of potassium, sulphur, calcium and magnesium in coal ash was higher

than in waste activated sludge. The content of potassium in hard coal ash was 6.5 times waste activated sludge while magnesium 44.1 times higher than in waste activated sludge.

Table 1

The content of select macroelements in sewage sludge and ash coal

Indicate macroelement	Sewage sludge	Ash coal
	g/kg^{-1} [d.m.]	
P	6.37	2.45
K	0.66	4.26
S	1.42	2.56
Ca	9.31	15.1
Mg	0.20	8.82

The high content of calcium and magnesium in hard coal ash might indicate its alkalizing properties.

The dry matter yield of Italian ryegrass (Table 2) oscillated within wide range from 1.47 g/pot d.m. from the 4th cut of not limed control and NPK to 9.70 g/pot d.m. from

Table 2

The yield [g · pot] of *Lolium multiflorum* dry matter

Liming		O			Ca		Means	Means
Combinations	Cuts	Fertilization		Means	Fertilization			
		O	NPK		O	NPK		
Object control	I	4.13	5.36	4.75	5.43	8.45	6.94	5.84
	II	2.64	4.16	3.40	2.16	3.20	2.68	3.04
	III	4.03	4.43	4.23	2.16	2.20	2.18	3.21
	IV	2.13	1.47	1.80	3.47	2.55	3.01	2.41
	Sum	12.95	15.42	14.18	13.22	16.40	14.81	14.50
Sludge + ash 2:1 15 %	I	4.66	5.16	4.91	5.53	5.96	5.75	5.33
	II	5.75	7.26	6.51	4.60	3.96	4.28	5.39
	III	5.80	9.46	7.63	5.70	4.56	5.13	6.38
	IV	3.20	4.33	3.77	2.93	2.83	2.88	3.32
	Sum	19.41	26.21	22.82	18.76	17.31	18.00	20.42
Sludge + ash 2:1 30 %	I	4.76	6.33	5.55	8.36	7.66	8.01	6.78
	II	4.93	6.33	5.63	5.30	6.86	6.08	5.86
	III	8.06	8.02	8.04	9.46	8.06	8.76	8.40
	IV	5.03	7.40	6.22	9.70	4.63	7.17	6.69
	Sum	22.78	28.08	25.44	32.82	27.21	30.20	27.73

	cuts				
	I	II	III	IV	sum
$LSD_{(0.05)}$ for:					
doses mixture of sewage sludge and ash	ns	1.55	2.87	2.88	1.65
liming	1.63	ns	ns	ns	ns
fertilization NPK	ns	1.04	ns	ns	ns
doses mixture of sewage sludge and ash x liming	ns	ns	ns	ns	2.33

the 4th cut of limed object with additional application of 30 % mixture of waste activated sludge and coal ash. The highest total grass yield as sum of four cuts was achieved from limed objects after application of 30 % mixture (32.82 g/pot d.m.), while the lowest – from not limed control object and without NPK (12.95 g/pot d.m.). The highest Italian ryegrass dry matter yields were achieved from the 1st and 3rd cuts, which can be elucidated by the rate of sewage sludge and hard coal ash mineralization rate [2, 3]. The lowest yields were recorded for the 4th cut of tested plant. Statistical analysis revealed significant influence of all studied experimental factors on plant yields in particular cuts. In the 1st cut, only liming considerably affected the yields. Sludge with hard coal ash mixture had significant effects on the yield of grass biomass in other three cuts and for sum yield of four cuts. Addition NPK fertilization significantly differentiated the biomass yield of grass only in the 2nd cut.

Also significiant influence was found for the interaction between the waste activated sludge and liming in the biomass for the yield of the sum of four cuts.

Nitrogen content in the biomass of Italian ryegrass (Table 3) was medium ranging from 16.8 g · kg^{-1} in the plant biomass harvested as biomass the 4th cut from not limed

Table 3

The content of nitrogen in *Lolium multiflorum* [g · kg^{-1}]

Liming		O			Ca			Means
Combinations	Cuts	Fertilization		Means	Fertilization		Means	
		O	NPK		O	NPK		
Object control	I	28.1	24.2	26.15	26.9	30.8	28.85	27.50
	II	31.0	36.9	33.95	27.8	30.1	28.90	31.43
	III	30.0	32.6	31.30	29.3	30.8	30.05	30.68
	IV	31.8	21.3	26.55	31.2	18.7	24.95	25.75
	Means	30.23	28.75	29.49	28.8	27.60	28.20	28.84
Sludge + ash 2:1 15 %	I	34.3	31.5	32.90	28.7	32.8	30.75	31.83
	II	32.2	32.5	32.35	29.4	29.9	29.65	30.00
	III	26.1	27.2	36.65	27.3	29.5	28.40	27.53
	IV	23.9	16.8	20.35	35.0	19.4	27.20	23.78
	Means	29.12	27.00	28.06	30.10	30.10	30.10	28.53
Sludge + ash 2:1 30 %	I	39.7	31.0	35.35	32.9	31.8	32.35	33.85
	II	30.7	39.2	34.95	39.1	28.7	33.90	34.43
	III	27.9	25.5	26.70	29.3	22.8	26.05	26.38
	IV	21.7	20.2	20.95	23.7	24.2	23.95	22.45
	Means	30.00	28.97	29.49	31.25	31.25	31.25	26.88

	cuts			
	I	II	III	IV
$LSD_{(0.05)}$ for:				
doses mixture of sewage sludge and ash	1.86	ns	2.09	ns
liming	ns	ns	ns	ns
fertilization NPK	1.25	ns	ns	3.40
doses mixture of sewage sludge and ash x liming	2.16	2.14	ns	ns
doses mixture of sewage sludge and ash x fertilization NPK	2.16	2.14	2.43	3.95
liming x fertilization NPK	1.76	ns	ns	ns

object with additional 15 % mixture and NPK, to 39.7 g · kg^{-1} in the 1st cut from not limed object with additional 30 % mixture application. The nitrogen content decreased in the biomass of grass harvested from objects fertilized with sludge with hard coal ash mixture in subsequent cuts (Table 3), which can indicate a fast rate of organic matter mineralization in applied sewage sludge with narrow C:N ratio. Statistical analysis revealed significant influence of sludge with coal ash mixture and NPK nutrition applied, while liming had not considerable impact on nitrogen concentration in the biomass of tested plants, which was consistent with observations made by Pronczuk [4], who found that the soil acidity had no influence on nitrogen accumulation in a fodder. Interaction between all investigated factors revealed significiant influence but in differentiated cuts for example between doses of mixture x liming for biomass harvested as 1st and 2nd cuts, for doses of mixture NPK in biomass of four cuts and for liming x NPK only in biomass harvested as 1st cut.

Hay containing 3 g of phosphorus · kg^{-1} d.m. is considered as balanced in reference to phosphorus content [5, 6]. Italian ryegrass grown in present experiment contained varied quantities of phosphorus, which is presented in Table 4. Many authors report that

Table 4

The content of phosphorus in *Lolium multiflorum* [g · kg^{-1}]

Liming		O			Ca			Means
Combinations	Cuts	Fertilization		Means	Fertilization		Means	
		O	NPK		O	NPK		
Object control	I	4.67	4.49	4.58	4.56	5.10	4.83	4.71
	II	4.41	4.81	4.61	5.14	4.10	4.62	4.62
	III	5.55	5.14	5.35	6.56	4.90	5.73	5.54
	IV	3.55	3.08	3.32	4.23	3.60	6.92	3.62
	Means	4.55	4.38	4.47	5.12	4.43	4.78	4.62
Sludge + ash 2:1 15 %	I	8.25	8.23	8.24	7.31	6.28	6.80	7.52
	II	6.24	5.74	5.99	5.49	4.62	5.06	5.52
	III	5.59	5.20	5.40	6.24	4.71	5.48	5.44
	IV	4.19	4.18	4.19	4.66	4.11	4.39	4.29
	Means	6.07	5.84	5.96	5.93	4.93	5.43	5.69
Sludge + ash 2:1 30 %	I	8.28	8.74	8.51	10.02	9.54	9.78	9.15
	II	8.03	6.01	7.02	7.35	6.68	7.02	7.02
	III	5.63	5.21	5.42	5.64	5.39	5.52	5.47
	IV	4.16	4.07	4.12	4.14	4.05	4.10	4.11
	Means	6.50	6.01	6.26	6.79	6.42	6.61	6.43

	cuts			
	I	II	III	IV
$LSD_{(0.05)}$ for:				
doses mixture of sewage sludge and ash	1.30	0.515	0.288	0.328
liming	ns	ns	ns	0.221
fertilization NPK	ns	0.347	ns	0.221
doses mixture of sewage sludge and ash x liming	1.84	0.728	ns	ns
mixture of sewage sludge and ash x fertilization NPK	ns	ns	ns	ns
liming x fertilization NP.	ns	0.407	ns	ns

phosphorus level at Italian ryegrass oscillates from 2.1 to 5.0 g · kg^{-1}. Phosphorus content in plants from the control object was within that range, while in objects where sludge with hard coal ash mixture plus NPK nutrition was applied, it often exceeded the optimum values, which was confirmed by other studies [7].

Like for nitrogen, phosphorus concentration in cultivated plants on objects treated with sewage sludge with hard coal ash decreased in subsequent cuts, which was associated with sludge organic matter mineralization. Statistical analysis revealed significant influence of all experimental factors on phosphorus level at tested grass. In the 1st, 2nd, and 4th cuts, both 15 % and 30 % mixture considerably increased the phosphorus content as compared with the control. Mineral fertilization of the 2nd, 3rd, and 4th cuts significantly decreased phosphorus concentration in reference to objects that were not NPK fertilized. Liming had significant effect on discussed trait only in the 4th cut. Italian ryegrass from that cut was characterized by significantly higher phosphorus content on limed objects.

Concentration of potassium at tested plant oscillated within wide range (Table 5) and in all cases it exceeded the optimum amounts for that element in a fodder [8]. NPK

Table 5

The content of potassium in *Lolium multiflorum* [g · kg^{-1}]

Liming		O			Ca			Means
Combinations	Cuts	Fertilization		Means	Fertilization		Means	
		O	NPK		O	NPK		
Object control	I	42.3	42.9	42.60	41.7	45.6	43.65	43.13
	II	36.5	44.3	40.40	42.3	27.5	34.90	37.65
	III	38.7	37.8	38.25	31.8	27.5	29.65	33.95
	IV	26.8	26.5	26.65	35.2	24.0	29.60	28.13
	Means	36.08	37.88	36.98	37.75	31.15	34.45	35.72
Sludge + ash 2:1 15 %	I	40.1	43.4	41.75	38.7	43.0	40.85	41.30
	II	41.3	43.5	42.40	35.1	42.1	38.60	40.50
	III	30.4	45.3	37.85	31.9	35.7	33.80	35.83
	IV	26.8	24.9	25.85	26.5	26.7	26.60	26.23
	Means	34.65	39.28	36.96	33.05	36.88	34.96	35.97
Sludge + ash 2:1 30 %	I	33.7	47.3	40.50	38.8	46.3	42.55	41.53
	II	28.1	41.6	34.85	39.3	33.7	36.50	35.68
	III	25.6	31.9	28.75	33.4	36.3	34.85	31.80
	IV	21.8	30.9	26.35	39.3	23.5	31.50	28.89
	Means	27.30	37.93	32.61	37.7	34.95	36.33	34.47

	cuts			
	I	II	III	IV
$LSD_{(0.05)}$ for:				
doses mixture of sewage sludge and ash	ns	4.02	3.40	ns
liming	ns	ns	ns	2.52
fertilization NPK	3.41	ns	2.29	2.52
doses mixture of sewage sludge and ash x liming	ns	ns	3.97	ns
doses mixture of sewage sludge and ash x fertilization	ns	4.71	3.97	ns
liming x fertilization NPK	ns	3.85	3.24	3.56

fertilization at the 1st, 3rd, and 4th cuts significantly affected the increase of potassium level in plants, which is fully plausible. Applying the mixture of sludge with ash at 30 % rate for the 2nd and 3rd cut grass considerably decreased the potassium level. Probably higher nitrogen dose introduced along with the sludge was the reason, which was also confirmed by other studies [9]. The liming effect was apparent in the 4th cut manifesting with the increase of potassium content at Italian ryegrass. Statistical analysis also revealed significant interactions of all studied factors with potassium amounts in the grass.

Calcium content at tested plants (Table 6) oscillated around values commonly considered as optimum (6.1 to 12.0 g · kg^{-1}): its highest levels were recorded in the 3rd cut grass. Sewage sludge with hard coal ash mixture significantly decreased the element concentration in all cuts as compared with the control, while liming had the opposite influence. Mineral nutrition in the 1st and 2nd cuts considerably decreased the calcium concentration at Italian ryegrass.

Table 6

The content of calcium in *Lolium multiflorum* [g · kg^{-1}]

Liming		O			Ca			Means
Combinations	Cuts	Fertilization		Means	Fertilization		Means	
		O	NPK		O	NPK		
Object control	I	8.11	7.67	7.89	8.28	8.69	8.69	8.19
	II	9.27	7.91	8.59	9.60	11.93	10.77	9.68
	III	12.46	10.41	11.44	12.94	12.30	12.62	12.03
	IV	7.86	6.88	7.37	9.86	9.41	9.62	8.50
	Means	9.43	8.22	8.82	10.17	10.58	10.38	9.60
Sludge + ash 2:1 15 %	I	7.29	7.29	7.29	8.64	7.12	7.88	7.59
	II	8.62	8.48	8.55	9.72	8.22	8.97	8.76
	III	10.16	9.77	9.97	11.92	9.60	10.76	10.37
	IV	6.80	6.76	6.78	7.31	7.92	7.62	7.20
	Means	8.22	8.08	8.15	9.40	8.22	8.81	8.48
Sludge + ash 2:1 30 %	I	7.06	5.92	6.49	8.02	6.40	7.21	6.85
	II	8.27	8.09	8.18	8.86	8.31	8.59	8.39
	III	9.99	10.64	10.32	10.17	10.38	10.28	10.30
	IV	6.60	6.50	6.55	5.72	6.65	6.19	6.37
	Means	7.98	7.79	7.89	8.19	7.94	8.07	7.98

	cuts			
	I	II	III	IV
$LSD_{(0.05)}$ for:				
doses mixture of sewage sludge and ash	0.799	0.587	0.840	0.661
liming	0.539	0.396	0.567	0.446
fertilization NPK	0.539	ns	0.567	ns
mixture of sewage sludge and ash x liming	ns	0.686	ns	0.773
doses mixture of sewage sludge and ash x fertilization NPK	ns	0.686	0.982	ns

The optimum magnesium content at tested grass is – according to Falkowski [8] – 2.5 g · kg^{-1}. Here examined Italian ryegrass contained from 1.96 g · kg^{-1} on control to 4.45 g · kg^{-1} of magnesium on object fertilized with the mixture of sewage sludge with hard coal ash at 30 % rate (Table 7). As similarly as for calcium, the highest magnesium content was recorded at plants from the 3rd cut. All examined factors significantly influenced on the element concentration, although sludge with ash mixtures, that significantly increased the magnesium content in all cuts of plants, had the strongest impact. That fact can be accounted for by high magnesium concentration in hard coal ash (8.82 g · kg^{-1}). Liming only in the 1st cut of Italian ryegrass increased magnesium level, while NPK nutrition applied for the 3rd cut significantly decreased the macronutrient content at tested plants.

Table 7

The content of magnesium in *Lolium multiflorum* [g · kg^{-1}]

Liming		O			Ca			Means
Combinations	Cuts	Fertilization		Means	Fertilization		Means	
		O	NPK		O	NPK		
Cbject control	I	2.32	2.40	2.36	2.35	2.74	2.55	2.46
	II	3.60	3.51	3.56	3.35	3.52	3.44	3.50
	III	3.71	3.50	3.61	3.90	3.39	3.65	3.63
	IV	2.21	1.96	2.09	2.35	2.35	2.35	2.22
	Means	2.96	2.84	2.91	2.99	3.00	3.00	2.95
Sludge + ash 2:1 15 %	I	2.50	2.83	2.67	3.43	2.93	3.18	2.93
	II	4.09	4.04	4.07	3.96	3.42	3.69	2.88
	III	4.27	3.84	4.06	4.35	3.85	4.10	4.08
	IV	3.16	2.86	3.01	3.01	2.97	2.99	3.00
	Means	3.51	3.39	3.45	3.69	3.29	3.49	3.47
Sludge + ash 2:1 30 %	I	3.51	2.78	3.15	3.80	3.12	3.46	3.31
	II	4.07	3.82	3.95	4.45	4.17	4.31	4.13
	III	4.23	4.15	4.19	4.31	4.15	4.23	4.21
	IV	2.99	2.77	2.88	2.52	2.88	2.70	2.79
	Means	3.70	3.38	3.54	3.77	3.58	3.68	3.61

	cuts			
	I	II	III	IV
$LSD_{(0.05)}$ for:				
doses mixture of sewage sludge and ash	0.473	0.282	0.322	0.224
liming	0.319	ns	ns	ns
fertilization NPK	ns	ns	0.217	ns
doses mixture of sewage sludge and ash x liming	ns	0.329	ns	ns
liming x fertilization NPK	ns	ns	ns	0.214

The values of the correlation coefficient between the uptake of nitrogen, phosphorus, potassium and calcium by the biomass of Italian ryegrass and the of those macroelements introduced into the soil with materials used for fertilization (waste activated sludges and the ash of hard coal) were significient and reach the following values respectivally: r = + 0.589*, r = + 0.659*, r = + 0.445* and r = + 0.449*.

Conclusions

1. Significant influence of the application of sewage sludge with hard coal ash mixture on the yield biomass of ryegrass harvested in the 2nd, 3rd, 4th cuts and the sum of all was found.

2. Liming significiantly increased the biomass yield of ryegrass expressed as the sum of four cuts harvested as during experiment.

3. The application of sewage sludge with hard coal ash mixture considerably increased phosphorus and magnesium contents at tested plants, while the mixture at 30 % rate significantly decreased calcium and potassium levels.

4. The biomass of Italian ryegrass contained significantly higher content calcium and phosphorus harvested from limed object than without application of lime.

References

[1] Antonkiewicz J.: Ecol. Chem. Eng. 2006, **13**(9), 865–874.
[2] Meller E.: Fol. Univ. Agric. Stetin. Agricultura 1999, **78**, 203–214.
[3] Strączyńska S.: Fol. Univ. Agric. Stetin. Agricultura 1998, **72**, 289–293.
[4] Prończuk J.: Zesz. Probl. Post. Nauk Roln. 1983, **276**, 29–35.
[5] Moraczewski R.: Łąki i pastwiska w gospodarstwie rolnym. SGGW, Warszawa 1996, 220 pp.
[6] Niczyporuk A. and Jankowska-Huflejt H.: Zesz. Probl. Post. Nauk Roln. 2001, **479**, 217–221.
[7] Kozłowski S., Goliński P., Zielewicz W. and Biniak J.: Zesz. Probl. Post. Nauk Roln. 2001, **479**, 163–171.
[8] Falkowski M., Kozłowski S. and Kukułka I.: Właściwości chemiczne roślin łąkowych. Wyd. AR Poznań, Poznań 1990, 110 pp.
[9] Kochanowska R. and Nowak W.: Roczn. Glebozn. 1992, **XLIII**(1/2), 99–111.

PLONOWANIE ORAZ ZAWARTOŚĆ MAKROELEMENTÓW W ŻYCICY WIELOKWIATOWEJ NA TLE NAWOŻENIA ORGANICZNEGO I WAPNOWANIA

Katedra Gleboznawstwa i Chemii Rolniczej
Akademia Podlaska w Siedlcach

Abstrakt: W doświadczeniu wazonowym badano wpływ mieszaniny osadów ściekowych z popiołem węgla kamiennego w warunkach dodatkowego nawożenia mineralnego i wapnowania na plon i zawartość makroelementów w życicy wielokwiatowej. Badane osady pochodziły z oczyszczalni ścieków w Siedlcach (ścieki przemysłowe i komunalne), które w końcowym procesie obróbki poddano fermentacji metanowej. Rośliną testową był rajgras włoski, w którym oznaczono plon suchej masy oraz zawartość makroelementów w biomasie życicy wielokwiatowej. Stosowanie mieszaniny znacznie zwiększyło plon rośliny testowej oraz zawartość w jej biomasie magnezu i fosforu, a obniżyło zawartość wapnia i potasu. Natomiast wapnowanie znacznie zwiększyło zawartość wapnia i fosforu w biomasie życicy wielokwiatowej.

Słowa kluczowe: rajgras włoski, plon, makroelementy, osady, popiół z węgla kamiennego, mieszanina, wapnowanie

ECOLOGICAL CHEMISTRY AND ENGINEERING A

Vol. 16, No. 11 2009

Jolanta BOHDZIEWICZ[1], Anna KWARCIAK-KOZŁOWSKA[2]
and Mariusz KUGLARZ[3]

IMPACT OF ULTRASONIC FIELD ON THE EFFICIENCY OF LANDFILL LEACHATE CO-TREATMENT IN ANAEROBIC DIGESTION – REVERSE OSMOSIS SYSTEM

WPŁYW POLA ULTRADŹWIĘKOWEGO NA EFEKTYWNOŚĆ WSPÓŁOCZYSZCZANIA ODCIEKÓW W UKŁADZIE ZINTEGROWANYM FERMENTACJA BEZTLENOWA – ODWRÓCONA OSMOZA

Abstract: The results of a research project pertaining to the specification of the influence of the ultrasonic, US field on the efficiency of landfill leachate co-treatment in the process of anaerobic digestion associated with reverse osmosis were presented. The biological process – methane fermentation – was conducted in the bioreactor equipped with submerged membrane module (MBR reactor). The concentration of the anaerobic sludge granules was maintained at the fixed level of 10 g/m^3. The samples both after and before ultrasonic disintegration underwent the digestion process. Hydraulic retention time was varied within the range of between 1 and 3 days, which allowed to increase the OLR (Organic Loding Rate) value from 1.3 kg COD/m^{3}d to 4.0 kg COD/m^{3}d. It was established that ultrasonic disintegration reduced the HRT value from 2 to 1.5 days, as compared with non-disintegrated samples. What is more, ultrasonic, US-facilitated samples exhibited a higher COD reduction as well as the overall biogas production, on average by 10 % and 11 %, respectively. Since the biologically treated effluent in both analysed modes (MBR and MBR+US) exhibited a high degree of contamination – which did not allow to release the effluent into the natural water – an attempt was made to post-treat it by means of a high-driven membrane process, ie reverse osmosis. The application of reverse osmosis enabled a high degree of pollutants reduction. However, the final volumetric permeate flux (in both cases, ie MBR and MBR +US) exhibited an excessive concentration of ammonia nitrogen, which did not allow to release the effluent into receiving water. It was suggested that further experiments should additionally be based on nitrogen ammonia removal processes, eg ammonia stripping.

Keywords: landfill leachate**,** anaerobic digestion, membrane reactor (MBR), reverse osmosis (RO), ultrasonic field

[1] Institute of Water and Wastewater Engineering, Silesian University of Technology, ul. S. Konarskiego 18, 44–100 Gliwice, Poland, email: jolanta.bohdziewicz@polsl.pl

[2] Institute of Environmental Engineering, Czestochowa University of Technology, ul. Brzeźnicka 60a, 42–200 Częstochowa, Poland, email: akwarciak@is.pcz.czest.pl

[3] Institute of Environmental Protection and Engineering, University of Bielsko-Biala, 43–309 Bielsko-Biała, Poland, email: mkuglarz@ath.bielsko.pl

By far the largest proportion of municipal solid waste (MSW) generated in Poland as well as in other countries is still disposed of by means of landfilling. Moreover, depositing municipal solid waste even at properly designed and serviced dumping sites constitutes a threat to the natural environment, in particular, to groundwaters. Generally, landfill leachate is caused by atmospheric precipitation percolating through the landfill bed as well as organic and inorganic substances – often toxic – leaching from the landfill bed [1–3]. Leachate chemical composition as well as its amount vary and depend on a number of factors, ie season of the year; type of landfilled waste; age of the landfill site as well as landfilling method used [4]. Additionally, in a number of dumping sites, anaerobic conditions results in the production of explosive gases, as well as vapor-phase volatile organic compounds. Taking into account the limited biodegradability of organic compounds in the leachate, their treatment requires the classic biological method to be augmented by additional processes, mainly physical or/and chemical.

The aim of the research project

The main objective of the research project was to establish the influence of the ultrasonic (US) field on the efficiency of landfill leachate and synthetic wastewater co-treatment. In particular, an attempt was made to establish if the treatment of landfill leachate – especially that generated in long existing landfill sites – involving digestion in an MBR reactor after ultrasonic disintegration (US) and subsequent treatment in the reverse osmosis process (RO), is a promising solution to the problem of leachate treatment or not.

Research material and methods

The research project is based on samples collected from the regional landfill site in Sobuczyny near Czestochowa, which has been in operation since 1987. Experiments were conducted on samples consisting of: raw leachate – 20 % vol. and synthetic wastewater – 80 % vol. The adopted proportion was considered optimal taking into account results from the early stages of the research project. Table 1 presents the physical and chemical parameters of raw landfill leachate.

Table 1

Characteristics of the raw landfill leachate

Parameter	Unit	Range of value
pH	[-]	8.2–8.4
COD	mgO_2/dm^3	3200–4600
BOD/COD	[-]	0.11–0.2
NH_4^+	mg/dm^3	800–1000
Cl^-	mg/dm^3	1800–2500

Samples both after and before ultrasonic disintegration underwent the digestion process – a methane fermentation in the reactor equipped with submerged membrane module. The concentration of sludge granules was maintained at the fixed level of 10 g/m^3. Hydraulic retention time was varied within the range of between 1 and 3 days, which allowed to increase the OLR (Organic Loading Rate) value from 1.3 kg COD/m^3d to 4.0 kg COD/m^3d. The ultrasonic field parameters applied: disintegration time: 300 s and amplitude of resonance – 25 m were specified during the early stages of the research project implementation. Samples after anaerobic digestion were transferred to the reverse osmosis module. The reverse osmosis process was conducted applying the following parameters: cross-flow velocity of 2 m/s and transmembrane pressure of 3 MPa.

Discussion

The core of the project focused on the determination of the most appropriate operating parameters of anaerobic digestion process, such as hydraulic retention time (HRT) and organic loading rate (OLR) of the bioreactor. Samples after anaerobic digestion were treated in the process of reverse osmosis with the aim to receive a high degree of pollutant removal.

The treatment of landfill leachate in an MBR reactor

Hydraulic retention time (HRT) initially adopted was 3 days, which was tantamount to 1.3 kg COD/$kg_{d.m.}$d of bioreactor organic loading rate (OLR). Under the conditioned specified, the leachate treated exhibited the COD value of 620 mgO_2/dm^3. In this case, COD reduction amounted to 84.5 %. Whilst samples treated in the same reactor without ultrasonic disintegration exhibited the COD value of 780 mgO_2/dm^3 and the COD reduction at the level of 80.5 %.

The HRT value was subsequently reduced by 12 hours and the corresponding COD changes recorded. Figure 1 presents COD values as well as COD reduction of the leachate samples in relation to the HRT value.

Firstly, the reduction of HRT value from 3 days to 2.5 days caused the OLR value to increase from 1.3 to 1.6 kgCOD/m^3d as well as positively effected the degree of COD reduction both with reference to disintegrated and non-disintegrated samples – Fig. 1.

Secondly, when the HRT was reduced to 2 days, the COD removal increased significantly and amounted to 87.2 % and 84 % for the US-facilitated and non--facilitated samples, respectively.

Thirdly, the application of HRT of 1.5 was associated with an increase in OLR value to 2.6 kgCOD/m^3d. Under such conditions, the degree of COD removal increased to 88 % for the US-facilitated sample. In case of non-disintegrated sample, the recorded degree of COD removal was lower and amounted to 81 %.

Finally, when the HRT was reduced the most to 1 day, and the corresponding OLR value amounted to 4.0 kgCOD/m^3d, degree of COD reduction for ultrasonically treated

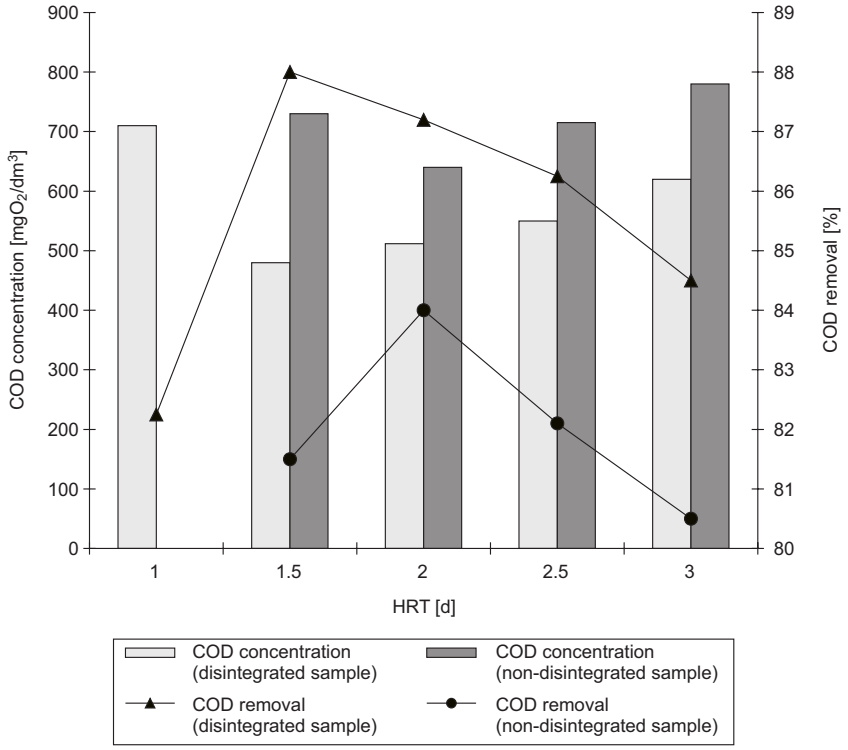

Fig. 1. Dependency of COD concentration as well as COD removal on HRT value in samples treated in MBR reactor

samples amounted to around 82.2 % and was lowered by 6 %, as compared with samples treated at HRT 1.5.

As the samples were undergoing digestion, the amount of biogas generated was recorded. It was observed that the reduction of HRT value lead to an increase in the amount of biogas generated. For, example, at the HRT of 3 days, the daily amount of biogas was about 14.8 and 13.5 dm^3 for US-facilitated and non-facilitated sample, respectively. Whilst at the HRT of 1 day, in both cases the amount of biogas generated increased by about 3 times. In comparison with the process which was not augmented by ultrasonic disintegration, the amount of biogas produced increased by 11 % on average. Figure 2 presents the amount of biogas generated at various HRT values for both conditioned and non-conditioned samples.

The results presented above allowed to specify the optimum HRT as well as the OLR value of the membrane reactor for both ultrasonically disintegrated and non-disintegrated samples. When the methane fermentation was conducted at 2.6 $kgCOD/m^3d$ and HRT of 1.5, the recorded degree of COD removal was the highest and amounted to 88 % in the MBR reactor coupled with ultrasonic disintegration. In the case of non-disintegrated process, the highest degree of COD removal, ie 84 % was recorded for the HRT of 2.0. It should be highlighted that the application of US-field allowed to

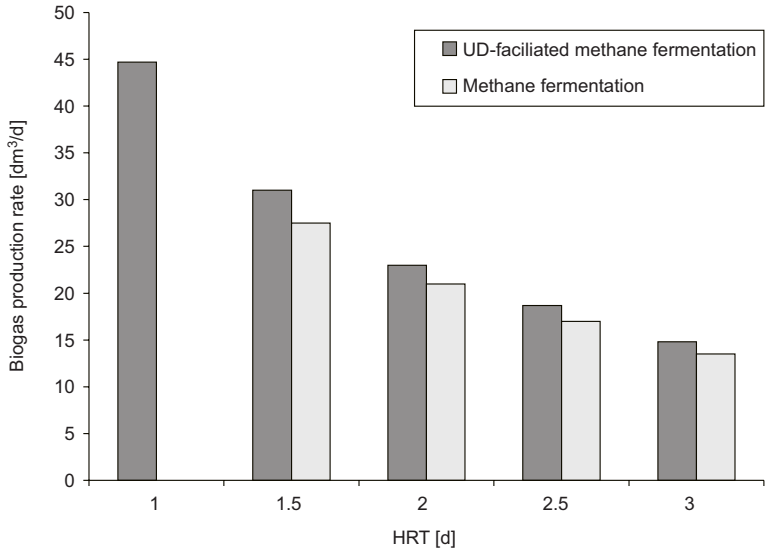

Fig. 2. The amount of biogas generated at various HRT values for both conditioned and non-conditioned samples

decrease the HRT value by 12 hours. What is more, US-facilitation positively impacted the overall biogas production – Fig. 2.

Post-treatment of landfill leachate in the process of reverse osmosis

Leachate samples treated in the process of anaerobic digestion, both disintegrated and non-disintegrated underwent the reverse osmosis process. In the beginning of the

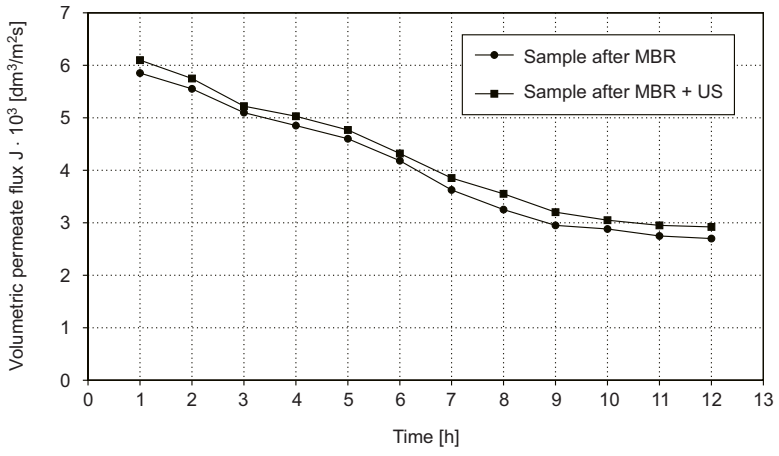

Fig. 3. Dependency of the volumetric permeate flux on the length [in hours] of the process

process, both volumetric permeate fluxes exhibited the same value of 8.13×10^{-3} dm^3/m^2s. After 12 hours of the process their value decreased significantly and amounted to 2.7 dm^3/m^2s for non-US facilitated sample and 2.9 dm^3/m^2s for UD-facilitated sample – Fig. 3.

As it was expected, the process of reverse osmosis turned out to be very effective. The COD and BOD values of samples after ultrasonic disintegration decreased by 97.5 % and 92.6 %, respectively. Whilst the concentration of chlorides and ammonia nitrogen was reduced by 90 % and 86 %, respectively, all compared with the values obtained after biological treatment. Likewise, posttreated samples which had been treated by means of anaerobic digestion without ultrasonic disintegration, allowed to receive a high degree of pollutant reduction. The values of COD and BOD decreased by 90.8 % and 96.2 %, respectively. The application of US field did not exert a positive influence on chlorides and ammonia nitrogen concentration, as compared with the values recorded for samples, which did not undergo US-facilitation. Table 2 presents the comparison of chemical parameters of the leachate treated in the MBR as well as MBR + US mode.

Table 2

Comparison of physical and chemical parameters of the leachate treated in the MBR and MBR+US mode

Indicator	Raw sample	Samples after anaerobic digestion		Samples after anaerobic digestion and reverse osmosis		Maximal discharge limits [5]
		MBR HRT = 2d	MBR + UD HRT = 1.5d	MBR +RO HRT = 2d	MBR + UD + RO HRT = 1.5d	
COD [mgO_2/dm^3]	4000	640	480	24	12	125
BOD_5 [mgO_2/dm^3]	1350	186	135	17	10	25
NH_4^+ [mg/dm^3]	280	207	207	20	29	10
Cl^- [mg/dm^3]	2500	2250	2300	209	210	1000

Conclusions

The application of the MBR reactor associated with a reverse osmosis process (RO) turned out to be effective for the treatment of the analyzed landfill leachate. It was established that ultrasonic disintegration reduced the HRT value from 2 to 1.5 days, as compared with non-disintegrated samples. Moreover, the COD removal as well as biogas production for each HRT value adopted was on average by 10 % and 11 % higher, respectively. However, landfill leachate after anaerobic digestion in both modes,

ie MBR and MBR+US, exhibited an excessive amount of contamination, which did not allow to discharge it into receiving water.

Post-treatment by means of reverse osmosis ensured a high degree of pollutant removal for both US-facilitated and non-facilitated modes. However, posttreated leachate exhibited an excessive amount of ammonia nitrogen – exceeding the discharge limits [5]. In order to overcome the problem, it was suggested that the leachate might subsequently undergo the process of ammonia stripping. It will be taken into consideration in the further stages of the research project.

Acknowledgements

The research project was supported by the Polish Ministry of Science and Higher Education (grant no. T09D 014 25).

References

[1] Surmacz-Górska J.: Degradacja związków organicznych zawartych w odciekach z wysypisk. Monografia nr 5. PAN Komitet Inżynierii Środowiska, Lublin 2001.
[2] Żygadło M.: Gospodarka odpadami komunalnymi, Wyd. Polit. Świętokrzyskiej, Kielce 2002.
[3] Szyc J.: Odcieki ze składowisk odpadów komunalnych. Monografia, Wyd. Naukowe Gabriel Borkowski, Warszawa 2003.
[4] El-Fadel M. and Findikakis N.: *Environmental impacts of solid waste landfiling*. J. Environ. Manage. 1997, **50**, 1–25.
[5] Rozporządzenie Ministra Środowiska z dnia 24 lipca 2006 r. w sprawie warunków, jakie należy spełnić przy wprowadzaniu ścieków do wód lub ziemi. DzU Nr 137, poz. 984.

WPŁYW POLA ULTRADŹWIĘKOWEGO NA EFEKTYWNOŚĆ WSPÓŁOCZYSZCZANIA ODCIEKÓW W UKŁADZIE ZINTEGROWANYM FERMENTACJA BEZTLENOWA – ODWRÓCONA OSMOZA

[1] Instytut Inżynierii Wody i Ścieków
Politechnika Śląska
[2] Instytut Inżynierii Środowiska
Politechnika Częstochowska
[3] Instytut Ochrony i Inżynierii Środowiska
Akademia Techniczno-Humanistyczna w Bielsku-Białej

Abstrakt: Przedstawiono wyniki badań dotyczące określenia wpływu pola ultradźwiękowego (UD) na efektywność współoczyszczania odcieków ze ściekami syntetycznymi w procesie fermentacji metanowej skojarzonym z odwróconą osmozą. Oczyszczanie ścieków metodą biologiczną realizowano w beztlenowym bioreaktorze z zanurzonym modułem membranowym (MBR), w którym stężenie osadu granulowanego utrzymywano na poziomie 10 g/dm^3. Czas zatrzymania w reaktorze zmieniano w zakresie wartości od 3 do 1 d, uzyskując dzięki temu wzrost obciążenia reaktora ładunkiem zanieczyszczeń od 1,3 do 4,0 kgChZT/m^{3}d. Stwierdzono, że kondycjonowanie odcieków w polu UD pozwoliło na skrócenie z 2 do 1,5 d hydraulicznego czasu zatrzymania mieszaniny współoczyszczanych ścieków w reaktorze MBR w porównaniu z procesem fermentacji prowadzonym dla odcieków nie poddawanych nadźwiękawianiu. Odnotowano również średnio o 10 % większy stopień usunięcia ChZT oczyszczonych ścieków dla każdego z przebadanych HRT i o 11 % większą objętość generowanego biogazu. Z uwagi na fakt, że ścieki po procesie beztlenowej biodegradacji w obu przebadanych układach (MBR i MBR+UD) nadal charakteryzowały się dużym ładunkiem zanie-

czyszczeń uniemożliwiającym ich bezpośrednie odprowadzenie do odbiornika naturalnego, podjęto próbę ich doczyszczania metodą odwróconej osmozy. Pomimo bardzo dużej retencji ładunku zanieczyszczeń, w otrzymanym permeacie stężenie azotu amonowego pozostało nadal na zbyt wysokim poziomie. W celu obniżenia pozostałego azotu amonowego poniżej wartości umożliwiającej odprowadzenie do odbiornika naturalnego zaproponowano, aby w kolejnych etapach badań włączyć do badanego układu proces odpędzania amoniaku.

Słowa kluczowe: odcieki ze składowisk odpadów komunalnych, fermentacja metanowa, reaktor membranowy (MBR), odwrócona osmoza (RO), pole ultradźwiękowe

ECOLOGICAL CHEMISTRY AND ENGINEERING A

Vol. 16, No. 11 2009

Jarosław ZAWADZKI[1] and Piotr FABIJAŃCZYK[1]

FIELD MAGNETOMETRY FROM GEOSTATISTICAL PERSPECTIVE

MAGNETOMETRIA TERENOWA Z GEOSTATYSTYCZNEJ PERSPEKTYWY

Abstract: Field magnetometry is a method used for investigations of soil pollution, especially for screening and determination of locations with the highest concentration of pollutants ("hot spots"). The advantages and limitations of this method are still intensively discussed in the literature.

Field magnetometry is an example of measuring method that can be effectively supported by geostatistical methods. Often, during field measurements, even several types of magnetometric measurements are carried out, frequently combined with chemical ones. In a result, obtained data sets differ in a precision and give different information about potential soil contamination with heavy metals. Similarly to other methods, also in field magnetometry the most convenient, rapid and cost-effective measurements performed on soil surface are simultaneously less precise and often perturbed by many environmental and anthropogenic factors. Such data are often characterized by complex spatial distributions and neighboring measurements are not spatially independent. Consequently, classical statistical methods have limited applications.

In the studies of soil quality, it is crucial to investigate spatial correlations of studied phenomena. Accordingly, improper location of the measurement points at the study area may be a source of uncertainty and errors that will be much higher than errors connected with measurement devices. In addition, the cost of the field surveys can increase.

Geostatistics can be very effective tool that makes it possible to plan optimal measuring nets, integrate different types of measurements, minimize the cost of field surveys, and perform complex analyses with the assumed precision. Additionally, applications of geostatistics in field magnetometry may enable to eliminate errors connected with often controversial expert evaluations.

This work outlines possible applications of geostatistical methods in field magnetometry, and gives some recommendations in this subject.

Keywords: field magnetometry, magnetic susceptibility, geostatistics, heavy metals, soils, data integration, ecological risk

One of the inseparable characteristics of environmental data is a spatial nature of phenomena and linked with that spatial correlations. If samples collected in the field will be investigated using classic statistical methods, there will be impossible to take

[1] Environmental Engineering Faculty, Warsaw University of Technology, ul. Nowowiejska 20, 00–661 Warszawa, Poland, email: j.j.zawadzki@gmail.com; piotr.fabijanczyk@is.pw.edu.pl

into account spatial relations between samples. In contrast, geostatistics provides many tools that makes it possible to analyze spatially correlated data and spatial relationships between them [1, 2]. It is possible to describe and analyze spatial correlations that characterize studied phenomena using different geostatistical measures of spatial variability. Apart from that, using a variety of methods as cokriging or Co_Est [3–5] it is possible to integrate different types of data due to cross-correlations that exists between different types of measurements performed in the field.Data integration finds application especially when some type of measurement is difficult to sample or too expensive.

Above-mentioned advantages of geostatistics are especially beneficial in environmental studies [6, 7], where very often some measurements are difficult to carry out or expensive. At the same time, it is possible to use large data sets of cheap and easy-to-measure data, like information about soil, forest type etc. Moreover, in the studies of soil quality, it is crucial to investigate spatial correlations of studied phenomena. Accordingly, improper location of the measurement points at the study area may be a source of uncertainty and errors that will be much higher than errors connected with measurement devices. In addition, the cost of the field surveys can be increased.

Geostatistics can be very effective tool that makes it possible to plan optimal measuring nets, integrate different types of measurements, minimize the cost of field surveys, and perform complex analyses with the assumed precision. Additionally, applications of geostatistics in field magnetometry may enable to eliminate errors connected with often controversial expert evaluations.

Geostatisitcs

In the beginning, geostatistics was developed for the needs of the mining and petroleum exploration industry. After some time, geostatistical methods found applications in numerous other branches like hydrology, geology, environmental engineering etc. The theory of geostatistics was started by works of Danie Krige in the 1950's and later the mathematical formalization was given by Georges Matheron. The main goal of geostatistics is to describe and analyze data considering its spatial characteristics and spatial variability.

One of the most important tools of geostatistics is a semivariance function, which is a measure of spatial continuity. [3–5, 8]. The experimental semivariance is calculated as one-half of the average squared difference between values measured at sample points separated by vector **h**. The following formula is used for the semivariance calculations:

$$\gamma(\mathbf{h}) = \frac{1}{2N}\sum_{i=1}^{N}[Z(\mathbf{x}_i) - Z(\mathbf{x}_i + \mathbf{h})]^2 \tag{1}$$

where $\mathbf{x}_i$ is a data location, **h** is a lag vector, $Z(x_i)$ is the data value at location $\mathbf{x}_i$, and N is the number of data pairs spaced a distance and direction **h** units apart.

The plot of experimental semivariance is often referred as to variogram and is usually characterized by a range of correlation that is the distance at values are no more spatially correlated, and a sill that is a plateau of the variogram. Another important parameter of a variogram is a nugget effect that represents the vertical discontinuity at the origin. It is a combination of sampling error and short-scale variation that occurs at a scale smaller than the closest sample spacing.

In geostatistics, it is possible to investigate spatial correlations not only between one variable but also between several variables. Such spatial correlations can be investigated using cross-semivariance:

$$\gamma_{WZ}(\mathbf{h}) = \frac{1}{2N}\sum_{i=1}^{N}[W(\mathbf{x}_i) - W(\mathbf{x}_i + \mathbf{h})][Z(\mathbf{x}_i) - Z(\mathbf{x}_i + \mathbf{h})] \tag{2}$$

where $\mathbf{x}_i$ is a data location, $\mathbf{h}$ is a lag vector, $Z(\mathbf{x}_i)$ and $W(\mathbf{x}_i)$ are the data values at location $\mathbf{x}_i$ of different quantities, and N is the number of different type data pairs separated by length of the vector $\mathbf{h}$. The cross-semivariogram quantifies the joint cross-correlation between two different variables. In some situations, it is necessary to calculate measure of joint spatial variability that is called the pseudo-cross-semivariogram:

$$\gamma_{WZ}(\mathbf{h}) = \frac{1}{2N}\sum_{i=1}^{N}[W(\mathbf{x}_i) - W(\mathbf{x}_i + \mathbf{h})]^2 \tag{3}$$

Such measure is especially useful in case of small data sets, when classic cross-variograms cannot be reliable.

The main geostatistical method of spatial estimation is kriging that is a linear estimator:

$$Z^* = \sum_{i=1}^{n}\lambda_i z_i \tag{4}$$

where: λ_i are the weights, z_i are the known data values.

Kriging weights are calculated by minimizing the variance of estimation and simultaneously the average estimation error is set to zero.

It is possible to perform spatial estimation using more than one variable. The method that makes is possible to use multiple variables, which ought to be strongly correlated with each other, is called cokriging [4, 5]. It finds application when samples of primary variable (often referred as to hard data) are difficult to collect, are too expensive or too rarely sampled. Data integration is done due to cross-correlations between primary and secondary variables (often referred as to soft data). Such integration of multivariate information is especially advantageous in environmental studies, where some measurements eg chemical ones are difficult to obtain or are expensive, whereas another type of information is cheap or relatively easy to obtain (eg magnetic susceptibility). Similarly to kriging, cokriging minimizes variance of estimation error of primary variable,

utilizing cross-correlations between primary variable and secondary variables. The value of primary variable, estimated at unknown location, is calculated using linear combination of both variables:

$$Z^*(\mathbf{x}_0) = \sum_{k=j}^{N_1} a_j \, z(\mathbf{x}_j) + \sum_{l=1}^{N_2} b_l \, w(\mathbf{x}_l) \tag{5}$$

where: $z(\mathbf{x}_j)$ is the j-th nearby sample primary value weighted by a_j, and $z(\mathbf{x}_l)$ is the i-th nearby secondary value weighted by b_i, N_1 and N_2 are, respectively, the numbers of nearby sample primary values and nearby secondary values.

Typically, cokriging gives more precise results than kriging. However, it is necessary that the hard and soft data must be strongly correlated, and the value of classical Pearson correlation coefficient should equal about 0.4 to 0.9. If correlations between hard and soft data are too weak, cokriging can give even worse estimation results than kriging. Conversely, if correlations between hard and soft data are very high and the Pearson correlation coefficient is close to one it is not advantageous to use cokriging because it gives the similar results like multivariate linear regression.

It is the most difficult to apply cokriging when only small number of measurements is available (often referred as to small dataset problem). If the number of soft data is large but the number of primary samples is too low, it can be very difficult, or almost impossible to calculate and model reliable variograms and cross-variograms. According to our experience with data integration in field magnetometry, at least 40 to 50 measurements of primary variable are needed to calculate reliable cross-variograms and use cokriging method. In such situations, it is necessary to use different methods of data integration (eg Co_Est method) or calculate some robust estimators instead of cross-variograms (eg pseudo cross-variograms).

The indicator methods that include both kriging and cokriging are especially usefully applied in field magnetometry. In this procedure, the measured values are transformed into indicator values: ie measured value is assigned with 0 if it is less than pre-defined cutoff level, or otherwise it is assigned with 1. Indicator techniques are very resistant to outliers and are appropriate for non-Gaussian distributions. Furthermore, using these methods it is possible to include in analyses also the additional qualitative information like soil type, land use, forest type, etc.

Field magnetometry

Field magnetometry is a method used for investigations of soil pollution, especially for screening and determination of locations with the highest concentration of pollutants (“hot spots”). The advantages and limitations of this method are still intensively discussed in the literature [2, 9–13].

Field magnetometry is an example of measuring method that can be effectively supported by geostatistical methods. Often, during field measurements, even several types of magnetometric measurements are carried out, frequently combined with chemical ones. In a result, obtained data sets differ in a precision and give different

information about potential soil contamination with heavy metals. Similarly to other methods, also in field magnetometry the most convenient, rapid and cost-effective measurements performed on soil surface are simultaneously the less precise and often perturbed by many environmental and anthropogenic factors. Such data are often characterized by complex spatial distributions and neighboring measurements are not spatially independent. Consequently, classical statistical methods have limited applications.

Geostatistical issues in field magnetometry

Selection and split of the study area

Frequently, a study area can be composed of sub-areas, with different types of forest (deciduous or coniferous) or of forest with different age. In case of high heterogeneity of a development of particular soil horizons, especially the top ones (Ol – organic litter, Of – organic fermentation, Oh – organic humic), magnetic particles of anthropogenic origin may be accumulated at different depths. Furthermore, magnetic particles may be also dispersed in soil layers of different thickness. In a result, it may happen that despite of the same industrial dust deposition the values of magnetic susceptibility measured at the soil surface will be different.

In such cases, it is advantageous to investigate these sub-areas individually. It is needed because of the possible significant differences in spatial variability of magnetic susceptibility measured at those sub-areas. However, in order to distinguish better these sub-areas it highly useful to calculate and model global semivariance, which shows the ranges of spatial correlations. Similarly, the vertical semivariances of magnetic susceptibility should be calculated and modeled separately for each heterogeneous sub-area.

Planning measuring net

Geostatistical methods allow for significant decrease of the cost of expensive environmental studies. However, magnetometric measurements should be carefully planned in order to maximize the effectiveness of geostatistical methods. Many geostatistical methods, especially those used for data integration (like cokriging), are very sensitive to sampling grid configuration, number of samples etc., but in the same time, there is no need for a use of strictly regular measuring networks. The negative effect of an irregularity in sampling grids may be decreased by use of geostatistical methods. Moreover, it is often even advantageous to avoid regular sampling schemes. Regular sampling may cause the appearance of the periodical effects, and in a result, difficulties in modeling of spatial variability of magnetic susceptibility.

Measurements of magnetic susceptibility should be carried out with such sampling density that assures that an average distance between samples is about 30 % to 50 % of characteristic scale of spatial variability (Fig. 1). An use of such sampling density enables to investigate spatial variability of magnetic susceptibility only in that scale that

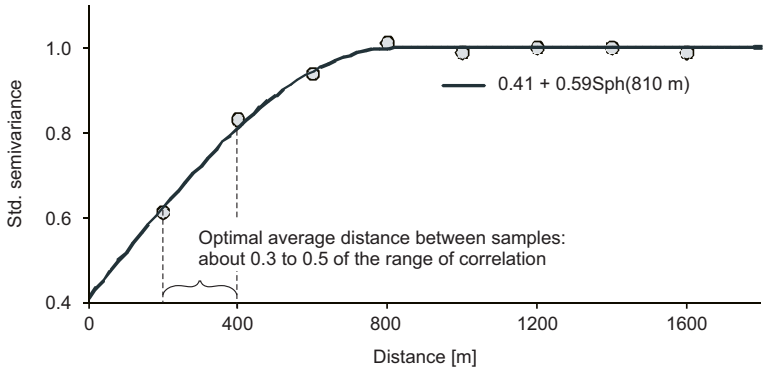

Fig. 1. Assessing of an optimal average distance between measuring points

will be used for modeling of spatial distributions. This way, spatial variability characteristic for smaller scale will not have negative influence on the modeled spatial distributions.

Proper densities of sampling grids should be determined also according to the local geological conditions. For example, during previous studies, significant differences in spatial variability of magnetic susceptibility measured at loam and sandy soil were also observed. Magnetic susceptibility measured at sandy soils was characterized by almost two-times shorter range of correlation. For that reason, it is recommended to use denser sampling grids at areas occupied by sandy soils. Particular attention should be drawn to the planning of sampling grids when measurements will be integrated using chosen geostatistical methods. Usually the number of hard measurements (eg chemical ones or magnetometric ones in soil profiles) should be greater than 40 to 50, although the number of these samples strongly depends on the scale of the study area as well as on the observed spatial variability. If the number of chemical samples exceeds several dozens, it should be sufficient to calculate reliable cross-variograms, and consequently to use multivariate geostatistical methods like cokriging. The number of magnetometric measurements at soil surface (soft measurements) should be at least a few times greater than the number of hard measurements.

If the number of hard measurements will be very low, it may happen that there will be a need for modeling pseudo cross-variograms or to use different methods of data integrations like Co_Est. In such cases, it is recommended not to perform chemical and magnetometric measurements at the same sample points because it will be impossible to use Co_Est method and to calculate pseudo cross-variograms. It is also useful to spread the locations of hard and soft measurements uniformly at the study area. Local clustering of data usually causes that modeling of spatial variability is more difficult.

It is also advisable to perform measurements in several stages. In the first one, it is recommended to perform the measurements of magnetic susceptibility with a MS2D sensor. This stage can be used as a fast screening method for preliminary recognition of the study area.

Typically, at the selected study area measurements can be performed beginning from the most imprecise, but the cheapest ones and finishing at the the most precise, but expensive ones. Firstly, the measurements of magnetic susceptibility at soil surface can be carried out, after that measurements of magnetic susceptibility in soil profile, and finally chemical analyses. Such measurements usually will not be performed at the same locations. For that reason, it might be difficult to investigate correlations using classic statistics and the Pearson correlation coefficient. It is recommended to use geostatistical measures of spatial correlations and cross correlations, like correlograms and cross--correlograms.

Planning the measurement at sample point

Apart from planning the measurement net, it is also important to use properly the information collected at single sample point. It is especially important in case of measurements that are cheap and easy-to-measure, but give imprecise information about studied phenomena. In field magnetometry, it concerns measurements of magnetic susceptibility performed at soil surface. Usually, at selected sampling point, magnetometric sensor was used to perform a series of 10 to 15 measurements of magnetic susceptibility in a circle of about 2 m diameter. Such methodology was recommended heretofore. However, it would be more advantageous not to average these values before applying further geostatistical analyses. It allows model the spatial variability of magnetic susceptibility more precisely, and no additional information from measurements is lost. It concerns especially the spatial variability in a micro-scale that contributes to the nugget effect. The nugget effect is also connected with measuring errors and it is important to assess the uncertainty of spatial distributions of magnetic susceptibility.

Assessing the extent of polluted area

The degree of development of uppermost soil horizons and its thickness can significantly affect the values measured with MS2D sensor due to its limited to 10 cm penetration range. To avoid these problems, it is recommended to geostatistically integrate these measurements with the thickness of Of, Ol and Ah horizons. Such methodology allows for taking into account the individual characteristic of the study area.

The assessment of the potentially polluted area should be performed rather using robust geostatistical methods like indicator or disjunctive kriging than ordinary one. This is caused due to usually observed complicated distributions of magnetometric data. In order to obtain better precision, geostatistical analyses can be performed separately for sub-areas with different thickness of Of, Ol and Ah horizons.

The extent of polluted area can be quantitatively assessed using measurements of magnetic susceptibility in a soil profile, especially the area under the curve of magnetic susceptibility against the depth. This area should be calculated beginning from the soil surface to the depth where the curve stabilizes. Spatial distributions should be then

modeled using some robust geostatistical methods like indicator kriging. However, as often as it is possible, measurements in a soil profile should be integrated with measurements of magnetic susceptibility performed at soil surface with a MS2D sensor. An area under the curve of magnetic susceptibility against the depth is more effective measure of potential pollution than other measures that can be calculated from the measurements in a soil profile, like maximum magnetic susceptibility, or magnetic susceptibility at specified depth. Such measures should be used rather as additional information, which may support the analyses.

Conclusions

Geostatistical methods are particularly suited for analyzing magnetometric measurements. Combining the field magnetometry and chemical analyses with geostatistical methods enables to better plan the measuring survey. By analyzing of the spatial variability of studied phenomenon (eg soil magnetic susceptibility or the content of heavy metals in soil), it is possible to use proper sampling density, and to place samples in the way that minimizes possible sampling errors and simultaneously maximizes the amount of information collected in the field.

Using geostatistical methods it is also possible to integrate different types of magnetometric measurements eg measurements of magnetic susceptibility in soil profile and those performed at the soil surface as well as combine the magnetometric measurements with geochemical ones, or geological information. Furthermore, it is possible to integrate magnetometric measurements with chemical analyses using geostatistical methods that allow for overcoming the problems connected with small data sets or irregular sampling designs.

References

[1] McBratney, A.B. and Webster R.: *Choosing function for semivariograms of soil properties and fitting them to sampling estimates*, J. Soil Sci. 1986, **37**, 617–639.
[2] Hanesch M. and Scholger R.: *Mapping of heavy metal loadings in soils by means of magnetic susceptibility measurements*, Environ. Geol. 2002, **42**(8), 857–870.
[3] Journel, A.G. and Huijbregts C.J.: Mining Geostatistics, Academic Press, London 1978.
[4] Isaaks E.H.R. and Srivastava M.: Applied Geostatistics, Oxford University, New York 1989.
[5] Goovaerts, P.: Geostatistics for Natural Resources Evaluation, Oxford University Press, New York 1997.
[6] Rouhani, S., Srivastava R., Desbarats A., Cromer M. and Johnson A.: Geostatistics for Environmental and Geotechnical Applications, STP 1283 1996.
[7] Zawadzki J.: *Geostatistical methods for continuity correlation evaluation: Studies of Fe, Pb and Zn concentrations in soil*, Inż. Ochr. Środow. 2002, **87**(3–4), 369–391.
[8] Gringarten E. and Clayton V.: *Deutsch Teacher's Aide Variogram Interpretation and Modeling*, Math. Geol. 2001, **33**(4), 507–534.
[9] Georgeaud V.M., Rochette P., Ambrosi J.P., Vandamme D. and Williamson D: *Relationship between heavy metals and magnetic properties in a large polluted catchments: the etang de Berre (south of France)*, Phys. Chem. Earth. 1997, **22**, 211–214.
[10] Strzyszcz Z.: *Magnetic susceptibility of soils in the area influenced by industrial emissions*, [in:] Soil Monitoring, Schulin R., Desalues A. (eds.). Birkhauser Verlag, Basel 1993, 1993, 255–269.
[11] Magiera T.: Wykorzystanie magnetometrii do oceny zanieczyszczenia gleb i osadów jeziornych. IPIŚ PAN, Zabrze 2004.

[12] Zawadzki J., Magiera T. and Strzyszcz Z.: *Analiza korelacji i regresji pomiędzy zawartością metali ciężkich w glebach Górnośląskiego Okręgu Przemysłowego, a ich podatnością magnetyczną*, Arch. Environ. Protect. 2004, **30**(2), 71–82.
[13] Magiera T., Lis J., Nawrocki J and Strzyszcz Z.: Podatność magnetyczna gleb Polski, PIG, Warszawa 2002.

MAGNETOMETRIA TERENOWA Z GEOSTATYSTYCZNEJ PERSPEKTYWY

Wydział Inżynierii Środowiska
Politechnika Warszawska

Abstrakt: Magnetometria terenowa jest metodą stosowaną do badań zanieczyszczenia gleby, w szczególności wykorzystywaną do wstępnego monitoringu jakości gleby na danym obszarze, wyznaczenia miejsc których występują największe stężenia zanieczyszczeń (“hot spots”). Zalety tej metody i jej ograniczenia są intensywnie dyskutowane w literaturze. Metoda ta jest rozwijana od wielu lat np. w ramach już zakończonego programu międzynarodowego MAGPROX.

Magnetometria terenowa jest wręcz klasycznym przykładem metody pomiarowej, w której można efektywnie wykorzystać metody geostatystyczne. W ramach badań magnetometrycznych zanieczyszczenia gleb wykonywanych jest często jednocześnie nawet kilka różnych typów pomiarów, którym towarzyszą nierzadko pomiary chemiczne. W rezultacie otrzymywane są zbiory danych charakteryzujące się różną precyzją oraz różnym rodzajem informacji na temat potencjalnego zanieczyszczenia gleb metalami ciężkimi. Podobnie jak w innych dziedzinach również w magnetometrii terenowej najbardziej wygodne, szybkie i tanie pomiary powierzchniowe gleby są jednocześnie najmniej dokładne oraz zaburzone poprzez różnorodne czynniki środowiskowe lub antropogenne. Dane te najczęściej mają skomplikowane rozkłady, sąsiednie pomiary nie są niezależne pomiędzy sobą. Tradycyjne obliczenia statystyczne mają więc bardzo ograniczoną przydatność.

Niezwykle ważną rolę w badaniach zanieczyszczenia gleb odgrywa znajomość korelacji przestrzennych badanych zjawisk. W związku z tym niewłaściwe rozplanowanie sieci pomiarowej na badanym obszarze może być przyczyną błędów oceny stężenia i rozkładu zanieczyszczenia gleby znacznie większych niż błędy pomiarowe związane z dokładnością aparatury pomiarowej. Może też radykalnie zwiększać koszty pomiarowe.

Geostatystyka może być również bardzo efektywnym narzędziem pozwalającym na właściwe rozplanowanie sieci pomiarowej, integrację różnorodnych pomiarów, minimalizację kosztów kampanii pomiarowych, wykonanie złożonych analiz i osiągnięcie założonej dokładności badań. Wykorzystanie geostatystyki w badaniach magnetometrycznych gleby pozwolić może w znacznym stopniu na eliminację dyskusyjnych ocen eksperckich. Jednym słowem, stosowanie geostatystyki może znacznie zwiększyć skuteczność stosowania metody magnetometrycznej.

Niniejsza praca prezentuje najważniejsze możliwości wykorzystania metod geostatystycznych w badaniach magnetometrycznej gleb, jak również prezentuje praktyczne zalecenia w tym zakresie.

Słowa kluczowe: magnetometria polowa, podatność magnetyczna, geostatyka, metale ciężkie, gleby, integracja danych, ryzyko ekologiczne

ECOLOGICAL CHEMISTRY AND ENGINEERING A

Vol. 16, No. 11 2009

Sabine FRIEDRICH[1] and Elly SPIJKERMAN[1]

CHLOROPHYLL *A* FLUORESCENCE AND ABSORPTION IN TWO *CHLAMYDOMONAS* SPECIES

FLUOROSCENCJA I ABSORPCJE CHLOROFILU *A* DWÓCH GATUNKÓW *CHLAMYDOMONAS*

Abstract: Phytoplankton densities in lakes and oceans are often measured via *in vivo* chlorophyll *a* (Chl *a*) fluorescence. This quick and non-invasive method has large advantages over traditional sampling and extraction methods. Here we hypothesize that measurements of *in vivo* fluorescence might overestimate the actual Chl *a* concentration when algal cells contain relatively high concentrations of Chl *a* degradation products, as a result of reaching the stationary phase in growth or living in a stress-full environment. Therefore the *in vivo* and *in vitro* fluorescence of Chl *a* was measured in two species of *Chlamydomonas* and compared with total Chl *a* content. Regular sampling over the full range of their growth curves was obtained. *Chlamydomonas reinhardtii* was selected as a species living in neutral, non-stressed environments and *Chlamydomonas acidophila* inhabits very acidic (pH 2.0–3.4), stress-full environments. Scattering of fluorescence during *in vivo* measurements resulted in an on average 25-fold lower Chl *a* concentration compared with *in vitro* measurements in both species. Cells of *C. reinhardtii* scattered approx. 1.5-fold more of the *in vivo* fluorescence than *C. acidophila*. The cellular Chl *a* content increased during the first fortnight period in both *Chlamydomonas* species. After reaching its maximum, the cellular Chl *a* content decreased with time in both species. This decrease was not accompanied by an increase of Chl *a* degradation products. The percentage of Chl *a* degradation products to total Chl *a* concentration was not significantly different between *C. acidophila* and *C. reinhardtii*; both species containing approximately 16 % of Chl *a* degradation products to total Chl *a*. Only 73–80 % of the concentration of Chl *a* measured by the *in vitro* fluorometric method was recovered in the HPLC. Therefore, despite the settings of the fluorometer, fluorescence possibly overestimated the Chl *a* concentration. In conclusion we find that external low pH or stationary growth does not result in increased concentrations of degradation products of Chl *a*. In addition, the extrapolation from the *in situ* detection of Chl *a* fluorescence with multiparameter sensors to concentrations of Chl *a* must be performed with great care as the use is subject to species-specific scattering of the fluorescence signal.

Keywords: *Chlamydomonas reinhardtii*, *Chlamydomonas acidophila*, freshwater ecology, chlorophyll *a* fluorescence, chlorophyll *a* absorption, *in vivo* measurements, *in vitro* measurements, growth, degradations products, multiparameter probe, HPLC

During the last decades, new methods have been introduced that detect *in situ* chlorophyll *a* (Chl *a*) fluorescence in order to estimate the phytoplankton population density and distribution over the water column [1]. Such measurements are non-

[1] Department of Ecology and Ecosystem Modelling, University of Potsdam, Am Neuen Palais 10, Potsdam, Germany, email: frieds@uni-potsdam.de; spijker@uni-potsdam.de

-invasive, fast, labour extensive and do not produce toxic waste, and are therefore very popular. Changes of *in vivo* Chl *a* fluorescence over time in freshwater has been recognized to be a good way to identify the factors controlling phytoplankton growth [2]. By using the fluorescence of Chl *a*, only the phytoplankton and not the bacteria or suspended matter is detected.

However, dependent on the growth phase or stress condition of an algal cell, Chl *a* can be converted to its degradation products chlorophyllide *a* and pheophytin *a* [3–4]. Besides growth phase and pH, numerous other variables can influence the degradation of Chl *a*, such as the presence of predators, oxygen concentration and microbial processing [5]. Under metal contaminated conditions, the exchange of magnesium by zinc is possible, changing the molecular characteristics of Chl *a*, but still enabling its use in light-harvesting [6]. The degradation products of Chl *a* have other absorption characteristics than Chl *a* and also another *in situ* fluorescence, but do not necessarily hamper or change light harvesting processes. It has been suggested that Chl *a* fluorescence in stress-full environments is higher than in other water bodies and that this enhanced fluorescence overestimates the Chl *a* concentration and consequently phytoplankton biomass present in the lake.

In a study to resolve the importance of the concentration of degradation products of Chl *a* compared to total Chl *a* concentration, Stich and Brinker [7] compared with uncorrected versus corrected Chl *a* concentrations taken from six different lakes in south-western Germany over a two-year period. The uncorrected Chl *a* concentration consisted of the sum of Chl *a* and its degradations products, whereas corrected ones consisted of Chl *a* concentrations only (the correction was performed via acidification of the extract that transforms all Chl *a* into pheophytin *a*). They concluded that uncorrected values were more reliable than corrected values, the method to determine uncorrected values was less timeconsuming and values measured on different types of spectrophotometers were comparable [7]. Their study emphasized that in lakes, the concentration of Chl *a* degradation products to the total Chl *a* concentration are usually insignificant.

Concentrations of Chl *a* and its degradation products can be measured using different methods, see eg [8–9]. Basically, two methods can be distinguished, a photometric and a fluorimetric determination after the extraction of the pigments in an alcohol. The *in situ* Chl *a* concentration can also be detected by these two methods, but scattering and re-absorption characteristics of particles prohibit quantification. Large effort has been made into the establishment of a reproducible and accurate determination of Chl *a* concentrations. In numerous studies, measuring devices, extraction solvents and procedures have been compared (eg [10–12]). From these comparisons, no method has been considered superior, as the efficiency of the extraction method and solvent varies with, for example, the composition of the phytoplankton community. When properly extracted, a fluorometric method with certain lamp and filter settings allows a fast and more reliable determination of Chl *a* in presence of Chlorophyll *b* (Chl *b*) and pheopigments than the photometric methods described thus far [13]. However, the method will not discriminate chlorophyllide *a* from Chl *a* because the two pigments have identical spectral properties, and only chromatographic analysis (HPLC) can separate between these two.

With the increasing use of *in situ* fluorescence probes it is of general interest to know to what extend measurements of the *in situ* fluorescence of Chl *a* equal those of the extracted concentration and, to know to what extend the *in situ* fluorescence signal is influenced by Chl *a* degradation products. Therefore, we compared the Chl *a* absorption and fluorescence of two *Chlamydomonas* species over their growth curve. To possibly detect the influence of external pH on the accumulation of Chl *a* degradation products we selected the acidophilic species *Chlamydomonas acidophila* and the mesophile *Chlamydomonas reinhardtii*.

Chlamydomonas species can be found in a wide variety of habitats worldwide [14]. *Chlamydomonas acidophila* is a dominant phytoplankton species in very acidic lakes [15–[16]. Although the pH of these lakes is extremely low, the internal pH of *C. acidophila* is neutral [17–18]. The maintenance of the large pH gradient over the plasma membrane is considered a stressful condition, likely enhancing metabolic costs [17]. *Chlamydomonas reinhardtii* is a well-described species abundant in neutral, eutrophic fresh water lakes and soils [19–23]. As a consequence of the neutral pH of its environment, *C. reinhardtii* has only a minor pH gradient over its plasma membrane.

Methods

Cultures

Growth experiments were started with 7 day-old pre-cultures of *Chlamydomonas reinhardtii* Dangeard (Algal collection Göttingen, SAG 11-32b) and *Chlamydomonas acidophila* Negoro (SAG 2045).The cell density at the beginning of the experiment were between 10,000 and 80,000 cells cm^{-3}. *C. reinhardtii* was grown in Woods Hole Medium at pH 7.0 [24].

C. acidophila was grown in 111 Medium at pH 2.65 [25]. The 111 Medium reflects the chemical composition of the water from Lake 111; an acidic, metal-rich lake in Lusatia, Germany. Cultures were maintained at 20 ± 1 ^{o}C at a light: dark cycle of 16:8 h. Incident light irradiance was 80 μmol PAR m^{-2} s^{-1}. Experiments were performed in triplicate. Every day or every second day about 80 cm^3 was aseptically removed from each culture for measurements.

Determination of cell density

For cell density, samples were fixed with 1 % Lugol solution and counted on an automatic particle counter (Casy 1, Model TT, Schärfe, Reutingen, Germany). Growth rates (μ) were calculated over the first 4 days assuming exponential growth.

Fluorometry

For *in vitro* determination of Chl *a* fluorescence, algal culture was filtered on Whatman GF/F filters, immediately rinsed with 0.1 M ammonium acetate [3] and extracted in 90 % ethanol by vigorous shaking for 5 minutes. The extract was then measured on a fluorometer (Turner TD-700, F4T41/2B2 lamp, ex: 436 nm (FS10), em:

680 nm (FS10), GAT Bremerhaven, Germany), which was calibrated with a commercially obtained Chl *a* standard (Sigma, Germany).

In vivo Chl *a* fluorescence was determined directly on life culture suspensions, eventually diluted with culture medium to avoid changes in the sensitivity settings of the fluorometer.

HPLC analysis

For total pigment analysis on HPLC, cultures were filtered as described above, immediately frozen in liquid nitrogen and stored at –80 ^{o}C till later analysis. Extraction with 90 % acetone was performed in dark and cold conditions using a Mini-Beadbeater (Biospec Products, Bartlesville, OK, USA). HPLC analysis was done following Gilmore and Yamamoto [26] using an ODS1-column (non-end capped, lightly carbon-coated, Spherimage-80, 5 μm, Knauer, Berlin, Germany). Absorbance was recorded at λ = 440 nm, 470 nm, 647 nm and 665 nm with a multiwavelength UV/VIS detector (PHD 601, GAT, Bremerhaven, Germany), but concentrations were only calculated by using the signal at λ = 440 nm. The system was calibrated using a commercial standard of Chl *a* and Chl *b* (Sigma, Germany).

Multiparameter probe

Fluorescence of Chl *a* from cell suspensions of life algal cultures with various cell density was measured with a multiparameter probe (Ocean Seven 316, with an integrated Seapoint chlorophyll fluorometer, Idronaut, Italy). The Seapoint chlorophyll fluorometer (SCF) uses modulated blue LED lamps and a blue excitation filter to excite chlorophyll *a*. The fluorescent light emitted by the chlorophyll *a* passes through a red emission filter and is detected by a silicon photodiode. More specific, the fluorometer had the following filters: ex: 470 nm CWL (30 nm FWHM), em: 685 nm CWL (30 nm FWHM). These settings suggest the detection of *Chl b* and pheopigments besides Chl *a* [13]. *In vivo* fluorescence of the same suspensions was simultaneously measured on the calibrated fluorometer as described above.

Calculations were performed in Excel software (Microsoft Office Excel 2003). Tests for significance were performed using SPSS software (version 15.0 for Windows, Chicago IL).

Results

Growth curves

Despite the difference in pH of the medium, no significant differences in growth rates between the two *Chlamydomonas* species were detected (Fig. 1). The exponential growth rates over the first 4 days were calculated as 0.52 ± 0.14 d^{-1} for *C. reinhardtii* and 0.39 ± 0.15 d^{-1} for *C. acidophila* (mean ± SE). No lag-phase in growth was detected in any of the cultures and exponential growth started immediately after inoculation. In both *Chlamydomonas* cultures, the stationary phase was reached after approximately

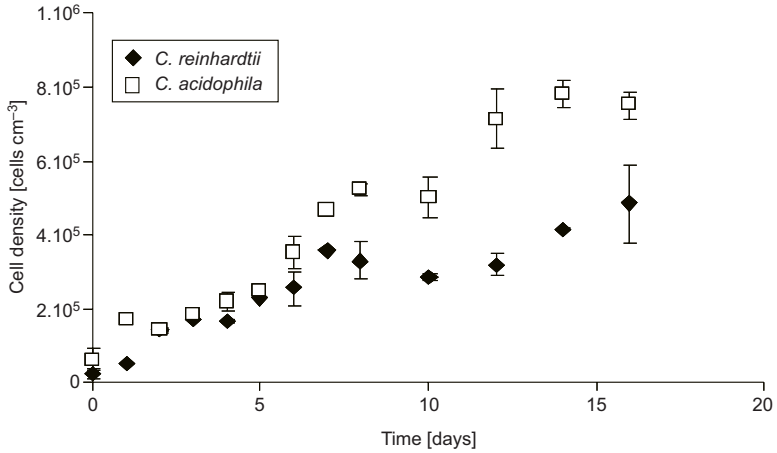

Fig. 1. Cell densities in [cells cm^{-3}] of *C. reinhardtii* and *C. acidophila* over time (in days) in batch culture (Mean ± SE of 3 replicates)

7–8 days. Increases in densities after the onset of the stationary phase were likely the result of evaporation or non-exponential growth resulting from increased CO_2 availability to the algal cells due to increased surface to volume ratio in the Erlenmeyer flasks. After reaching the stationary phase, *C. acidophila* cultures were denser than cultures of *C. reinhardtii*, this difference being nearly 2-fold.

In vivo Chl *a* fluorescence

The *in vivo* fluorescence increased over time, similar to increases in cell density for both Chlamydomonas species (Fig. 2). The increase in Chl *a* fluorescence was faster in

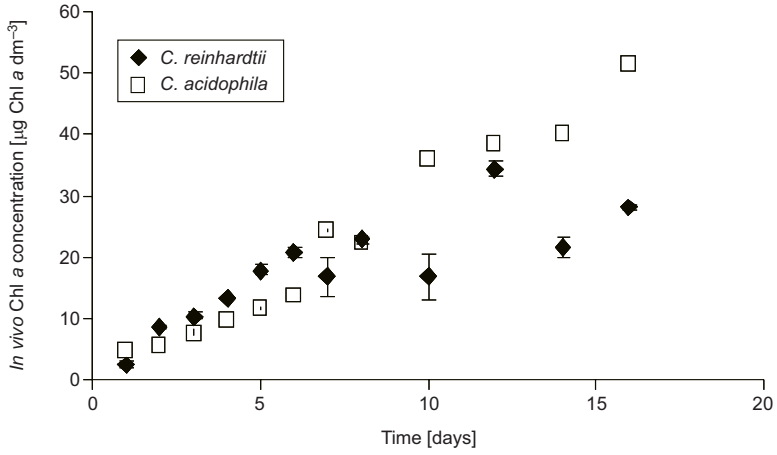

Fig. 2. *In vivo* fluorescence of Chl *a* in [µg Chl *a* dm^{-3}] in cultures of *C. reinhardtii* and *C. acidophila* over time (in days) in batch cultures (Mean ± SE of 3 replicates)

cultures of *C. reinhardtii* than in those of *C. acidophila* (3.5 and 1.9 µg Chl *a* dm^{-3} d^{-1} for *C. reinhardtii* and *C. acidophila*, respectively). Although the differences of Chl *a* fluorescence in both species reached in the stationary phase was smaller than the difference in cell density (Fig. 1), comparable to differences in cell density, *in vivo* fluorescence of Chl *a* was greater in cultures of *C. acidophila* than in cultures of *C. reinhardtii* (Fig. 2).

Cellular Chl *a* content

The cellular Chl *a* content of both *Chlamydomonas* species increased over time (Fig. 3). After reaching the highest value, the cellular Chl *a* content decreased again in *C. reinhardtii*, whereas it remained more or less constant in *C. acidophila* (Fig. 3). The results show a faster increase of cellular Chl *a* content in *C. reinhardtii* during the first 10 days of culturing, but equal cellular Chl *a* contents in both species after 16 days. The maximum cellular Chl *a* content in *C. reinhardtii* was 2.8 pg $cell^{-1}$ and in *C. acidophila* only 1.4 pg $cell^{-1}$ (Fig. 3).

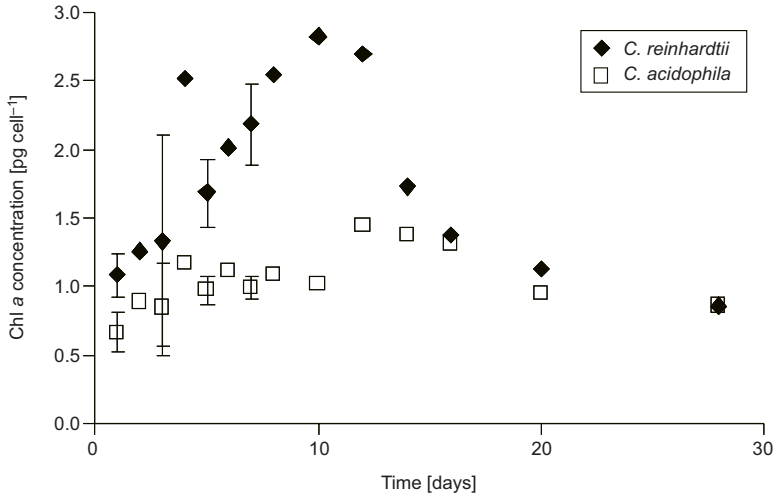

Fig. 3. Cellular chlorophyll *a* content in [pg Chl *a* $cell^{-1}$] over time (in days) in batch cultures of *C. reinhardtii* and *C. acidophila* (Mean ± SE of 2 replicates)

In vitro and *in vivo* fluorescence of Chl *a*

There was a linear relationship between the *in vitro* fluorescence and the *in vivo* fluorescence of Chl *a* in both species (Fig. 4a, b). In both species the measurement of the *in vivo* Chl *a* fluorescence was lower than that of the *in vitro* fluorescence**.** On average, the *in vivo* Chl *a* concentration was about a 23-fold lower than the *in vitro* concentration. For *C. reinhardtii* the *in vivo* Chl *a* fluorescence was 31-fold lower than the *in vitro* fluorescence (Fig. 4a) and for *C. acidophila* this was only 15-fold (Fig. 4b).

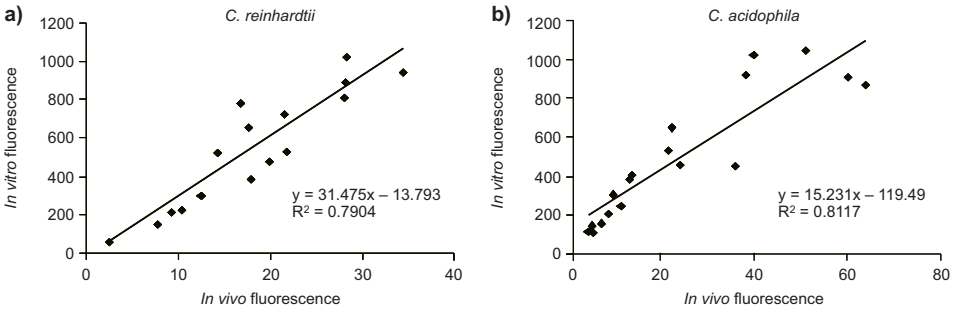

Fig. 4. The *in vitro* Chl *a* fluorescence in relation to the *in vivo* fluorescence in *C. reinhardtii* (a) and *C. acidophila* (b)

These results therefore show that *C. reinhardtii* scatters approximately 1.5-fold more of the emitted light than *C. acidophila*.

Comparison between fluorescence and absorption

The concentration of Chl *a* obtained via HPLC was linearly related to the concentration of Chl *a* obtained via fluorescence in both Chlamydomonas species (Fig. 5a, b). The slopes of the curves reveal that only 73–80 % of the concentration of Chl *a* measured via fluorescence was recovered when measuring via absorption in the HPLC (Fig 5a, b; Table 1). The recovery increased to 86–91 % when the concentration of degradation products of Chl *a* were included in the analysis of this linear relationship (Table 1). These degradation products mainly consisted of chlorophyllides *a* as hardly any pheophytin a was detected (results not shown).

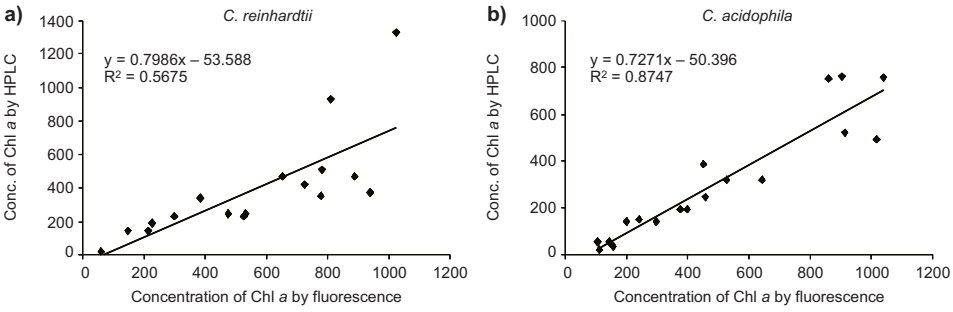

Fig. 5. The concentration of Chl *a* as measured by HPLC in relation to the concentration of Chl *a* as measured by fluorescence in *C. reinhardtii* (a) and *C. acidophila* (b). The fluorescence on both axis is given in [μg Chl *a* dm^{-3}]

The recovery of measurements of the Chl *a* concentration in the HPLC was always higher in *C. reinhardtii* than in *C. acidophila*, suggesting that either the measurement of total pigment composition via HPLC was more problematical in *C. acidophila* or that

the Chl *a* molecules in *C. acidophila* were more fluorescent (Table 1). These differences were, however, smaller than 5 % and were therefore considered not important.

Table 1

The square of the correlation coefficient (R^2) and the slope of linear regressions through the concentration of Chl *a* or Chl *a* + degradation products as measured by HPLC against Chl *a* fluorescence as measured by fluorometer

		R^2	Slope
C. reinhardtii	Chl *a* concentration	0.57	0.80
	Chl *a* + degrad. prod. concentration	0.60	0.91
C. acidophila	Chl *a* concentration	0.87	0.73
	Chl *a* + degrad. prod. concentration	0.92	0.86

Concentration of degradations products of Chl *a*

When analysing the percentage of Chl *a* degradation products to total Chl *a* concentration in both *Chlamydomonas* species, it was observed that there was no significant difference between *C. reinhardtii* and *C. acidophila* (Paired T-test, t = –2.1, df = 13, p = 0.056; Fig. 6). On average, the percentage of Chl *a* degradation products to total Chl *a* concentration was slightly higher in *C. acidophila* compared with *C. reinhardtii*, but this difference was not significant (ie 5.6 %). In addition, the percentage of Chl *a* degradation products in relation to the concentration of Chl *a* did not change over growth in *C. reinhardtii* (ANOVA, F = 1.13, df = 1,12, p = 0.31) and also not in *C. acidophila* (ANOVA, F = 3.97, df = 1.12, p = 0.07; Fig. 6).

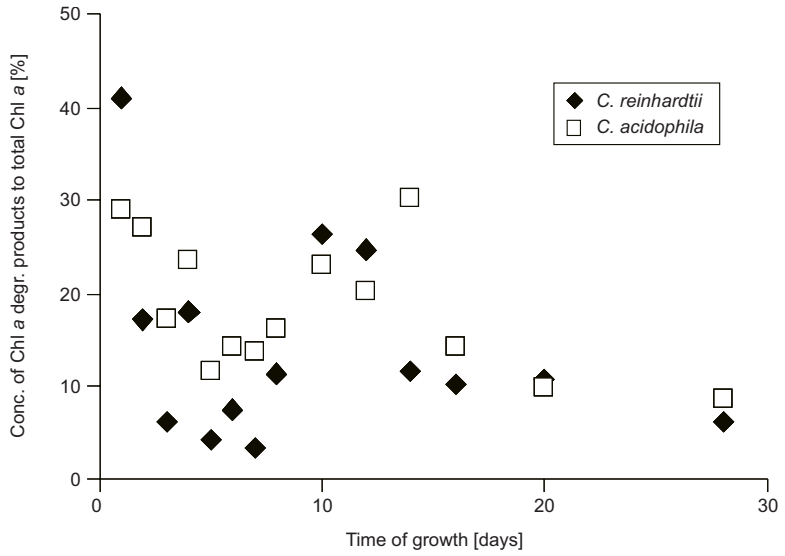

Fig. 6. The percentage of Chl *a* degradation products to total Chl *a* concentration in *C. reinhardtii* and *C. acidophila* over the time of growth

Multiparameter probe

The measurements of Chl *a* fluorescence made by the multiparameter probe were linearly related to the measurements of Chl *a* fluorescence gathered by the fluorometer (Fig. 7). The measurements reveal that the same signal of the multiparameter probe (here in mV) resulted in a higher fluorescence of Chl *a* in the fluorometer in *C. acidophila* than in *C. reinhardtii* (Fig. 7). The difference in fluorescence between the two *Chlamydomonas* species was approximately 1.5-fold.

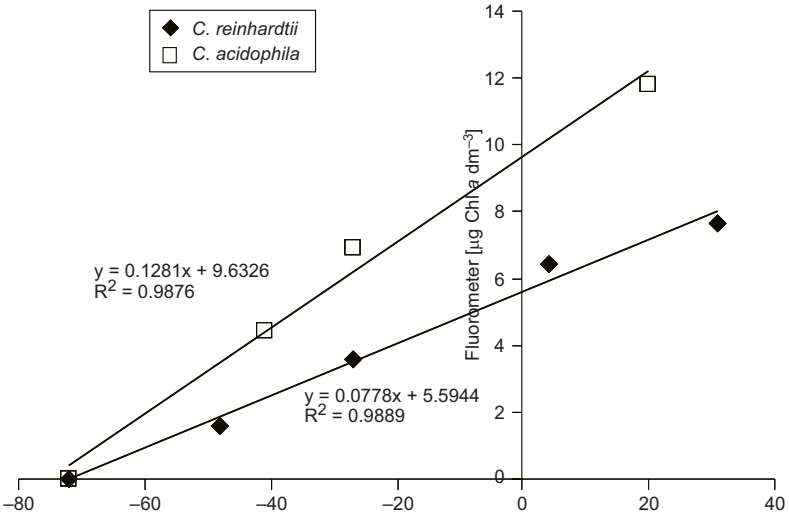

Fig. 7. *In vivo* chlorophyll a fluorescence of *C. reinhardtii* and *C. acidophila* measured with a fluorometer in relation to measurement with a multiparameter sensor

Discussion

In this study we compared the chlorophyll a fluorescence and absorption in an acidophilic and a mesophilic *Chlamydomonas* species over their growth curve. We hypothesized that stress conditions such as the stationary phase in growth or a low external pH increases the cellular concentration of Chl *a* degradation products and consequently enhances fluorescence of Chl *a* compared with its absorption.

In contrast to expectations, no increase in the concentration of Chl *a* degradation products was found in either *Chlamydomonas* species over the course of time of growth in batch culture. Several studies suggest that stressful conditions, such as nutrient limitation, high oxygen concentrations, or the presence of predators will enhance the conversion of Chl *a* to its degradation products, chlorophyllide *a* and pheophytin *a* [3–5]. During batch growth, light or nutrients start limiting growth and upon entering the stationary phase, stress increases by some growth limiting condition. In support to our findings, recent experiments with *C. acidophila* showed [27] no enhanced

concentration of pheophytin a to Chl *a* + pheophytin *a* in P-limited cells compared with P-saturated ones.

In our study, the maximum cellular Chl *a* content of *C. acidophila* (1.4 pg cell^{-1}) was approximately 2-fold lower than that of *C. reinhardtii* (2.8 pg cell^{-1}), although the acidophilic species can reach a Chl *a* content similar to that of *C. reinhardtii*, ie 2.2–2.5 pg cell^{-1} [28–29]. Obviously, some nutrient in the 111 Medium inhibited the Chl *a* synthesis. Studying the elemental ratios in the medium provokes that Chl *a* synthesis is most likely inhibited by a limitation of nitrogen, provided as ammonium [25]. The molar N to P ratio in 111 Medium is 3.7, whereas this is 20 in, for example, Woods Hole medium [24]. A molar N : P ratio below 16 would suggest N-limiting conditions according to the Redfield ratio [30]. An N-limitation can explain the low cellular Chl *a* content in *C. acidophila* as it will decrease the Chl *a* content in algae [31].

Between the results gathered from the two *Chlamydomonas* species only a minor difference was found, this being a slightly higher fluorescence of Chl *a* compared with its absorption measured *via* HPLC in *C. acidophila* than in *C. reinhardtii*. Assuming a higher fluorescence of Chl *a* degradations products than from Chl *a* itself, the results suggests that *C. acidophila* contains more degradation products than *C. reinhardtii*. The latter was found although the difference was not significant (Fig. 6), and therefore our results support this hypothesis. The enhanced concentrations of Chl *a* degradation products (especially in the form of chlorophyllide *a*) in *C. acidophila* could both be the result of the low external pH in the growth medium, but could also have resulted from the N-limitation. In contrast, Meyns et al [32] obtained a lower Chl *a* concentration of 10 to15 % in HPLC than in absorption measurements. They assumed that the presence of degradations products provided part of the explanation for this difference, but could not fully explain their observations. Possibly, the lower Chl *a* concentration estimation by HPLC is a general problem related to the attachment and detachment of Chl *a* molecules to the column?

There are several well-known degradation products of Chl *a*: pheophytin *a*, chlorophyllide *a* and pheophorbide *a* [8, 33]. In addition, a red pigment accumulated during growth in a Chl *b*-less mutant of *C. reinhardtii* that was considered a breakdown product of Chl *a* [34]. This red pigment had a larger similarity to carotenoids than chlorophylls in its absorption characteristics and was water soluble. In contrast to their experiments under aerobic conditions [34], under anaerobiosis pyropheophorbide *a* was the main Chl *a* degradation product [22]. Pyropheophorbide *a* is a pigment more similar to pheophytins in its absorption characteristics. The difference in Chl degradation in response to oxygen concentration can explain the presence of degradation products in field samples and might explain the accumulation of pheopigments in stationary phase grown algal cultures, when cell densities are very high and oxygen gradients within the culture can be significant.

A full description of Chl *a* degradation to other products such as chlorophyllide *a* is provided by Mantile et al [33]. In the HPLC measurements, we detected mainly chlorophyllide *a* and hardly any pheophytin *a*. This is a logic result of the fact that pheophytin *a* does not absorb much light at λ = 440 nm, the wavelength of our Chl *a* detection in the HPLC. In contrast, the absorption spectrum of chlorophyllide *a* is

largely identical to that of Chl *a* and both pigments absorb well at $\lambda = 440$ nm [8]. The absorption spectra of pheophytin *a* and pheophorbide *a* are also alike and are called pheopigments. Welschmeyer [13] described a fluorometric method with a certain lamp and filter settings that allows for a reliable measurement of Chl *a*, without interference of Chl *b* and pheopigments. However, the fluorescence method will not discriminate chlorophyllide *a* and Chl *a* because they have nearly identical absorption spectra. Most likely, the enhance concentrations of chlorophyllide *a* in our fluorescence measurements resulted in an overestimation of the 'true' Chl *a* concentration by minimal 10 and maximal 27 %.

The percentage of Chl *a* degradation products to total Chl *a* concentration ranged between 3 and 40 %, the average value being only 16 % (Fig. 6). These results support the study from Stich and Brinker [7] who emphasized that in lakes, the concentration of Chl *a* degradation products to the total Chl *a* concentration are usually insignificant. Unfortunately, in their investigations only a comparison between acidified and non-acidified extracts was made, without any information on the possible concentrations of Chl *a* degradation products [7].

The use of *in vivo* fluorescence measurements via multiparameter probes has become eg [1, 35] and it is therefore of importance to what extend measurements of the *in situ* fluorescence of Chl *a* equal those of the extracted concentration and to know to what extend the *in situ* fluorescence signal is influenced by Chl *a* degradation products. In Jeffrey et al [8] contour plots of Chl *a* are provided recorded in the Pacific Ocean from measurements with a calibrated multiparameter probe and with HPLC, showing remarkably similar contours (Fig. 4.14, page 150). In contrast, our data show already 1.5-fold differences in scattering and re-absorption characteristics between two species of *Chlamydomonas*, expecting much larger differences in measurements on natural phytoplankton. The advantages of using a multiparameter probe in measuring the *in vivo* Chl *a* concentration (ie non-invasive, fast, labour extensive and not producing any toxic waste) largely compensate for the disadvantages (ie calibration difficulty). Based on our results we emphasize to take care for interpreting the *in vivo* Chl *a* concentration into the Chl *a* quantification as the *in vivo* fluorescence will be influenced by concentrations of eg chlorophyllide *a*, Chl *b*, species specific scattering and re-absorption of emitted light.

Acknowledgements

This work has been supported by the German research foundation (DFG, SP695/2) and a European Union Marie Curie Development Host Fellowship (HPMD-CT-2001-00103).

References

[1] Tittel J., Bissinger V., Zippel B., Gaedke U., Bell E., LorkeA. and Kamjunke N.: Mixotrophs combine resource use to outcompete specialists: Implications for aquatic food webs – P.N.A.S., USA. 100, 2003, 12776–12781.

[2] Leboulanger C., Quiblier C. and Dufour P.: *Rapid assessment of multiple-limiting factors of phytoplankton biomass: in vivo chlorophyll a fluorescence and factorial design*, Arch. Hydrobiol. 2006, **166**, 433–451.

[3] Rücker J. and Liepelt A.: Pigmentbestimmung in sauren Tagebauseen – Probleme und Lösungsansätze – DGL – Tagungsbericht (Braunschweig), Tuzing 2003.
[4] Develi E.E., Kideys A.E. and Tugrul S.: *Effect of nutrients on culture dynamics of marine phytoplankton*, Aquat. Sci. 2006, **68**, 28–39.
[5] Szymczak-Zyła M., Grazyna Kowalewska G. and William Louda J.: *The influence of microorganisms on chlorophyll a degradation in the marine environment*, Limnol. Oceanogr. 2006, **53**, 851–862.
[6] Ikegami I., Nemoto A. and Sakashita K.: *The formation of Zn-Chl a in Chlorella heterotrophically grown in the dark with an excessive amount of* Zn^{2+}, Plant Cell Physiol. 2005, **46**, 729–735.
[7] Stich H.B. and Brinker A.: *Less is better: Uncorrected versus Pheopigment-corrected photometric chlorophyll-a estimation*, Arch. Hydrobiol. 2005, **162**, 111–120.
[8] Jeffry S.W., Mantoura R.F.C. and Wright S.W.: Phytoplankton pigments in oceanography, UNESCO Publishing, Paris 1998.
[9] Kohl J.-G. and Nicklisch A.: Ökophysiologie der Algen, G. Fischer Verlag, Stuttgart, New York 1988.
[10] Mantoura R.F.C., Jefrey S.W., Liewelyn C., Claustre H. and Moralies C.B.: *Comparison between spectrophotometric, fluorometric and HPLC methods for chlorophyll analysis*, [In:] Jeffry S.W., Mantoura R.F.C. and Wright S.W.: Phytoplankton pigments in oceanography, UNESCO Publishing, Paris 1997, 361–381.
[11] Wright S.W., Jefrey S.W. and Mantoura R.F.C.: *Evaluation of methods and solvents for pigment extraction*, [In:] Jeffry S.W., Mantoura R.F.C. and Wright S.W.: Phytoplankton pigments in oceanography, UNESCO Publishing, Paris 1997, 261–282.
[12] Webb D.J., Burnson B.K., Trimbee A.M. and Prepas E.E.: *Comparision of chlorophyll-a extraction with ethanol and dimethyl-sulfoxide/acetone, and concern about spectrophotometric phaeopigment correlation.* Can. J. Fish. Aquat. Sci. 1992, **49**, 2331–2336.
[13] Welschmeyer N.A.: *Fluorometric analysis of chlorophyll a in the presence of chlorophyll b and pheopigments*. Limnol. Oceanogr. 1994, **39**, 1985–1992.
[14] Ettl H.: Süßwasserflora von Mitteleuropa 9, Chlorophyta 1, 1st ed. Gustav Fischer Verlag, Jena 1983.
[15] Doi H., Kikuchi E., Hino S., Itoh T., Takagi S. and Shikano S.: *Seasonal dynamics of carbon stable isotope ratios of particulate organic matter and benthic diatoms in strongly acidic Lake Katanuma,* Aquat. Microb. Ecol. 2003, **33**, 87–94.
[16] Gerloff-Elias A., Spijkerman E. and Schubert H.: *Light acclimation of Chlamydomonas acidophila accumulating in the hypolimnion of an acidic lake (pH 2,6)*, Freshw. Biol. 2005, **50**, 1301–1314.
[17] Messerli M.A., Amaral-Zettler L.A., Zettler E., Jung S.-K., Smith P.J.S. and Sogin M.L.: *Life at acidic pH imposes an increased energetic cost for a eukaryotic acidophile*, J. Exp. Biol. 2005, **208**, 2569–2579.
[18] Gerloff-Elias A., Deepak B., Möllich A. and Spijkerman E.: *Temperature- and pH- dependent accumulation of heat-shock proteins in the acidophilic green alga Chlamydomonas acidophila*, FEMS Microbiol. Ecol. 2006, **56**, 345–354.
[19] Briantais J.-M., Cornic G. and Hodges M.: *The modification of chlorophyll fluorescence of Chlamydomonas reinhardtii by photoinhibition and chloramphenicol addition suggests a form of photosystem II less susceptible to degradation*, FEBS Letters 1988, **236**, 226–230.
[20] Förster B., Osmond C.B., Boynton J.E. and Gillham N.W.: *Mutants of Chlamydomonas reinhardtii resistant to very high light*, J. Photochem. Photobiol. 1999, **48**, 127–135.
[21] Förster B., Osmond C.B. and Boynton J.B.: *Very high light resistant mutant of Chlamydomonas reinhardtii: responses of photsystem II, nonphotochemical quenching and xanthophyll pigments to light and* CO_2. Photosynthesis Res. 2001, **67**, 5–15.
[22] Doi M., Inage T. and Shioi Y.: *Chlorophyll degradation in a Chlamydomonas reinhardtii mutant: An accumulatiom of pyropheophorbide a by anaerobiosis*, Plant Cell Physiol. 2001, **42**, 469–474.
[23] Nishikawa K., Machida H., Yamakoshi Y., Ohtomo R., Saito K., Saito M. and Tominaga N.: *Polyphosphate metabolism in an acidophilic alga Chlamydomonas acidophila KT-1 (Chlorophyta) under phosphate stress*, Plant Science 2006, **170**, 307–313.
[24] Nichols H.W.: Growth media-freshwater, Stein J.R. (Ed.), Handbook of Phycological Methods: Culture Methods and Growth Measurements. Cambridge University Press, Cambridge 1973, 7–24.
[25] Bissinger V., Jander J. and Tittel J.: *A new medium free of organic carbon to cultivate organisms from extremely acidic mining lakes (pH 2.7)*, Acta Hydrochim. Hydrobiol. 2007, **28**, 310–312.
[26] Gilmore A.M. and Yamamoto H.Y.: *Resolution of lutein and zeaxanthin using a non endcapped, lightly carbon-loaded C18 high-performance liquid chromatographic column*, J. Chromatography 1991, **543**, 137–145.

[27] Fach B.: *Growth and photosynthesis of C. acidophila grown in acidic, iron-rich lake water*, Diploma Thesis University of Potsdam, Potsdam 2008.

[28] Gerloff-Elias A., Spijkerman E. and Proeschold T.: *Effect of external pH on the growth, photosynthesis and photosynthetic electron transport of Chlamydomonas acidophila Negoro, isolated from an extremely acidic lake (pH 2.6*), Plant Cell Environ. 2005, **28**, 1218–1229.

[29] Spijkerman E., Barua D., Gerloff-Elias A., Kern J., Gaedke U. and Heckathorn S.A.: *Stress responses and metal tolerance of Chlamydomonas acidophila in metal-enriched lake water and artificial medium*, Extremophiles 2007, **11**, 551–562.

[30] Geider R.J. and La Roche J.: *Redfield revisited: variability of C: N: P in marine microalgae and its biochemical basis*, Eur. J. Phycol. 2002, **37**, 1–17.

[31] Geider R.J., MacIntyre H.L., Graziano L.M. and McKay R.M.L.: *Responses of the photosynthetic apparatus of Dunaliella tertiolecta (Chlorophyceae) to nitrogen and phosphorus limitation.* Eur. J. Phycol. 1998, **33**, 315–332.

[32] Meyns S., Illi R. and Rob B.: *Comparision of chlorophyll-a analysis by HPLC and spectrophotometry: Where do the differences come from?* Acta Hydrobiol. 1994, **1032**, 129–139.

[33] Mantile P., Hörtensteiner S. and Thomas H.: *Chlorophyll a degradation.* Ann. Rev. Plant Physiol. Plant. Mol. Biol. 1999, **50**, 67–95.

[34] Doi M., Shima S., Egashira T., Nakamura K. and Okayama S.: *New bile pigment excreted by a Chlamydomonas reinhardtii mutant o possible breakdown catabolite of chlorophyll a.* J. Plant Physiol. 1997, **150**, 504–508.

[35] Tittel J., Bissinger V., Gaedke U. and Kamjunke N.: *Inorganic carbon limitation and mixotrophic growth in Chlamydomonas from an acidic mining lake*, Protist. 2005, **156**, 63–75.

FLUOROSCENCJA I ABSORPCJE CHLOROFILU *A* DWÓCH GATUNKÓW *CHLAMYDOMONAS*

Abstrakt: Zagęszczenia fitoplanktonu w jeziorach i oceanach często jest mierzone *in vivo* za pomocą fluorescencji chlorofilu *a* (Chl *a*). Ta szybka i nieinwazyjna metoda ma dużą przewagę nad tradycyjnymi metodami pobierania próbek i ekstrakcji. W tej pracy badamy hipotezę, że pomiary *in vivo* fluorescencji rzeczywistego stężenia Chl *a* mogą prowadzić do zawyżonych ocen stężeń, jeśli komórki glonów zawierają stosunkowo duże stężenia produktów rozpadu Chl *a* w wyniku osiągnięcia stanu stacjonarnego wzrostu lub w wyniku przebywania w środowisku zawierającym wiele czynników stresowych. Zmierzono fluorescencję Chl *a in vivo* i *in vitro* dla dwóch gatunków *Chlamydomonas* i porównano z całkowitą zawartością Chl *a*. Uzyskano próbki w pełnym zakresie ich krzywej wzrostu. *Chlamydomonas reinhardtii* został wybrany jako gatunek żyjący w warunkach naturalnych, nie stresowych, a *Chlamydomonas acidophila* zamieszkuje stresogenne, bardzo kwaśne środowisko (pH 2,0–3,4). Rozpraszanie fluorescencji w czasie pomiarów *in vivo* wskazywało na średnio 25-krotnie mniejsze stężenie Chl *a* w porównaniu z pomiarami *in vitro* dla obu gatunków. W warunkach *in vivo* komórki *C. reinhardtii* rozpraszały ok. 1,5-krotnie silniej niż *C. acidophila*. W okresie pierwszych dwóch tygodni eksperymentu zawartość Chl *a* w komórkach rosła u obu gatunków *Chlamydomonas*. Po osiągnięciu maksimum zawartość Chl *a* zmniejszała się z czasem u obu gatunków. Stosunki zawartości produktów rozpadu Chl *a* do całkowitej zawartości Chl *a* nie różniły się statystycznie istotnie pomiędzy *C. acidophila* i *C. reinhardtii*. Oba gatunki zawierały około 16 % produktów degradacji Chl *a* w stosunku do całkowitego jego stężenia. Tylko 73–80 % stężenia Chl *a* mierzonego metodą fluorymetryczną *in vitro* zostało oznaczone za pomocą HPLC. Dlatego też, niezależnie od ustawienia fluorymetru, metoda fluorescencyjna prawdopodobnie zawyża stężenie Chl *a*. W rezultacie okazuje się, że niskie zewnętrzne pH lub stacjonarna równowaga wzrostu nie powodują zwiększenie stężenia produktów rozkładu Chl *a*. Ponadto ekstrapolacje fluorescencyjnego wykrywania Chl *a in situ* za pomocą czujnika wieloparametrowego do stężenia Chl *a* muszą być wykonane z dużą starannością ze względu na zależność rozpraszania fluorescencyjnego od rodzaju badanego gatunku.

Słowa kluczowe: *Chlamydomonas reinhardtii, Chlamydomonas acidophila*, ekologia wód słodkich, fluorescencja chlorofilu *a*, absorpcja chlorofilu *a*, pomiary *in vivo*, pomiary *in vitro*, wzrost, produkty rozkładu, sondy wieloparametrowe, HPLC

ECOLOGICAL CHEMISTRY AND ENGINEERING A

Vol. 16, No. 11 2009

Ewa B. MOLISZEWSKA[1] and Violetta SMIATEK[1]

TOXIC PROPERTIES OF *Alternaria radicina* CULTURE FILTRATES AGAINST CARROT SEEDS AND SEEDLINGS

WŁAŚCIWOŚCI TOKSYCZNE PRZESĄCZY POHODOWLANYCH *Alternaria radicina* W STOSUNKU DO NASION I SIEWEK MARCHWI

Abstract: The carrot seed samples health condition and their germination ability were discussed for the period 1997–2003. For the discussed period, the average infection of seed plots was 9.8 % and the seeds' percentage germination was 68.4 %. These parameters were correlated each other. The culture filtrates of five isolates of *Alternaria radicina* were tested in the laboratory experiments. *A. radicina* isolates were obtained from carrot seeds. Toxic activity of metabolites included in culture filtrates showed different activity against seeds and seedlings depending on the isolate type. Their phytotoxic influence was observed against germination of seeds; more dead seeds and abnormal seedlings were observed under their influence as well as the time of germination was prolonged. The influence on the normally developed and healthy seedlings showed the phytotoxic activity for more concentrated culture filtrates and a positive activity for low concentrated culture filtrates (1 %, 2 %) of isolates 001 and 003. The direct relationships between culture filtrates and their concentrations were not observed.

Keywords: carrot, *Alternaria radicina*, toxins, culture filtrate

Carrot (*Daucus carota* L.) is one of the major vegetable plant. It is grown in many cultivars and varieties because of the roots which are rich source of the β-carotene. Carrot roots can also accumulate some substances harmful for human beings. This can be prevented by use of healthy carrot seeds. Seeds frequently are contaminated by *Alternaria dauci* and *A. radicina* [1–3].

A. radicina is a seed-transmitted pathogen and causes seed rot, decreases seed germination percentage and reduces seedlings survival [4, 5]. Increase in seed infestation/infection by this pathogen results in the reduced germination of carrots [1,

[1] Department of Biotechnology and Molecular Biology, Opole University, ul. kard. B. Kominka 4, 45–035 Opole, Poland, phone/fax 77 401 60 50, email: ewamoli@uni.opole.pl

[2] Regional Station of Plant Protection and Seed Evaluation in Opole, ul. Wrocławska 172, 45–810 Opole, Poland, phone/fax 77 474 46 19, email: fiolaf@op.pl

2]. The black rot of carrot roots is a postharvest disease important during the storage and cultivation carrots for seed-yield. Carrot seeds and debris have been considered to be the critical primary inoculum of the disease in the field [2, 4].

A. radicina produces phytotoxins: radicin (RAD), radicinol (ROH) and *epi*-radicinol (*epi*-ROH). These phytotoxins were found in carrot samples naturally contaminated with *Alternaria* and showing black rot symptoms. Toxic activity of *A. radicina* is expressed on carrot tissues. Radicins are reported as not hazard for consumers but otherwise they express its phytotoxic activity important to obtain good quality of plant material [2].

The aim of this work was to evaluate a toxic activity of five strains of *A. radicina,* isolated from diseased carrot seeds, against carrot seeds and seedlings.

Materials and methods

The natural infestation by *A. radicina* and *A. dauci* of carrot seed samples was measured according to routine methods used for seed evaluation [6]. Beside this the seed samples germination ability was evaluated. Data obtained in 1997–2003 for samples from Bydgoszcz, Opole and Poznan were analyzed.

The five isolates of *A. radicina* were obtained from diseased carrot seeds cv. Krakowia during routine tests in Regional Station of Plant Protection and Seed Evaluation in Opole in 2003 [6]. Isolates were incubated on PDA medium as well as they were stored on PDA slants at +4 ^{o}C.

The toxic activity of *A. radicina* strains 001, 003, 004, 005, 006 was investigated in liquid Czapek medium used as culture filtrates after the time of incubation of fungi. The Erlenmayer flasks filled with 250 cm^3 of medium, were inoculated with three 3-mm discs of PDA medium overgrown by the particular isolate and cut from the margin parts of one-week-old colony, then incubated at room temperature for three weeks. Then the culture filtrates were used for toxicogenic activity. The tests for toxic activity of culture filtrate to carrot seeds and seedlings were conducted in plastic boxes lined with sterile blotting paper. The blotting papers in each box were soaked with culture filtrates using concentrations: 100 %, 50 %, 25 %, 12 %, 6 %, 3 %, 2 %, 1 % (v:v) of the raw filtrates. In each box 25 carrot seeds cv. Krakowia were separately sown and incubated in thermostat in eight-hours temperature intervals 30 ^{o}C and 20 ^{o}C. Incubation was made for 21 days, the toxic activity was estimated four times, first time after 7, next after 10, 14 and 21 days. In the control combination, instead of a culture filtrate, sterile distilled water was used. Experiment was done in four replications.

For evaluating the phytotoxic activity of tested strains metabolites against healthy, normally developed seedlings the modified method given by Sulek-Pieta [7] for investigation *Fusarium oxysporum* f. sp. *phaseoli* toxic activity against *Phaseolus vulgaris* L. was used. The healthy and normally developed seedlings were transferred to the solutions of culture filtrates (concentrations the same as in the previous tests as well as the control combination). Their condition and living time were observed comparing with the control. Test was done in four replications.

Results were statistical estimated by the variance method, significant differences between averages were measured according to Duncan's multiple range test ($\alpha = 0.05$).

Results

The infestation of carrot seed samples was significantly correlated with their germination ability. The average infestation of seed samples in the period 1997–2003 was 9.8 % and the germination of seeds was 68.4 %. Average seed germination ranged from 66.0 % to 80.4 % (Table 1).

Table 1

Quality of carrot seeds in three locations illustrated by average infection by *A. radicina*, average seed germination and correlation coefficients between infection and germination of seed samples (significant > 0.306 for $\alpha = 0.05$; significant > 0.432 for $\alpha = 0.01$)

Year	Source of samples	No. of samples	Average infection [%]	Average germination [%]	Correlation coefficient ($\alpha = 0.05$; $\alpha = 0.01$)
1997	Bydgoszcz, Opole	30	22.2	66.8	**–0.6319**
1998	Bydgoszcz, Poznan	48	7.7	68.5	–0.0113
1999	Bydgoszcz, Poznan	51	8.5	71.5	**–0.4426**
2000	Bydgoszcz, Opole, Poznan	69	8.8	66.0	–0.2766
2001	Bydgoszcz, Opole, Poznan	41	10.1	68.9	**–0.4963**
2002	Bydgoszcz, Poznan	41	7.7	66.3	**–0.4675**
2003	Bydgoszcz, Poznan	8	3.8	80.4	**–0.9756**
1997–2003	Bydgoszcz, Opole, Poznan	288	9.8	68.4	**–0.3466**

The test with culture filtrates (CFs) showed that seedlings obtained in CFs environment were smaller and weaker as well as the time of germination was prolonged even to 21 days, although the most germinated seeds were observed in 7th day and next in 10th day of the experiment. In case of CFs of isolates 005 and 006 more germinated seeds were denoted for the concentration 1 % in 7th day. The feature was not observed in 10th day and showed that 1 % concentrated CFs of isolates 005 and 006 could speed up the germination process. The seedlings condition (normal/abnormal) and their health were more significant in accordance with the higher CFs concentrations. Seedling roots were more frequently deformed and shortened than hypocotyls and cotyledons. CFs tested in the experiment showed different phytotoxic properties depending on the origin (fungal isolate) and the concentration level. Seeds treated with not diluted culture filtrates gave only a few normally developed seedlings. For the isolate 003 the lowest phytotoxicty was found in case of CF used in a concentration 25 % – there were 50 % of normally germinated seeds (Table 2, Fig. 2). CF used in low concentrations showed a minute ability to reduction of seed germination although the isolate 003 was the most toxic for carrot seeds comparing with the other ones (Table 2). In most cases, CFs used in the concentration 12 % showed greater ability to reducing seeds germination than

culture filtrates used in conc. 50 % or 25 %. Clean (not diluted) CF caused very high decrease of seed germination or they did not germinated at all in case of isolates 001 and 004 (Table 2). In all test combinations the percentage of seed germination was worse than in the control combination, although in the cases of isolate 004, 005 and 006 it was not statistically different from the control (Table 2).

Table 2

Carrot seed germination ability measured after 21 days

Concentration [%]	*Alternaria radicina* isolate				
	001	003	004	005	006
100	0 a*	5 a	0 a	1 a	3 a
50	25 b	28 b	6 ab	16 b	32 b
25	37 c	50 e	42 c	48 cd	47 c
12	41 c	24 b	17 b	42 c	31 b
6	37 c	31 bc	32 c	48 cd	48 c
3	39 c	42 cde	40 c	51 cd	55 cd
2	57 de	34 bcd	42 c	57de	56cd
1	54 d	47 de	65 d	60 de	60 cd
0 (control)	66 e	66 f	66 d	66 e	66 d

* Data indexed by the same letter are statistically not significant in columns.

The condition of seeds and seedlings influenced by culture filtrates was different and depended on the isolate. A minute number of normally developed seedlings were

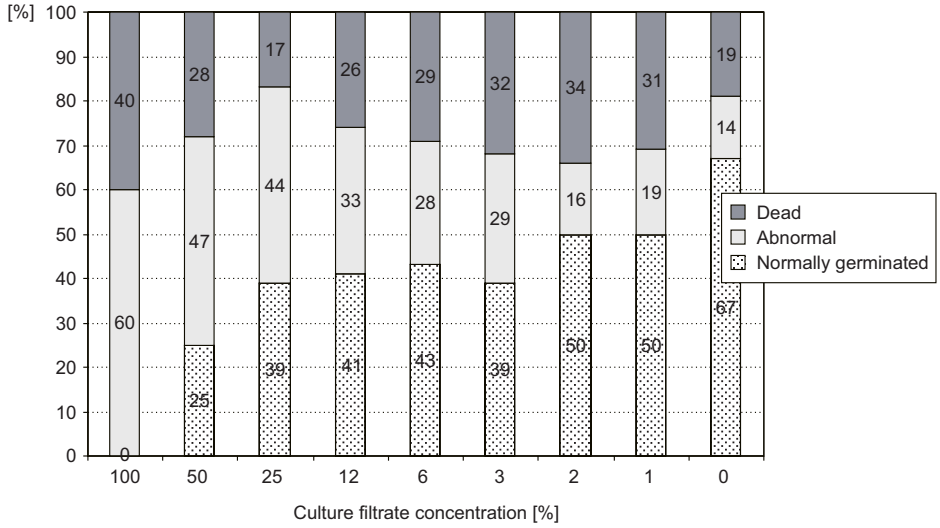

Fig. 1. The influence of culture filtrate of *A. radicina* 001 on the germination process of carrot seeds

observed under pure culture filtrates in case of isolates 003, 005 and 006 (5 %, 1% and 3 %, respectively). The isolate 004 used in conc. 50 % showed very similar activity – only 6 % of normally germinated seeds. For filtrates of 003, 004 and 006 in conc. 12 % we observed higher toxic activity than in case of twice more concentrated CFs (Figs. 1–5). In the combinations with the CFs of isolates 005 and 006 a high number of

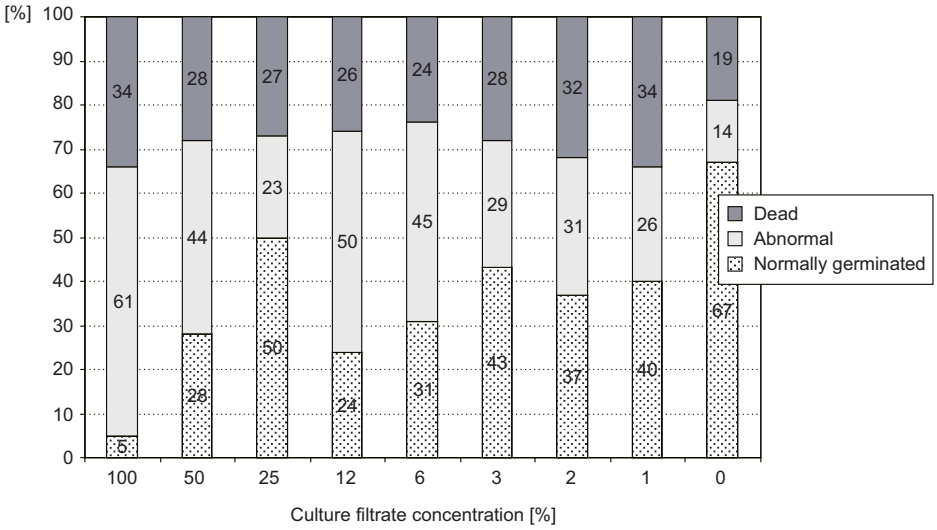

Fig. 2. The influence of culture filtrate of *A. radicina* 003 on the germination process of carrot seeds

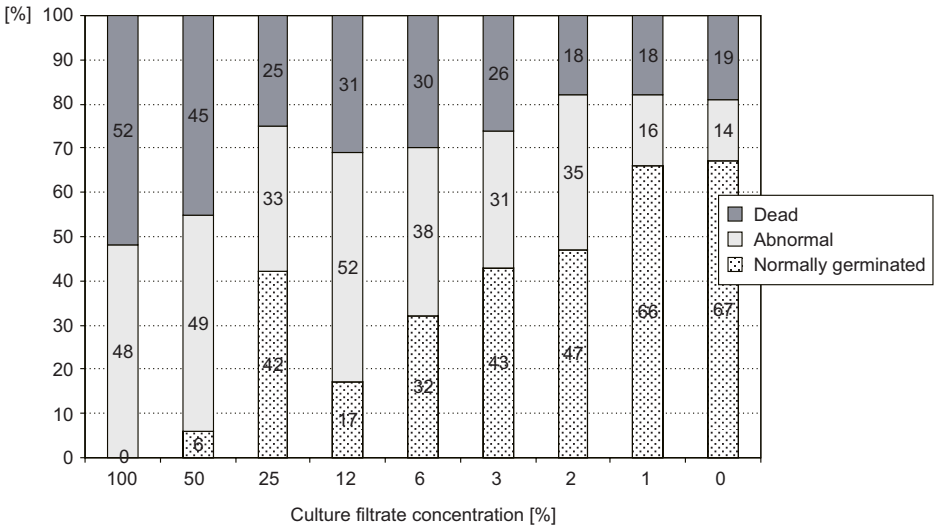

Fig. 3. The influence of culture filtrate of *A. radicina* 004 on the germination process of carrot seeds

abnormally germinated seeds were not observed in conc. 6–3 % to 1 % comparing with the control, but the number of dead seeds was higher (Figs. 4, 5). Higher concentrated CFs (100–12 %) showed the phytotoxic influence directed rather against seedlings than seeds. The lowest concentrated CFs had not significant activity. The effect on seeds ranged from 57 % and 52 % of dead seeds for not diluted CFs of isolate 006 and 004,

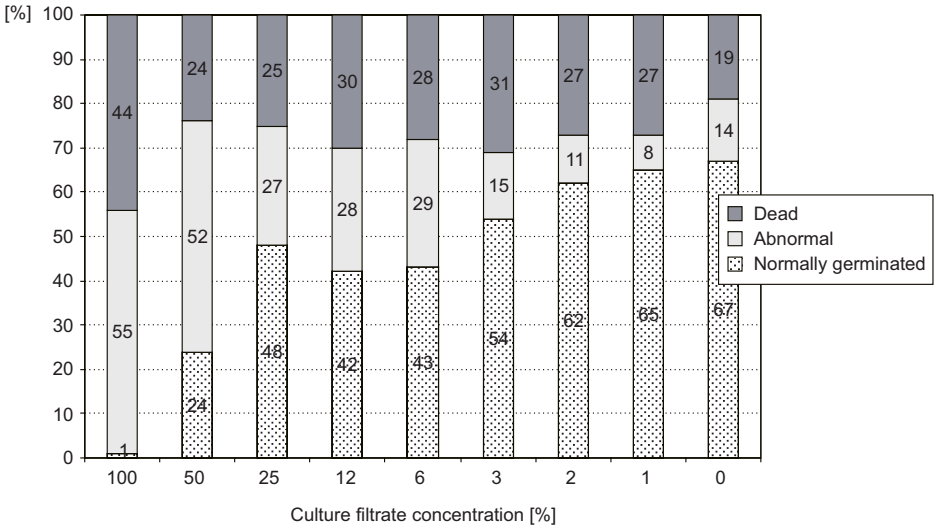

Fig. 4. The influence of culture filtrate of *A. radicina* 005 on the germination process of carrot seeds

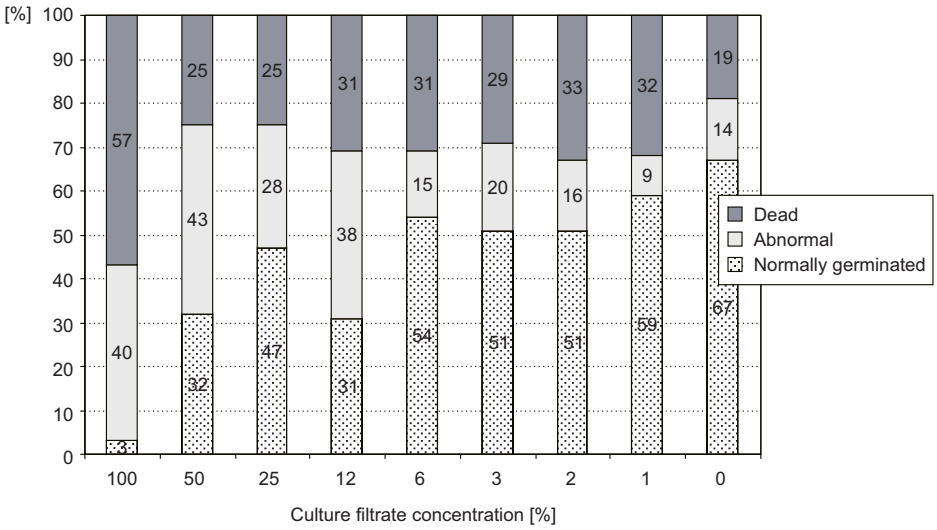

Fig. 5. The influence of culture filtrate of *A. radicina* 006 on the germination process of carrot seeds

respectively to 18 % of dead seeds for CF of isolate 004 in conc. 2 % and 1 % (Figs. 1–5). The results show that fungal metabolites activity is a combination of the influence on the seeds and seedlings condition but they depend on the CFs origin (fungal isolate) and their concentration.

Normally developed carrot seedlings were put on the Petri dishes lined with the blotting paper and soaked with diluted CFs. The influence of tested CFs on seedlings showed that the best results were obtained for low concentrated culture filtrates (2 %, 1 %) comparing with the control. The time of seedlings persisting/living was for one week longer for seedlings treated with low (1 %, 2 %) concentrated CFs of isolates 001 and 003. For filtrates of other isolates the results for highly diluted CF were comparable with the control (Table 3). The isolates 001 and 003 showed the weaker influence on the seedlings than the other isolates. The strongest phytotoxic activity showed the isolate 004 (Table 3).

Table 3

The influence of culture filtrates of *A. radicina* isolates on the time of living [days] of healthy and normally developed carrot seedlings

Culture filtrate concentration [%]	*Alternaria radicina* isolate				
	001	003	004	005	006
100	4.0 a*	4.8 a	2.3 a	3.0 a	3.0 a
50	5.0 a	6.0 a	4.3 b	3.5 a	3.0 a
25	8.3 ab	8.3 ab	3.8 ab	3.8 a	3.8 a
12	8.0 ab	7.5 ab	4.8 b	5.8 ab	3.5 a
6	8.8 ab	10.5 bc	5.5 bc	7.3 bc	5.8 ab
3	10.0 b	14.3 cd	7.0 c	8.8 cd	8.0 bc
2	16.0 c	13.3 cd	9.5 d	9.8 cd	8.5 bc
1	18.5 c	17.3 d	10.25 d	11.0 d	10.8 c
0 (control)	10.5 b	10.5 bc	10.5 d	10.5 d	10.5 c

* Data indexed by the same letter are statistically not significant in columns.

Discussion

The phytotoxic activity of radicines is related with carrot tissues. The carrot plant is biennial and pathogens correlated with carrot seeds originate from the carrot plants develop in their second year of cultivation. Because of this the health condition of taproots used in growing plants for seeds is very important. *A. radicina* existing on the taproots can develop on the plants in the second year of growing and then infect seeds. Fungicides used in the controlling root pathogens prevent only those ones free of pathogens but do not those originally infected [1, 8]. Avoiding infection of taproots is important both for commercially produced carrots and for seed production. Contamination of seed plots by *A. radicina* achieved even a 99 % of them at level ranging

from 0.5 % to 82.5 % for Polish samples in the period 1984–1988 and equally for samples from other countries but in infection rates to 35 % [1]. The investigated carrot seed plots were average infected 9.8 % in the period 1997–2003, and the highest rate of infection was 22.2 % (Table 1). These results show that the seeds quality in the experiment was better than quality of seed lots in 1984–1988. This is important in carrot cultivation because use of *A. radicina*-free seed is the first and perhaps most important step toward the integrated management of black rot of carrot. *A. radicina* was found also on seeds treated with thiram and/or iprodione at levels of 0.2 % to 14 % [1], so this highlights that contamination of carrot seeds is a continuing problem. The importance of contamination was shown in germination tests. *A. radicina* isolates and their metabolites (radicins) showed negative influence on the seed percentage germination and their quality as well as their time of germination. In our tests the germination was prolonged to even 21 days although the typical time of carrot seed germination is 7 to 12 days [1]. A risk of damping-off increases if the time of germination is prolonged and if seed samples are infected by pathogens and results in reduced stands and yield. Tests showed also that radicins can influence on the seedlings. They reduced a number of normally developed plants, and the number of abnormal seedlings was higher under their influence as well as the living time of normally developed plants was reduced. The low concentrated toxins were not a hazard for seedlings, we observed even that they could live for longer time than in the control. One of the reason was the non-specific mode of action of radicins and probably remnant of medium diluted together with metabolites, but naturally grown seedlings use nutrients from soil-solution as well. The mode of action of culture filtrates of *A. radicina* observed in our investigation showed its non-specific features [9] and the differentiation between fungal isolates in the ability of producing the phytotoxic components.

References

[1] Farrar J., Pryor B.M. and Davis R.M.: *Alternaria diseases of carrot*. Plant Dis. 2004, **88**(8), 776–784.

[2] Solfrizzo M., De Girolamo A., Vitti C., Tylkowska K., Grabarkiewicz-Szczęsna J., Szopińska D. and Dorna H.: *Toxigenic profile of Alternaria alternata and Alternaria radicina occuring on umbelliferous plants*. Food Addit. Contaminants 2005, **22**(4), 302–308.

[3] Pryor B.M.: *Survival and persistence of Alternaria dauci in carrot cropping systems*. Plant Dis. 2002, **86**, 1115–1122.

[4] Chen T.W. and Wu W.S.: *Biological control of carrot black rot*. J. Phytopathol. 1999, **147**, 99–104.

[5] Santos P., Nuneu J.J. and Davis R.M.:*Influence of giberelic acid on carrot growth and severity of Alternaria leaf blight*. Plant Dis. 2000, **84**, 555–558.

[6] Tylkowska K.: Ćwiczeniaz nasiennictwa ogrodniczego, część IV, oznaczanie zdrowotności nasion, Wyd. Akad. Roln. Poznań 1989.

[7] Sułek-PiętaD.: *Badania nad podatnością różnych odmian fasoli na porażenie przez Fusarium oxysporum Schil. f. sp. phaseoli Kend. Snyder*. Z. Probl. Post. Nauk Roln. 1983, **275**, 131–141.

[8] Kućmierz J., Mazur S. and Bartyńska M.: *Wpływ przedplonu na zdrowotność korzeni marchwi (Daucus carota L.)*. Phytopathol. Polon. 1990, **XI**, 395–405.

[9] Lucas J.A.: Plant pathology and plant pathogens, 3rd ed., Blackwell Science Ltd., UK 1998.

WŁAŚCIWOŚCI TOKSYCZNE PRZESĄCZY POHODOWLANYCH *Alternaria radicina* W STOSUNKU DO NASION I SIEWEK MARCHWI

[1] Katedra Biotechnologii i Biologii Molekularnej
Uniwersytet Opolski
[2] Wojewódzki Inspektorat Ochrony Roślin i Nasiennictwa w Opolu

Abstrakt: Porównano zdrowotność oraz zdolność kiełkowania partii nasion marchwi pochodzących z trzech rejonów Polski w latach 1997–2003. Średnie porażenie nasion w omawianym okresie wynosiło 9,8 %, a średnia zdolność kiełkowania – 68,4 %. Obydwa parametry były ze sobą skorelowane. W doświadczeniach laboratoryjnych zbadano wpływ przesączy pohodowlanych pięciu izolatów *Alternaria radicina* uzyskanych z nasion marchwi. Metabolity zawarte w przesączach pohodowlanych wykazywały działanie fitotoksyczne zarówno na nasiona marchwi, jak i na jej siewki. Obserwowano zwiększoną śmiertelność nasion, rozwój siewek anormalnych oraz przedłużenie kiełkowania. Roztwory przesączy pohodowlanych wpływały także negatywnie na żywotność zdrowych i normalnie rozwiniętych siewek marchwi, jednak filtraty izolatów 001 i 003 w małych stężeniach (1 %, 2 %) wykazywały się zdolnością do przedłużania życia siewek w porównaniu do kontroli. Nie obserwowano bezpośredniej zależności działania badanych przesączy od ich stężenia.

Słowa kluczowe: marchew, *Alternaria radicina*, toksyny, przesącz pohodowlany

Varia

INVITATION
FOR ECOPOLE '10 CONFERENCE

CHEMICAL SUBSTANCES IN ENVIRONMENT

We have the honour to invite you to take part in the 19th annual Central European Conference ECOpole '10, which will be held in **13–16 X 2010** (Thursday–Saturday) on Wilhelms Hill at Uroczysko in Piechowice, the Sudety Mts., Lower Silesia, PL.

The Conference Programme includes oral presentations and posters and will be divided into five sections:

- **SI Chemical Pollution of Natural Environment and its Monitoring;**
- **SII Environment Friendly Production and Use of Energy;**
- **SIII Risk, Crisis and Security Management**;
- **SIV Forum of Young Scientists and Environmental Education;**
- **SV Impact of Environment Pollution on Food and Human Health.**

The Conference language is English.

Contributions to the Conference will be published as:

- abstracts on the CD-ROM (0.5 page of A4 paper sheet format);
- extended Abstracts (4-6 pages) in the semi-annual journal *Proceedings of ECOpole*;
- full papers will be published in successive issues of the *Ecological Chemistry and Engineering/Chemia i Inżynieria Ekologiczna* (Ecol. Chem. Eng.) ser. A and S.

Additional information one could find on the Conference website:

ecopole.uni.opole.pl

The deadline for sending the Abstracts is **15.07.2010** and for the Extended Abstracts: **1.10.2010**. The actualised list (and the Abstracts) of the Conference contributions accepted for presentation by the Scientific Board, one can find (starting from 15.07.2010) on the Conference website.

The papers must be prepared according to the Guide for Authors on Submission of Manuscripts to the Journals.

At the Reception Desk each participant will obtain a CD-ROM with abstracts of the Conference contributions as well as Conference Programme (the Programme will be also published on the Conference website).

At the Reception Desk each participant will obtain a CD-ROM with abstracts of the Conference contributions as well as Conference Programme (the Programme will be also published on the Conference website).

Maria Waclawek

Further information is available from:
Dr hab. Maria Wacławek, prof. UO
Chairperson of the Organising Committee
of ECOpole '10 Conference
Opole University
email: Maria.Waclawek@uni.opole.pl
and mrajfur@o2.pl
tel. +48 77 455 91 49 and +48 77 401 60 42
fax +48 77 401 60 51

Conference series

1. 1992 Monitoring '92 Opole
2. 1993 Monitoring '93 Turawa
3. 1994 Monitoring '94 Pokrzywna
4. 1995 EKO-Opole '95 Turawa
5. 1996 EKO-Opole '96 Kędzierzyn Koźle
6. 1997 EKO-Opole '97 Duszniki Zdrój
7. 1998 CEC ECOpole '98 Kędzierzyn Koźle
8. 1999 CEC ECOpole '99 Duszniki Zdrój
9. 2000 CEC ECOpole 2000 Duszniki Zdrój
10. 2001 CEC ECOpole '01 Duszniki Zdrój
11. 2002 CEC ECOpole '02 Duszniki Zdrój
12. 2003 CEC ECOpole '03 Duszniki Zdrój
13. 2004 CEC ECOpole '04 Duszniki Zdrój
14. 2005 CEC ECOpole '05 Duszniki Zdrój
15. 2006 CEC ECOpole '06 Duszniki Zdrój
16. 2007 CEC ECOpole '07 Duszniki Zdrój
17. 2008 CEC ECOpole '08 Piechowice
18. 2009 CEC ECOpole '09 Piechowice

ZAPRASZAMY
DO UDZIAŁU W ŚRODKOWOEUROPEJSKIEJ KONFERENCJI
ECOpole '10
w dniach 13–16 X 2010

SUBSTANCJE CHEMICZNE W ŚRODOWISKU PRZYRODNICZYM

Będzie to dziewiętnasta z rzędu konferencja poświęcona badaniom podstawowym oraz działaniom praktycznym dotycząca różnych aspektów ochrony środowiska przyrodniczego. Odbędzie się ona w ośrodku „Uroczysko" na Wzgórzu Wilhelma w Piechowicach koło Szklarskiej Poręby. Doroczne konferencje ECOpole mają charakter międzynarodowy i za takie są uznane przez Ministerstwo Nauki i Szkolnictwa Wyższego.

Obrady konferencji ECOpole '10 będą zgrupowane w pięciu sekcjach
- **SI Chemiczne substancje w środowisku przyrodniczym oraz ich monitoring;**
- **SII Odnawialne źródła energii i jej oszczędne pozyskiwanie oraz użytkowanie;**
- **SIII Zarządzanie środowiskiem w warunkach kryzysowych;**
- **SIV Forum Młodych (FM) i Edukacja prośrodowiskowa;**
- **SV Wpływ zanieczyszczeń środowiska oraz żywności na zdrowie ludzi**.

Materiały konferencyjne będą opublikowane w postaci:
- abstraktów (0,5 strony formatu A4) na CD-ROM-ie;
- rozszerzonych streszczeń o objętości 4-6 stron w półroczniku *Proceedings of ECOpole*;
- artykułów: w abstraktowanych czasopismach: *Ecological Chemistry and Engineering/Chemia i Inżynieria Ekologiczna* (*Ecol. Chem. Eng.*) ser. A i S oraz niektórych w półroczniku *Chemia – Dydaktyka – Ekologia – Metrologia*.

Termin nadsyłania angielskiego i polskiego streszczenia o objętości 0,5–1,0 strony (wersja cyfrowa + wydruk) planowanych wystąpień upływa w dniu 15 lipca 2010 r. Lista prac zakwalifikowanych przez Radę Naukową Konferencji do prezentacji będzie sukcesywnie publikowana od 15 lipca 2010 r. na stronie webowej

ecopole.uni.opole.pl

Aby praca (dotyczy to także streszczenia, które powinno mieć tytuł w języku polskim i angielskim, słowa kluczowe w obydwu językach) przedstawiona w czasie konferencji

mogła być opublikowana, jej tekst winien być przygotowany zgodnie z wymaganiami stawianymi artykułom drukowanym w czasopismach *Ecological Chemistry and Engineering* ser. *A* oraz *S*, które jest dostępne w wielu bibliotekach naukowych w Polsce i zagranicą. Są one takie same dla prac drukowanych w półroczniku *Chemia – Dydaktyka – Ekologia – Metrologia*.

Po konferencji zostaną wydane 4-6-stronicowe rozszerzone streszczenia wystąpień w półroczniku *Proceedings of ECOpole*. Artykuły te winny być przesłane do **1 października 2010 r**. Wszystkie nadsyłane prace podlegają zwykłej procedurze recenzyjnej. Wszystkie streszczenia oraz program Konferencji zostaną wydane na CD-ROM-ie, który otrzyma każdy z uczestników podczas rejestracji. Program będzie także umieszczony na stronie webowej Konferencji.

dr hab. inż. Maria Wacławek, prof. UO
Przewodnicząca Komitetu Organizacyjnego
Konferencji ECOpole ’10

Wszelkie uwagi i zapytania można kierować na adres:
Maria.Waclawek@uni.opole.pl
lub mrajfur@o2.pl
tel. 77 401 60 42
tel. 77 455 91 49
fax 77 401 60 51

Kalendarium

1. 1992 Monitoring ’92 Opole
2. 1993 Monitoring ’93 Turawa
3. 1994 Monitoring ’94 Pokrzywna
4. 1995 EKO-Opole ’95 Turawa
5. 1996 EKO-Opole ’96 Kędzierzyn Koźle
6. 1997 EKO-Opole ’97 Duszniki Zdrój
7. 1998 ŚEK ECOpole ’98 Kędzierzyn Koźle
8. 1999 ŚEK ECOpole ’99 Duszniki Zdrój
9. 2000 ŚEK ECOpole 2000 Duszniki Zdrój
10. 2001 ŚEK ECOpole ’01 Duszniki Zdrój
11. 2002 ŚEK ECOpole ’02 Duszniki Zdrój
12. 2003 ŚEK ECOpole ’03 Duszniki Zdrój
13. 2004 ŚEK ECOpole ’04 Duszniki Zdrój
14. 2005 ŚEK ECOpole ’05 Duszniki Zdrój
15. 2006 ŚEK ECOpole ’06 Duszniki Zdrój
16. 2007 ŚEK ECOpole ’07 Duszniki Zdrój
17. 2008 ŚEK ECOpole ’08 Piechowice
18. 2009 ŚEK ECOpole ’09 Piechowice

15th ICHMET

15th International Conference on Heavy Metals in the Environment
September 19–23, 2010
Gdańsk, Poland

Organized by
Chemical Faculty, Gdańsk University of Technology (GUT)
together with
Committee on Analytical Chemistry of the Polish Academy Sciences (PAS)

15th ICHMET – is a continuation of a series of highly successful conferences that have been held in major cities of the world since 1975. These conferences typically draw 500–1000 participants from countries in many parts of the world. Well over 5000 scientists have taken part in this series of conferences including most leaders in the field. Apart from the city's natural beauty, Gdansk is logical choice for the 15th Conference to highlight the outstanding work that is being done on heavy metals in central Europe. The venue for the meeting will be the Gdansk University of Technology (GUT) which features many tourist attractions.

The Conference will include a number of invited lectures treating frontier topics prepared by specialist with international reputation, oral presentation and poster sessions. ICHMET welcomes contributions on all aspects of any heavy metal in the environment. All presentation will be connected with such topics as:

- Risk assessment and risk management pertaining to toxic metals in the environment
- Susceptibility and protection of children from toxic metals in their environment
- Measurement and exposure assessment
- Biomarkers of exposure and effects of heavy metals
- Gene-environment-metal interactions
- Trend tracking/analysis of heavy metal data – spatial and temporal
- Risk communication pertaining to heavy metals
- Life cycle analysis for metalliferous consumer products
- Soil quality criteria
- Remediation technologies
- Control strategies for heavy metal emissions and deposition
- Metal mixtures – mechanistic and epidemiological studies
- Nutrient-metal interactions
- Advancements in analytical tools (procedures and measurement devices)

– Toxicology of heavy metals, from cellular and genomic to ecosystem levels
– Heavy metals in foods
– Impact of global change on heavy metal cycle

For further information on the conference, please contact:

Professor Jacek Namieśnik (Conference Chairman)
Gdansk University of Technology,
Chemical Faculty, Department of Analytical Chemistry
G. Narutowicza 11/12, 80–233 Gdansk, (Poland),
e-mail: chemanal@pg.gda.pl
homepage: http://www.pg.gda.pl/chem/ichmet/

GUIDE FOR AUTHORS
ON SUBMISSION OF MANUSCRIPTS

A digital version of the Manuscript addressed –

Professor Witold Wacławek
Editorial Office of monthly *Ecological Chemistry and Engineering*
(Ecol. Chem. Eng.)
Uniwersytet Opolski
ul. Oleska 48, 45–951 Opole, Poland
Tel. +48 77 452 71 34, fax +48 77 455 91 49,
Email – waclawek@uni.opole.pl

should be sent by email to the Editorial Office Secretariat – mrajfur@o2.pl

The Editor assumes, that an author submitting a paper for publication has been authorised to do that. It is understood the paper submitted to be original and unpublished work, and is not being considered for publication by another journal. After printing, the copyright of the paper is transferred to *Towarzystwo Chemii i Inżynierii Ekologicznej* (*Society for Ecological Chemistry and Engineering*). In preparation of the manuscript please follow the general outline of papers published in the most recent issues of *Ecol. Chem. Eng*., a sample copy can be sent, if requested.

Papers submitted are supposed to be written in English language and should include a summary and keywords, if possible also in Polish language. If not then the Polish summary and keywords will be provided by the Editorial Office. All authors are requested to inform of their current addresses, phone and fax numbers and their email addresses.

It is urged to follow the units recommended by the *Systéme Internationale d'Unites* (SI). Graph axis labels and table captions must include the quantity units. The use of the following commonly applied expressions is recommended: mass – m/kg, time – t/s or t/min, current intensity – I/A; thermodynamic temperature – T/K, Celsius scale temperature – t/°C or θ/°C (if both time and Celsius scale units need to be used, the symbol θ/°C for temperature is to be taken) etc.

Symbols recommended by the International Union of Pure and Applied Chemistry (Pure and Appl. Chem., 1979, **51**, 1–41) are to be followed.

Graphics (drawings, plots) should also be supplied in the form of digital vector – type files, *e.g*. Corel-Draw, Grapher for Windows or at least in a bitmap format (TIF, PCK, BMP). In the case of any query please feel free to contact with the Editorial Office.

Footnotes, tables and graphs should be prepared as separate files.

References cited chronologically should follow the examples given below:

[l] Kowalski J. and Malinowski A.: Polish J. Chem. 1990, **40**(3), 2080–2085.

[2] Nowak S: Chemia nieorganiczna, WNT, Warszawa 1990.

[3] Bruns I., Sutter K., Neumann D. and Krauss G.-J.: *Glutathione accumulation – a specific response of mosses to heavy metal stress*, [in:] Sulfur Nutrition and Sulfur Assimilation in Higher Plants, P. Haupt (ed.), Bern, Switzerland 2000, 389–391.

Journal titles should preferably follow the Chem. Abst. Service recommended abbreviations.

Receipt of a paper submitted for publication will be acknowledged by email. If no acknowledgement has been received, please check it with the Editorial Office by email, fax, letter or phone.

ZALECENIA DOTYCZĄCE PRZYGOTOWANIA MANUSKRYPTÓW

Praca przeznaczona do druku w miesięczniku *Ecological Chemistry and Engineering A/Chemia i Inżynieria Ekologiczna A* powinna być przesłana na adres Redakcji:

Profesor Witold Wacławek
Redakcja Ecological Chemistry and Engineering
Uniwersytet Opolski
ul. Oleska 48, 45–951 Opole
tel. 077 401 60 42, fax 077 455 91 49
email: waclawek@uni.opole.pl

w postaci cyfrowej w formacie Microsoft Word (ver. 7.0 dla Windows) emailem (mrajfur@o2.pl) lub na dyskietce.

Redakcja przyjmuje, że przesyłając artykuł do druku autor w ten sposób oświadcza, że jest upoważniony do tego oraz zapewnia, że artykuł ten jest oryginalny i nie był wcześniej drukowany gdzie indziej i nie jest wysłany do druku gdzie indziej oraz, że po jego wydrukowaniu copyright do tego artykułu uzyskuje Towarzystwo Chemii i Inżynierii Ekologicznej.

W przygotowaniu manuskryptu należy przede wszystkim wzorować się na postaci najnowszych artykułów opublikowanych w *Ecological Chemistry and Engineering*, na przykład zamieszczanych na stronie webowej Towarzystwa: http://tchie.uni.opole.pl/tchie/index.php?option=content&pcontent=1&task=view&id=49&Itemid=76

Prace przesyłane do publikacji winny być napisane w języku angielskim oraz zaopatrzone w streszczenia oraz słowa kluczowe w języku angielskim oraz polskim.

Zalecamy, ażeby artykuł zawierał adresy i emaile oraz numery telefonów i faksów wszystkich autorów danej pracy, szczególnie głównego autora, którego nazwisko wyróżniamy gwiazdką.

Usilnie prosimy o stosowanie układu jednostek SI. Zwracamy uwagę, że osie wykresów oraz główki tabel powinny bezwzględnie zawierać jednostki stosownej wielkości. Polecamy symbolikę zalecaną przez PTChem (Symbole i terminologia wielkości i jednostek stosowanych w chemii fizycznej, Ossolineum, Wrocław 1989; Pure Appl. Chem. 1979, **51**, 1–41). Materiał graficzny (rysunki, wykresy), obok wersji na papierze, powinien również być dostarczony w postaci cyfrowych plików wektorowych, np. za pomocą programu: CorelDraw wersja 3.0–8.0, Grafer dla Windows lub przynajmniej bitowe (TIF, PCX, BMP). W przypadku trudności z wypełnieniem tego warunku Redakcja

zapewnia odpłatne wykonanie materiału graficznego na podstawie dostarczonego szkicu, bliższe informacje można uzyskać telefonicznie 077 401 60 42.

Przypisy i tabele podobnie jak rysunki zapisujemy jako osobne pliki.

Literaturę prosimy zamieszczać wg poniższych przykładów:

[1] Kowalski J. and Malinowski A.: Polish J. Chem. 1990, **40**, 2080–2085.

[2] Nowak S.: Chemia nieorganiczna, WNT, Warszawa 1990.

[3] Bruns I., Sutter K., Neumann D. and Krauss G.-J.: *Glutathione accumulation – a specific response of mosses to heavy metal stress*, [in:] Sulfur Nutrition and Sulfur Assimilation in Higher Plants, P. Haupt (ed.), Bern, Switzerland 2000, 389–391.

Tytuły czasopism należy skracać zgodnie z zasadami przyjętymi przez amerykańską Chemical Abstracts Service. Autor może, jeżeli uważa to za wskazane, podawać też tytuł cytowanych artykułów z czasopism, który będzie składany kursywą oraz numer zeszytu danego woluminu (w nawiasie, po numerze woluminu).

Redakcja potwierdza emailem otrzymanie artykułu do druku. W przypadku braku potwierdzenia prosimy o interwencję: emailem, faksem, listem lub telefonicznie.

REDAKTOR TECHNICZNY
Halina Szczegot

SKŁAD KOMPUTEROWY
Jolanta Brodziak

PROJEKT OKŁADKI
Marian Wojewoda

Druk: „Drukarnia Smolarski", Józef Smolarski, 45–326 Opole, ul. Sandomierska 1. Objętość: ark. wyd. 10,50, ark. druk. 8,00.